Elsevier Editorial System(tm) for Journal of Non-Crystalline Solids

Manuscript Draft

Manuscript Number:

Title: Molecular dynamic in binary mixtures and polymer blends with large difference in glass transition temperatures of the two components: a critical review

Article Type: VSI: GUPTA

Keywords: Dynamics; Mixtures; polymer blends; Johari-Goldstein relaxation; glasses

Corresponding Author: Professor Kia L Ngai, PHD

Corresponding Author's Institution: IPCF

First Author: Kia Ngai

Order of Authors: Kia Ngai; Sofia Valenti, M.S.; simone capaccioli, Ph D

Abstract: By mixing a molecular or polymeric glass-former with another one, its dynamic and thermodynamic properties can be modified to various degrees depending on the composition. The study of the modifications is beneficial not only in basic research on glasses and glass transition but also in applications. When the difference in glass transition temperatures of the two components Tg is not too large (less than 100 K), commonly observed in miscible mixtures is a single glass transition temperature coming from a single structural a-relaxation, which is accompanied by a Johari-Goldstein (JG) b-relaxation strongly connected in dynamic properties. Satisfactory explanation of the connected dynamics of the two relaxations and changes with composition have been given by the Coupling Model. The dynamics and thermodynamics in highly asymmetric mixtures (i.e., when Tg is large) are more complex. Two a-relaxations (a1 and a2) and correspondingly two glass transitions temperatures (T_g^α1 and T_g^α2) were clearly identified at high and moderate values of c2 of the lower-Tg2 component. However, at low values of c2, only the a1-relaxation and its glass transition at T_g^α1 were found together with a fast relaxation having approximately an Arrhenius temperature dependence for its relaxation time at low temperatures. There are two ways to interpret the data. One interpretation of the observed fast relaxation is the JG b-relaxation, and the 2-relaxation is not resolved due to low c2. Some researchers interpretated the fast relaxation as the 2-relaxation, but its properties and the associated T_g^α2 are drastically modified at low c2, and the JG -relaxation is either unresolved or non-existent. They further proposed that the drastic modification of the 2-relaxation is due to confinement of the low-Tg2 component by the frozen high-Tg1 component. It is transformed to local relaxation within the confined spaces, and becomes identifiable with the observed fast relaxation having Arrhenius T-dependence. This view and interpretation of the dynamics of highly asymmetric mixtures and polymer blends are maintained to be valid up to the present time. In this paper we review exhaustively the experimental data of many highly asymmetric mixtures and blends to show unequivocally that the observed fast relaxation is the JG b-relaxation and not the a2-relaxation.

Notwithstanding, the a2-relaxation with its associated $T_g^{\alpha 2}$ is also present, albeit not easily resolved due to weak relaxation strength at low c2. The value of $T_g^{\alpha 2}$ increases monotonically on decreasing c2, without exhibiting a maximum as concluded by one group. The fast relaxation is demonstrated to be the JG b-relaxation from its connection to both the a1 and the a2 relaxations in its properties including the pressure dependence of its relaxation time. Established also is the significant increase of $T_g^{\alpha 2}$ with pressure, and hence also the relaxation time of the a2-relaxation, despite it is confined. Only experimental data are utilized in this review, and therefore the conclusions we arrived at are totally objective.

Suggested Reviewers: Thomas Blochowicz Ph D
Prof., Institut fur Festkorperphysik, TU-Darmstadt
thomas.blochowicz@physik.tu-darmstadt.de
He has done the most extensive studies using different spectroscopies including neutron scattering. His data are critical in this review. None of the authors have published with him.

Osamu Urakawa PH D
Prof., Department of Macromolecular Science, University of Osaka
urakawa@chem.sci.osaka-u.ac.jp
His is the leader of the Japanese group working on dynamics and thermodynamics of polymer blends and mixtures of molecules with polymers. His data are important contributions and cited in the review. None of the authors has published paper with him.

G GOULART SILVA PH D
Prof., G. GOULART SILVA, ICEx/UFMG
glaura@lcc.ufmg.br
He or she published important paper cited in the review.

George Floudas PH D
Prof., Physics, University of Ioannina
gfloudas@uoi.gr
He published important data on this subject and his paper is cited in this review

K.L. Ngai
Dipartimento di Fisica, Universita di Pisa,
Largo Bruno Pontecorvo 3, I-56127, Pisa, Italy

Telephone 39 050 221 4322 (lab), 4537(office) e-mail: kia.ngai@ pi.ipcf.cnr.it
kia.ngai@pi.ipcf.cnr.it,
kiangai@yahoo.com

February 22nd, 2019

Prof. Edgar Dutra Zanotto
Editor
J.Non-Cryst.Solids

Dear Prof. Zanotto,

I am submitting the manuscript entitled " **Molecular dynamic in binary mixtures and polymer blends with large difference in glass transition temperatures of the two components: a critical review** " by K. L. Ngai, Sofia Valenti, and Simone Capaccioli, for your consideration of publication as a Review article in the special issues of "Frontiers of Glass Science" and "PK Gupta".

The dynamics of the equilibrium liquid and glassy states of mixtures of two molecular glass-formers, mixture of moleuclar glass-former with polymer, and polymer blends are active research areas for the past few decades and continues to the present time. Currently of particular interest are the highly asymmetric mixtures and blends, which are composed of two components with very large difference in their glass transition temperatures. As expected, novel phenomena emerge from the experimental studies of these systems, and are challenging for fundamental understanding. In the course of the last twenty years, several attempts were made to interpret the experimental data and explain the phenomena. However, no consensus of interpretation and explanation have been reached, possibly due not all experimental facts were taken into consideration in past attempts. Thus, in this review we collect and consider all relevant experimental data. This undertaking is instrumental in arrive at an interpretation consistent with all available experiments. Since only experimental data are considered, this review is totally objective, and can be used as a basis for others to make their contributions.

For reviewers I suggest the following reserchers who made contributions to the subject, and are referred to in the review.

(1) Prof. Thomas Blochowicz, Institut fur Festkorperphysik, TU-Darmstadt, 64289 Darmstadt, Germany, who have done the most extensive studies using different spectroscopies including neutron scattering. thomas.blochowicz@physik.tu-darmstadt.de

(2) Prof. George Floudas, University of Ioannina, Department of Physics, and Foundation for Research and Technology-Hellas (FORTH), gfloudas@uoi.gr

(3) G. Goulart Silva (glaura@lcc.ufmg.br).

(4) Prof. Osamu Urakawa, Department of Macromolecular Science, Osaka University, Toyonaka, Osaka 560-0043, Japan, urakawa@chem.sci.osaka-u.ac.jp

We did not have any publication with these researcher in publication. One exception is my collaboration with George Floudas, which was more than 30 years ago and when he was a graduate student.

Sincerely,

Journal of
Non-Crystalline Solids

Confirmation of Authorship

Please save a copy of this file, complete and upload as the "Confirmation of Authorship" file.

As corresponding author, I K.L. Ngai, hereby confirm on behalf of all authors that:

1. This manuscript has not been published, was not, and is not being submitted to any other journal. If presented at a conference, the conference is identified. If published in conference proceedings, substantial justification for re-publication must be presented.

2. All necessary permissions for publication were secured prior to submission of the manuscript.

3. All authors listed have made a significant contribution to the research reported and have read and approved the submitted manuscript, and furthermore, all those who made substantive contributions to this work have been included in the author list.

***Abstract**

By mixing a molecular or polymeric glass-former with another one, its dynamic and thermodynamic properties can be modified to various degrees depending on the composition. The study of the modifications is beneficial not only in basic research on glasses and glass transition but also in applications. When the difference in glass transition temperatures of the two components ΔT_g is not too large (less than 100 K), commonly observed in miscible mixtures is a single glass transition temperature coming from a single structural α-relaxation, which is accompanied by a Johari-Goldstein (JG) β-relaxation strongly connected in dynamic properties. Satisfactory explanation of the connected dynamics of the two relaxations and changes with composition have been given by the Coupling Model. The dynamics and thermodynamics in highly asymmetric mixtures (i.e., when ΔT_g is large) are more complex. Two α-relaxations (α1 and α2) and correspondingly two glass transitions temperatures ($T_g^{\alpha 1}$ and $T_g^{\alpha 2}$) were clearly identified at high and moderate values of c_2 of the lower-T_{g2} component. However, at low values of c_2, only the α1-relaxation and its glass transition at $T_g^{\alpha 1}$ were found together with a fast relaxation having approximately an Arrhenius temperature dependence for its relaxation time at low temperatures. There are two ways to interpret the data. One interpretation of the observed fast relaxation is the JG β-relaxation, and the α2-relaxation is not resolved due to low c_2. Some researchers interpretated the fast relaxation as the α2-relaxation, but its properties and the associated $T_g^{\alpha 2}$ are drastically modified at low c_2, and the JG β-relaxation is either unresolved or non-existent. They further proposed that the drastic modification of the α2-relaxation is due to confinement of the low-T_{g2} component by the frozen high-T_{g1} component. It is transformed to local relaxation within the confined spaces, and becomes identifiable with the observed fast relaxation having Arrhenius *T*-dependence. This view and interpretation of the dynamics of highly asymmetric mixtures and polymer blends are maintained to be valid up to the present

time. In this paper we review exhaustively the experimental data of many highly asymmetric mixtures and blends to show unequivocally that the observed fast relaxation is the JG β-relaxation and not the α2-relaxation. Notwithstanding, the α2-relaxation with its associated $T_g^{\alpha 2}$ is also present, albeit not easily resolved due to weak relaxation strength at low c_2. The value of $T_g^{\alpha 2}$ increases monotonically on decreasing c_2, without exhibiting a maximum as concluded by one group. The fast relaxation is demonstrated to be the JG β-relaxation from its connection to both the α1 and the α2 relaxations in its properties including the pressure dependence of its relaxation time. Established also is the significant increase of $T_g^{\alpha 2}$ with pressure, and hence also the relaxation time of the α2-relaxation, despite it is confined. Only experimental data are utilized in this review, and therefore the conclusions we arrived at are totally objective.

Molecular dynamic in binary mixtures and polymer blends with large difference in glass transition temperatures of the two components: a critical review

K.L. Ngai[a], Sofia Valenti[b] , S. Capaccioli[a,b]

[a]*CNR-IPCF, Largo Bruno Pontecorvo 3 ,I-56127, Pisa, Italy*

[b]*Dipartimento di Fisica, Università di Pisa, Largo Bruno Pontecorvo 3 ,I-56127, Pisa, Italy*

Abstract

By mixing a molecular or polymeric glass-former with another one, its dynamic and thermodynamic properties can be modified to various degrees depending on the composition. The study of the modifications is beneficial not only in basic research on glasses and glass transition but also in applications. When the difference in glass transition temperatures of the two components ΔT_g is not too large (less than 100 K), commonly observed in miscible mixtures is a single glass transition temperature coming from a single structural α-relaxation, which is accompanied by a Johari-Goldstein (JG) β-relaxation strongly connected in dynamic properties. Satisfactory explanation of the connected dynamics of the two relaxations and changes with composition have been given by the Coupling Model. The dynamics and thermodynamics in highly asymmetric mixtures (i.e., when ΔT_g is large) are more complex. Two α-relaxations (α1 and α2) and correspondingly two glass transitions temperatures ($T_g^{\alpha 1}$ and $T_g^{\alpha 2}$) were clearly identified at high and moderate values of c_2 of the lower-T_{g2} component. However, at low values of c_2, only the α1-relaxation and its glass transition at $T_g^{\alpha 1}$ were found together with a fast relaxation having approximately an Arrhenius temperature dependence for its relaxation time at

low temperatures. There are two ways to interpret the data. One interpretation of the observed fast relaxation is the JG β-relaxation, and the α2-relaxation is not resolved due to low c_2. Some researchers interpretated the fast relaxation as the α2-relaxation, but its properties and the associated $T_g^{\alpha 2}$ are drastically modified at low c_2, and the JG β-relaxation is either unresolved or non-existent. They further proposed that the drastic modification of the α2-relaxation is due to confinement of the low-T_{g2} component by the frozen high-T_{g1} component. It is transformed to local relaxation within the confined spaces, and becomes identifiable with the observed fast relaxation having Arrhenius *T*-dependence. This view and interpretation of the dynamics of highly asymmetric mixtures and polymer blends are maintained to be valid up to the present time. In this paper we review exhaustively the experimental data of many highly asymmetric mixtures and blends to show unequivocally that the observed fast relaxation is the JG β-relaxation and not the α2-relaxation. Notwithstanding, the α2-relaxation with its associated $T_g^{\alpha 2}$ is also present, albeit not easily resolved due to weak relaxation strength at low c_2. The value of $T_g^{\alpha 2}$ increases monotonically on decreasing c_2, without exhibiting a maximum as concluded by one group. The fast relaxation is demonstrated to be the JG β-relaxation from its connection to both the α1 and the α2 relaxations in its properties including the pressure dependence of its relaxation time. Established also is the significant increase of $T_g^{\alpha 2}$ with pressure, and hence also the relaxation time of the α2-relaxation, despite it is confined. Only experimental data are utilized in this review, and therefore the conclusions we arrived at are totally objective.

Corresponding author: kiangai@yahoo.com; kia.ngai@pi.ipcf.cnr.it

1. Introduction

The study of the dynamics of a component in binary mixtures of two glass-formers has been an active research effort in the past decades and continued till the present time [1-87].The binary systems studied include (1) molecular glass-former and polymer [1,6,29,79,84,85,88], (2) two amorphous polymers [2-5,7-28,30-67,80.86,87], and (3) two van der Waals molecular glass-formers [68-78,81-83,85],. One particular area of pursuit and the focus of this paper is the dynamics of the component having glass transition temperature T_{g2} lower than T_{g1} of the other component, and the changes with the composition of the mixture. Most spectacular change in the dynamics of the lower-T_g component was observed when its concentration c_2 is drastically reduced. Examples include mixtures of two van der Waals molecular glass-formers, where the difference in their glass transition temperatures, $\Delta T_g = T_{g1} - T_{g2}$, is not large and only one glass transition was observed in calorimetry or by dielectric spectroscopy [68-78]. In these cases, the relaxation time $\tau_{\alpha 2}$ and the frequency dispersion width of the structural α-relaxation of the lower-T_g compone nt both increase monotonically on decreasing c_2. At the same time, a secondary or β-relaxation with relaxation time τ_β emerges, which is not resolved in the lower-T_g component when in the pure state. The ratio $\tau_\beta/\tau_{\alpha 2}$ increases with decreasing c_2 for any fixed $\tau_{\alpha 2}$. Moreover, τ_β is not only pressure P dependent, but also the ratio $\tau_\beta(P,T)/\tau_{\alpha 2}(P,T)$ is invariant to variations of P and T while keeping τ_α constant. These properties shown for 10 wt% of quinaldine in tristyrene or PS370 [70,73] picoline in tristyrene [72] and 10 mole% of cyanobenzene in tristyrene [74] in Fig.1, as well as in neat glass-formers [89,90] and polymer [91], indicate the strong connection of the β-relaxation to the α-relaxation and its fundamental importance. It belongs to the special class of secondary relaxations with properties strongly connected to the α-

relaxation [92,93], which we called them the Johari-Goldstein β-relaxations. This choice of nomenclature turns out to be unwise because other researchers use the term, Johari-Goldstein relaxations [94,95], for all secondary relaxations without discrimination and distinction. The Johari-Goldstein β-relaxations belonging to the special class was found ubiquitous in neat glass-formers of various types [92,93,95-103].

The JG β-relaxation is the precursor of the cooperative structural α-relaxation in analogy to the primitive relaxation of the Coupling Model (CM), but need to be emphasized is that they are not the same process [92-103]. The primitive relaxation is an independent relaxation of individual molecules, or repeat units in the case of polymers, having correlation function exp(-t/τ_0). On the other hand, the JG β-relaxation is composed of a distribution of processes. Increasing number of molecules participate in the processes with longer relaxation times and larger length-scales, and the primitive relaxation of the model is the precursor [92,93,98-102]. Thus, the experimentally deduced most probable value of τ_β is expected to be in *approximate* agreement with the primitive relaxation time τ_0, and this is conveyed symbolically by $\tau_\beta(P,T) \approx \tau_0(P,T)$. The CM relates τ_0 to the α-relaxation time τ_α by the equation [80,97,104-109],

$$\tau_0(P,T) = (t_c)^n[\tau_\alpha(P,T)]^{1-n}, \quad (1)$$

where (1-n)≡β_{KWW} is the fractional exponent of the Kohlrausch correlation function, $\phi(t) = \exp[-(t/\tau_\alpha)^{1-n}]$, of the α-relaxation, and t_c=1 to 2 ps for polymers and van der Waals molecular glass-formers determined by quasielastic neutron scattering [28,51,52,80,110,111]. Thus one way to verify that the secondary relaxation in mixtures is the JG β-relaxation is to calculate $\tau_0(P,T)$ by Eq.(1) and show that it is about the same as the experimental $\tau_\beta(P,T)$. In other words, we need to verify the approximate relation,

$$\tau_\beta(P,T) \approx (t_c)^n[\tau_\alpha(P,T)]^{1-n}. \quad (2)$$

This was indeed verified in several mixtures, all having ΔT_g = T_{g1} - T_{g2} not large [70-76,80]. Examples are shown in Fig.1 by the approximate agreement between the corresponding frequencies $f_\beta(P,T)$ and $f_0(P,T) = 1/(2\pi\tau_\beta(P,T))$ in the two mixtures.

A different scenario for the dynamics presents itself in highly asymmetric binary mixtures [29,77-79,81-85,87,103] and polymer blends [20-28,31,32,39-52,54-66] where the difference in the glass transition temperatures, ΔT_g = T_{g1} - T_{g2}, is large. If the concentration c_2 of the low-T_g component is not low, each component generates its own cooperative α-relaxation. The results are the α1-relaxation with a shorter $\tau_{\alpha 1}(T)$ and a lower $T_g^{\alpha 1}$ than the pure higher-T_{g1} component determined mainly by the higher-T_{g1} component, and the α2-relaxation with a longer $\tau_{\alpha 2}(T)$ and a higher $T_g^{\alpha 2}$ than the pure lower-T_{g1} component dominated by the low-T_{g2} component. The temperature dependences of $\tau_{\alpha 1}(T)$ and $\tau_{\alpha 2}(T)$ are of the Vogel-Fulcher-Tammann kind, and $T_g^{\alpha 1}$ and $T_g^{\alpha 2}$ both increase monotonically with decrease of c_2. Coexisting with the α1-relaxation and α2-relaxation are possible secondary relaxation originating from intramolecular degree of freedom in the molecule of either one of the components [77-79,81,103,], and the supposedly ubiquitous Johari-Goldstein (JG) β-relaxation like that seen before in mixtures with smaller ΔT_g [68-79].

However, a different scenario presents itself when c_2 is low. The predominant higher-T_{g1} component is expected to contribute principally to a structural α1-relaxation of the mixture. Its relaxation times $\tau_{\alpha 1}$ increases with falling temperature and the molecules contributing to the α1-relaxation becomes vitrified at some $T_g^{\alpha 1}$ lower than T_{g1}. At temperatures below $T_g^{\alpha 1}$, cooperative motion is arrested because of very long $\tau_{\alpha 1}$. There are two proposed dynamics of the low-T_{g2} component. One is by Lorthioir, Alegria and Colmenero (LAC) [24,25] based on their dielectric

study of polystyrene-poly(vinyl methyl ether) (PS-PVME) blends. At temperatures below $T_g^{\alpha 1}$ they envisaged the low-T_{g2} PVME component are completely surrounded by the frozen PS chains, and thus the α' or $\alpha 2$ of the low-T_{g2} PVME component occurs in a confined environment, and they proposed the confinement induces a speeding up of the PVME dynamics. This relaxation is attributed to rather localized, weakly cooperative PVME motions resulting from the topological constraints imposed by the frozen PS chains [58]. Kahlau et al. and Bock et al. (B&K) proposed similar dynamics of the low-T_{g2} component based on the combined dielectric [81,83] and ^{2}H and ^{31}P nuclear magnetic resonance (NMR) [82,83] studies of tripropyl phosphate (TPP) mixtures with polystyrene (PS). The authors [81-83] proposed that "two fractions of TPP molecules are identified, one joining the glass transition of PS in the mixture ($a1$-process), the second reorienting isotropically ($a2$-process) even in the rigid matrix of PS, although at low concentration resembling a secondary process regarding its manifestation in the DS spectra."; and "the mobile low-T_g component still performs liquid-like dynamics within the matrix of the more or less immobilized high-T_g component.". It is important to recognize that the process of the low-T_g component, α'-relaxation of LAC and the $\alpha 2$-relaxation of K&B are nevertheless different, even though both emphasize confinement by the frozen or rigid high-T_{g1} component PS. The α'-relaxation of LAC is localized and non-cooperative. The $\alpha 2$-relaxation of B&K is liquid-like, isotropic, and cooperative, but the amplitude of the motion is highly restricted. The change of entropy and free volume with temperature is suppressed in the highly restricted (or confined) cooperative $\alpha 2$-relaxation, and consequently $\tau_{\alpha 2}$ has Arrhenius temperature dependence or close to Arrhenius over a range of low temperature when c_2 is low. The Arrhenius T-dependence of the confined $\tau_{\alpha 2}$ resembles that of the relaxation time of the ubiquitous Johari-Goldstein (JG) β-relaxation, and this common property can lead to the mistake of identifying the

JG β-relaxation as the confined α2-relaxation if the former was resolved and observed but not the latter, possibly in the cases of LAC and B&K. This mistake can be discerned by the fact that the activation energy E_β of the JG β-relaxation is usually no more than 30 times the glass transition temperature [112], while the activation energy $E_{\alpha 2}$ of the confined but cooperative α2-relaxation is much larger as shown from the data of experiments later. The Arrhenius-like *T*-dependence of $\tau_{\alpha 2}$ was not recognized by us earlier in considering the highly asymmetric 20%PEO/80%PMMA blend [80], where our focus was not on the confined α2-relaxation. Confined by the frozen PMMA chains, the α2-relaxation of the PEO component cannot experience the change of density and entropy with temperature of normal α-relaxation in equilibrium liquid. Thus the *T*-dependence of $\tau_{\alpha 2}$ is Arrhenius, and the use in Ref.[80] by us of a Vogel-Fulcher-Tammann (VFT) temperature dependence to interpolate the short PEO deuterium NMR $\tau_{\alpha 2} < 10^{-8}$ s [27,28] and the enthalpy relaxation time $\tau_{\alpha 2}$=100 s at $T_g^{\alpha 2}$obtained by DSC [39] is not appropriate. This mistake is rectified when we reconsider this blend in Section 2.2 later, where the VFT dependence of $\tau_{\alpha 2}(T)$ at high temperatures is replaced by an Arrhenius dependence at lower temperatures, which takes $\tau_{\alpha 2}$ to reach 100 s at $T_g^{\alpha 2}$.

None of the proposals of confined α2-relaxation by LAC [24,25] and B&K [81-83] considered the presence of the Johari-Goldstein (JG) β-relaxation which is known to have strong ties to the α-relaxation, and supposed to be ubiquitous [92-103]. Instead mentioned or discussed are the unimportant intramolecular secondary relaxation in PVME [24,25] and in TPP [81-83]. Both $\tau_{\alpha'}$ of the confined and local α′ relaxation of PVME in 10-30% PVME mixtures with PS, and $\tau_{\alpha 2}$ of the restricted but still cooperative α2-relaxation of the 8, 10, 18 and 20% TPP mixtures with PS, are expected respectively by LAC and B&K to have Arrhenius-like *T*-

dependence, like the τ_β of the JG β-relaxation. Because of the similar *T*-dependence, LAC mistakenly identified the actually observed JG β-relaxation as their α′-relaxation, which was not resolved. The α2 process of the 8, 10, 18 and 20% TPP mixtures also was not resolved and for the same reason B&K mistakenly identified the resolved JG β-relaxation as their α2 process. The difficulty of resolving the confined α2-relaxation is because it lies in between the α1-relaxation and the intense JG β-relaxation [81-83], and it has low relaxation strength due to its highly restricted motion and the low values of c_2. The mistake of B&K was confirmed by the work of Valenti et al. [87], where the α2-relaxation in 20%TPP mixture with PS was identified to be the JG β-relaxation by its relation to the α1-relaxation from various properties such as the pressure *P* dependence of its relaxation time τ_β, the invariance of the ratio $\tau_{\alpha1}/\tau_\beta$ to variations of *P* and *T*,and the approximate agreement between τ_β and the primitive relaxation time τ_0 of the Coupling Model [87].

The mistakes of identifying the JG β-relaxation as the assumed localized α′ relaxation of PVME in 10-30% PVME mixtures with PS by LAC [24,25] in 2003 could have been recognized immediately by LAC had they taken into consideration of the detection of $T_g^{\alpha2}$=293 K in the 20% PVME blend by the thermally stimulated depolarization current (TSDC) technique by Leroy et al. in 2002 [26]. The TSDC result assures at least some of the PVME are contributing to the α2-relaxation with relaxation time of the order of 100 s at $T_g^{\alpha2}$=293 K. It contradicts the interpretation of LAC that *all* PVME are confined by the frozen PS chains and have relaxation time of about 10^{-4} s at $T_g^{\alpha2}$=293 K. This contradiction originates from the mistake made by LAC of identifying the resolved JG β-relaxation time as $\tau_{\alpha2}$ of the unresolved confined α2-relaxation. Unfortunately this obvious contradiction has not changed LAC in interpreting their data since the

same interpretation is maintained in other papers [45-47,55,56] and in more recent reviews [58,86]. Such persistent interpretation may have led others including the authors of Refs.[81-84] to mistakenly identify the JG β-relaxation in the case of the 8-20% TPP mixtures with PS as the confined α2-relaxation, and the additional wrong conclusion that $T_g^{\alpha 2}$ does not continue the monotonic increase with decrease of c_2 found at higher values of c_2. Instead $T_g^{\alpha 2}$ reaches a maximum at some low value of $c_2 \approx 0.35$, and decrease on further decrease of c_2. This result is false because the JG β glass transition temperature $T_{g\beta}$ obtained by extrapolating the Arrhenius temperature dependence of τ_β to 100 s was wrongly taken as $T_g^{\alpha 2}$ for c_2 lower than 0.3. Efforts were made by us in 2013 [80] and 2018 [87] to demonstrate by experimental evidences and theoretical considerations that the JG β-relaxation was mistaken as either the local α′-relaxation in the blends of PVME with PS [24,25] or the restricted α2-relaxation in mixtures of TPP with PS [81-83]. Furthermore, new dielectric measurements by Valenti et al. [87] on 20% TPP/80%PS mixture at elevated pressures and compared with NMR data have shown unequivocally that the purported α2-relaxation is the JG β-relaxation. Hence proven wrong is the conclusion of $T_g^{\alpha 2}$ exhibiting a maximum at c_2=0.35 in the mixtures of TPP with PS. Notwithstanding, in a chapter of a book published in 2018, Bock et al. [85] acknowledged the publication of the paper by Valenti et al. but avoided mentioning or addressing the experimental evidences given therein. Instead, they reaffirmed their interpretation by reproducing the figure showing the existence of a maximum of the purported $T_g^{\alpha 2}$ as a function of c_2 of TPP in the mixtures with PS. In addition, to bolster the commitment to their interpretation, they show a similar figure from the mixture of *m*-tricresyl phosphate (*m*-TCP) with a nonpolymeric high-T_g glass formers DH based on spirobichroman derivatives in a paper published by Pötzschner et al. [84], which was not addressed in the paper by Valenti et al. The dielectric data and the

interpretation of Pötzschner et al. as confined α2-relaxation was made use by Alegria and Colmenero in a 2016 review [86] to support the interpretation by LAC [24,25] of a faster relaxation with Arrhenius *T*-dependence in the PVME/PS with $c_2 \leq 30\%$ as confined α2-relaxation, which we had shown that it is actually the JG β-relaxation [80]. It is disconcerting that Alegria and Colmenero had not so far responded to the experimental evidences and theoretical considerations we gave in ref.[80] to refute the interpretation of LAC. Instead they cited the meager data from Pötzschner et al.[84] for support, which we shall discuss later and show they made the same mistake of identifying the resolved JG β-relaxation as the confined α2-relaxation..

From the discussions in the above, it is clear that the controversy in the interpretation of the relaxation processes in highly asymmetric binary mixtures with low concentration c_2 of the low-T_g component remains unresolved since 2003. It calls for comprehensive, in-depth, and critical investigation into the experimental facts to uncover the true interpretation of the dynamics and to resolve the controversy once and for all. This is the objective of this paper. The first task is to demonstrate that the faster process with Arrhenius *T*-dependence identified by LAC and Pötzschner et al. as the confined α2-relaxation is actually and truly the JG β-relaxation. This will be accomplished by providing multiple and indisputable experimental evidences combined with theoretical considerations. The second task is to uncover the true confined but cooperative α2-relaxation detectable by conventional DSC, temperature-modulated DSC (TMDSC) or thermally stimulated depolarization current (TSDC) in some mixtures and blends despite it has weak relaxation strength and sandwiched between the α1-relaxation and the JG β-relaxation, and show it does exist and reveal its properties. The third and final task is to reassert the universal presence of the JG β-relaxation and revive its fundamental importance by showing

the various strong connections in properties it has with the α1-relaxation as well as with the confined and still cooperative α2-relaxation. We deem our genuine effort and the materials presented in this review either settle the controversy or deserve conscientious response from others if they still maintain their own interpretations.

Another way and perhaps the best to settle the controversy is to invoke direct evidences of the coexistence of the confined α2-relaxation and the JG β-relaxation together with the undisputed α1-relaxation from experiments in highly asymmetric mixtures and polymer blend. It would be ideal if the thermodynamics and dynamic properties of all three processes and the relations between them are characterized in the experimental results, as well as the determination of the two glass transition temperatures, $T_g^{\alpha 1}$ and $T_g^{\alpha 2}$. These facts can be used to unequivocally identify the processes in the mixtures and polymer blends, particularly in those cases where the confined α2-relaxation was not resolved and mistaken as the resolved JG β-relaxation [24,25,45-47,56,81-86]. Fortunately, such experiments had been performed by Blochowicz and coworkers and reported in a series of studies of either methyltetrahydrofuran or tetrahydrofuran in mixtures with tristyrene [77], polystyrene [79], oligo-PMMA [78]. Their results are presented first in the next section to pave the way in resolving the controversy in the interpretation of the other mixtures [81-85] and polymer blends [24,25,45-47,56,86].

2. Evidences of coexistence of confined α2-relaxation, α1-relaxation, and JG β-relaxation

Examples of highly asymmetric mixtures and polymer blends are taken from the literature to show coexistence of the confined α2-relaxation, the α1-relaxation, and the JG β-relaxation, and the two glass transition temperatures $T_g^{\alpha 2}$ and $T_g^{\alpha 1}$. This expose should make easier for us to

demonstrate convincingly the mistake made by others [24,25,81-84] in identifying the resolved JG β-relaxation as the confined α2-relaxation in the next section.

2.1 Highly asymmetric mixtures

(A) MTHF and THF in tristyrene

For highly asymmetric mixtures, the examples are taken from the comprehensive studies of methyltetrahydrofuran (MTHF, T_{g2}=90K) or tetrahydrofuran (THF) with tristyrene (T_{g1} =233 K) [77,78] as well as MTHF with polystyrene having M_w=60 000 g/mol (PS60k, T_{g1}=373 K) [79] by Blochowicz and coworkers using a variety of experimental techniques including dielectric spectroscopy, differential scanning calorimetry, ^{2}H nuclear magnetic resonance, depolarized dynamic light scattering, and incoherent quasielastic neutron scattering, which enable selectively probing the dynamics of the components over broad range of time or frequency.

Present in dielectric spectra of the mixtures of MTHF with tristyrene [77] are two secondary relaxations, β and δ. The slower β-relaxation was identified as the JG β-relaxation [103] with relaxation times $\tau_\beta(T)$ weakly dependent on concentration c_2 of MTHF ranging from 70% down to 6% and having an activation energy of about 3000 K. This is an interesting property of the JG β-relaxation in mixtures, which seems general as shown later on in mixtures of TPP with PS [81-85] and blends of PVME with PS [24,25,80]. The data of $\tau_\beta(T)$ plotted against reciprocal temperature are shown in Fig.2. The dashed lines emanating from the $\tau_\beta(T)$ data are the primitive relaxation times, τ_0, calculated from the α-relaxation times of the α1-process $\tau_{\alpha 1}$ at c_2 = 8%, 12%, 50% and 70% with coupling parameters n given in the figure. The α2- or α′-relaxation were resolved in the dielectric spectra times of mixtures with c_2 = 6%, 12%, 25%, 40% and 50%. The $\tau_{\alpha 2}$ or $\tau_{\alpha'}$ are represented by closed dark grey symbols lying close to the grey dashed line: inverted triangles (6% MTHF), diamonds (12% MTHF), and circles (50%

MTHF). Evidently the data of $\tau_{\alpha 2}$ or $\tau_{\alpha'}$ are limited and are much shorter than 100 s in any of the three cases of c_2= 6%, 12%, and 25% to allow determination of the dielectric $T_g^{\alpha 2}(c_2)$ without large uncertainty by extrapolating the assumed Arrhenius *T*-dependence of $\tau_{\alpha'}$ to 100 s. Nevertheless this was done by the authors of Ref.[77], and the results of the dielectric $T_g^{\alpha 2}$ shows very small increase on decreasing c_2 from 50% down to 12%. However there is a small decrease of $T_g^{\alpha 2}$ from c_2=12% to 6%. The mini 'maximum' at 12% should not be taken seriously due to scarcity of $\tau_{\alpha'}$ data and since error estimates were not given.

We do not follow Blochowicz et al. in drawing a line to represent the common Arrhenius dependence of $\tau_{\alpha'}$ for mixtures with different c_2 and extrapolate it to reach 100 s to determine $T_g^{\alpha 2}(c_2)$. For details, see Fig.3 in Ref.[77] or Fig.S3 in Supplementary Information (SI). This is because the data are too meagre to support that $\tau_{\alpha'}$ or $\tau_{\alpha 2}(T)$ as well as $T_{g\alpha 2}(c_2)$ is independent of c_2. Despite the uncertainty of the Arrhenius *T*-dependence of $\tau_{\alpha'}$, it can be seen from Fig.2 that $E_{\alpha 2}$ for any c_2 is much larger than E_β of the JG β-relaxation, as it should be.

On the other hand, $\tau_{\alpha'}$ deduced from DSC increases with decreasing c_2 from 50% down to 25%, but decrease slightly at c_2 =12%. Unfortunately the DSC data for c_2 =12% were not presented, and there is no way to judge the value of the DSC $\tau_{\alpha'}$ reported. The analysis of the 25% DSC data and error estimate were not given either to judge the DSC $\tau_{\alpha'}$ reported. By no means we are implying that Blochowicz and coworkers advocated the existence of a maximum in $T_g^{\alpha 2}$. In fact they drew a line through the data points in their Fig.4 in Ref. [77] and reproduced as Fig.S1 in SI, and also in Fig.1 in ref.[79] or Fig.S2 in SI suggesting monotonic increase with decrease of c_2. The purpose of this discussion is to preempt others to use the data as support of presence of maximum in mixtures of MTHF with tristyrene.

Blochowicz and coworkers also studied the mixtures of tetrahydrofuran (THF) with tristyrene at three c_2 =33%, 20% and 10% by dielectric spectroscopy and observe all four relaxation, α1, α2 or α′, β, and δ as in the mixtures of MTHF with tristryene. From the relaxation times of α1, α2, and β relaxations reported in separate figures in Ref.[78], we have combined the data of $\tau_{\alpha 2}$, τ_{β}, $T_g^{\alpha 1}$ and $T_g^{\alpha 2}$ in one Fig.3 here. Values of $\tau_{\alpha 2}(T)$ or $\tau_{\alpha'}(T)$ determined in the experiments have Arrhenius *T*-dependence of confined α2-relaxation for all three THF mixtures, and its concentration dependence in the THF mixtures is much clearer than from the data of the MTHF mixtures shown before in Fig.2. The activation energy $E_{\alpha 2}$ of $\tau_{\alpha 2}(T)$ for any c_2 in Fig.3 is larger than E_{β} of the JG β-relaxation.

By extrapolating the Arrhenius T-dependence of $\tau_{\alpha'}(T)$ to 100 s, the $T_g^{\alpha 2}$ of the three mixtures are determined. The $T_g^{\alpha 1}$ were determined before in Ref.[78] from the VFT-dependence of $\tau_{\alpha 1}(T)$ as the temperature at which $\tau_{\alpha 1}(T)$=100 s. The dependences of $T_g^{\alpha 2}$ and $T_g^{\alpha 1}$ on c_2, the concentration of THF, are presented in the lower panel of Fig.3 to show the monotonic increase of $T_g^{\alpha 2}$ with decrease of c_2. The coexistence of the α1-relaxation, the confined α2-relaxation, and the JG β-relaxation in the THF mixtures is clearer than in the MTHF mixtures. There is no doubt from the data of this highly asymmetric mixture that $T_g^{\alpha 2}$ does not exhibit a maximum at some low value of c_2.

(B) 50%MTHF in PS60k

Replacing tristyrene by PS60K (polystyrene with M_w= 60 kDa) the difference $\Delta T_g = T_{g1} - T_{g2}$ is increased from 143 K to 283 K, and consequently increased is the difference, $T_g^{\alpha 1}(c_2) - T_g^{\alpha 2}(c_2)$, and more separated is the α′- or α2-relaxation from the α1-relaxation to make it easier to

resolve. This trend can be seen by comparing the relaxation times $\tau_{\alpha 2}(T)$, $\tau_{\alpha 2}(T)$, and $\tau_{\beta}(T)$ of the MTHF-3styrene mixtures in Fig.2 with the MTHF-PS60K mixtures in the left panel of Fig.4 for c_2=50%. The coexistence of the JG β-relaxation and the confined α2-relaxation with $\tau_{\alpha 2}(T)$ having Arrhenius *T*-dependence is clear. Not pointed out before in Ref.[103] is the change of temperature dependence of $\tau_{\beta}(T)$ on crossing some temperature in the neighborhood of $T_g^{\alpha 2}$ determined by either DSC (thinner vertical dashed line) or dielectrically (thicker vertical dashed line) from the definition, $\tau_{\beta}(T_g^{\alpha 2})$=100 s. Brought out by the red full line and black dashed lines with different slopes in Fig.4, the crossover in temperature dependence of $\tau_{\beta}(T)$ at $T_g^{\alpha 2}$ is proof of that the β-relaxation is the JG β-relaxation as usually found in binary mixtures of rigid dielectric probes [70, 72]. The separation of $\tau_{\alpha 2}(T)$ from $\tau_{\beta}(T)$ measured by the length of either one of the two vertical dashed lines is consistent with that calculated from the CM Eq.(2) for a value of *n* of 0.44. These properties indicate the α2-relaxation is a genuine cooperative α-relaxation detected by DSC (see upper inset in Fig.S2), and connected to the JG β-relaxation by the CM Eq.(2) like in single component glass-formers [92,93,96-102]. Thus the α2-relaxation of the low-T_g component MTHF still performs liquid-like dynamics despite being confined within the matrix of the immobilized high-T_g component PS60K. Not too far above $T_g^{\alpha 2}$, the temperature dependence of $\tau_{\alpha 2}(T)$ is Arrhenius as well as that of $\tau_{\beta}(T)$. It is evident from Fig.4 that the activation energy $E_{\alpha 2}$ of $\tau_{\alpha 2}(T)$ is a few times larger than E_{β} of $\tau_{\beta}(T)$. The much larger size of $E_{\alpha 2}$ than E_{β} can be used to identify the JG β-relaxation and not to mistaken it as the confined α2-relaxation, especially in cases where the latter was not resolved [24,25,81-85]. It can be seen by inspection of the spectra in the upper right panel of Fig.4 that the dielectric strength $\Delta\varepsilon_{\alpha 2}(T)$ of the confined α2-relaxation increases with decrease of temperature according to the Curie-Weiss

law, while the opposite trend is shown by $\Delta\varepsilon_\beta(T)$ of the JG β-relaxation. Again, the contrasting *T*-dependences of the dielectric strength is another simple way to distinguish the two relaxations.

At higher temperatures, the short relaxation times represented in Fig.4 by closed red circles were measured by quasielastic neutron scattering. Considered together with the dielectric $\tau_{\alpha 2}(T)$ and $\tau_\beta(T)$, these neutron scattering data suggest the α2-relaxation has already merged with the JG β-relaxation, and hence the relaxation times $\tau_{\alpha 2}(T)$ are identifiable with $\tau_\beta(T)$. The dielectric frequency dispersions of the α1-relaxation measured at 190 and 200 K were fitted by the Fourier transform of the Kohlrausch function to determine the values of n=0.77 and 0.75 respectively in the right lower panel of Fig.4. The corresponding primitive relaxation times $\tau_0(T)$ calculated by Eq.(2) with these n values and $\tau_{\alpha 1}(T)$ are shown by the two black triangles in left panel, and they are in approximate agreement with $\tau_\beta(T)$. This result shows the relaxation times of the JG β-relaxation and the slowest α1-relaxation are also related by Eq.(2), in accord with the CM prediction.

It is remarkable that Blochowicz et al. had been able to detect the α2-relaxation and determine $\tau_{\alpha 2}(T)$ over 15 decades from 10^4 to 10^{-11} s by the combinations of DSC, dielectric relaxation, and neutron scattering. Their data in Fig.4 indicate the α2-relaxation has merged with the JG β-relaxation at higher temperatures, and there the short relaxation times $\tau_{\alpha 2}(T)$ probed by neutron scattering become $\tau_\beta(T)$. This is the reason why the temperature dependence of $\tau_{\alpha 2}(T)$ is so weak in the range $10^{-11} < \tau_{\alpha 2}(T) < 10^{-9}$ s, and different from the stronger Arrhenius *T*-dependence of $\tau_{\alpha 2}(T)$ observed at longer times down to 10^3 s at temperature lower than $T_g^{\alpha 2}$ from DSC of the truly confined α2-relaxation. By contrast, dielectric data of $\tau_{\alpha 2}(T)$ at long times and the DSC $T_g^{\alpha 2}$ were absent in the neutron scattering studies of three highly asymmetric polymer

blends of 25%PEO in poly(meth methacrylate) (PMMA) ($T_{g\mathrm{PEO}}$=220 K, $T_{g\mathrm{PMMA}}$=400 K) by Genix et al. [45], 20%PEO in poly(vinylacetate) (PVAc) (T_{gPEO} =220 K, T_{gPVAc} =315 K) by Tyagi et al. [46,56], and 25%PEO in polyethersulfone (PES) ($T_{g\mathrm{PEO}}$=220 K, $T_{g\mathrm{PES}}$=382 K) by Genix et al. [47]. The neutron data of $\tau_{\alpha 2}(T)$ from PEO in the three blends with PMMA, PVAc, and PES have $\tau_{\alpha 2}(T)$ shorter than $10^{-9.5}$ s, and with weak temperature dependence like that of the neutron scattering $\tau_{\alpha 2}(T)$ in 50%MTHF in PS60k in Fig.4, which we had identified with $\tau_{\beta}(T)$. Without the benefit of this knowledge possible only from more complete set of data such as those of Blochowicz and coworkers, the authors of the neutron scattering studies of the three polymer blends [45-47] interpreted the neutron $\tau_{\alpha 2}(T)$ data of PEO component as confinement by the rigid environments. In fact they stated explicitly in Ref.[46] for $\tau_{\alpha 2}(T)$ of 20%PEO in PVAc by the statement: "The activation energy of the confined motions is of about 0.26 eV, much lower than those shown by the secondary relaxations in this system. Thus, the observed phenomenon cannot be identified with those processes.". This interpretation is questionable because the neutron $\tau_{\alpha 2}(T)$ were taken at temperatures above and slightly below $T_g^{\alpha 1}$ where the high-T_{g1} component is at or near equilibrium respectively and is not hard frozen (see Fig.S4). Moreover, by extrapolating the Arrhenius temperature dependence of the $\tau_{\alpha 2}(T)$ from neutron scattering with its activation energy of 0.26 eV to lower temperatures, its value is many orders of magnitude shorter than the value of $\tau_{\alpha 2}(T)$ at the viscoelastic $T_g^{\alpha 2}$ of 245 ± 5 K determined by Urakawa et al. in the same blend [113]. The same interpretation of confined α2-relaxation based on the neutron $\tau_{\alpha 2}$(T) with Arrhenius *T*-dependence of 25%PEO in PMMA [45] is contradicted by the observation of the calorimetric $T_g^{\alpha 2}$ by several groups [16,39,54]. Moreover, as shown before for the mixture of 50%MTHF in PS60k in Fig.4, the neutron $\tau_{\alpha 2}(T)$ has merged with and becomes the JG relaxation time $\tau_{\beta}(T)$, supported by finding that $\tau_{\beta}(T)$ is the same as the primitive

relaxation time $\tau_0(T)$. Therefore, the short $\tau_{\alpha 2}(T)$ from neutron scattering of 25%PEO in PVAc, PMMA, and PES is not associated with the confined α2-relaxation and cannot be interpreted as such in Refs.[45-47,56] and in the review [58].

High frequency deuteron NMR experiments have found that segmental relaxation times, $\tau_{\alpha 2}$, in the range, $-8.5 \geq \log(\tau_{\alpha 2}/\mathrm{s}) \geq -11.5$, of the fast PEO component in blends with PMMA are nearly independent of composition for blends from 3 to 30% d_4PEO over the wide temperature regime studied, and $\tau_{\alpha 2}$ is hardly influenced by the presence of the PMMA [23,27,28]. Shown in Fig.S6 of SI, the result holds for a wide range of temperatures extending to well below the glass transition of the PMMA matrix, where the segmental relaxation times of PMMA are about 12 orders of magnitude longer than $\tau_{\alpha 2}$ of PEO. Similar behavior is observed by deuteron NMR in PEO blends with PVAc (polyvinyl acetate) [59]. In the range $-9 \geq \log(\tau_{\alpha 2}/\mathrm{s}) \geq -11.8$, the $\tau_{\alpha 2}$ of PEO in 2% PEO blend differs little from that in 50% PEO and 100%PEO blends by about half a decade and one decade respectively. The effect seems general, not only found in highly asymmetric polymer blends but also in all blends [80]. For instance, the same effect was found by quasielastic neutron scattering (QENS) in the PEO/PMMA blends by Sakai et al. [51,52]. The explanation was given by the CM in Refs.[28,80], and the details will be given later in the section on polymer blends.

In the neutron scattering study of the blend of 25% of PEO in PES [47], Genix et al. pointed out that the PEO neutron $\tau_{\alpha 2}(T)$ seem to approach, within the experimental uncertainties, the extrapolation of the timescales obtained for the secondary γ-relaxation in semicrystalline PEO or the β′-relaxation in 10 and 20%PEO in PMMA as shown in their Fig.6 [47] or Fig.S5 in SI. By this they implied that the confined motion of PEO in the blend could correspond to those involved in the γ-relaxation of PEO. Although they said that this is a question that deserves

further work, they reasserted the belief by saying: "Apparently, PES provides an environment for PEO which seems to be effectively very similar to its own, and therefore the confined motion shows the features of the secondary process in the pure polymer. We emphasize that this is not the regular case, as demonstrated for PEO in PEO/PMMA,[18] and PEO/PVAc.[21]". This belief is incompatible with the confined α2-relaxation time $\tau_{\alpha 2}(T)$ have much larger Arrhenius activation energy $E_{\alpha 2}$ than E_β of the JG β-relaxation in mixtures of MTHF with either tristyrene or PS60k shown in Figs.2 and 4, and also in the mixture of MTHF with oligo-PMMA to be presented next.

(C) 40%MTHF/oligo MMA

There is yet another detailed study of the structure and dynamics mixture of MTHF with oligomeric methyl metacrylate (MMA) with a large difference of 249 K between T_{g1}=340 K and T_{g2}=91 K of the pure components by Schramm et al. [78]. Although the study was principally on concentration fluctuations in the mixture of 40%MTHF/oligo MMA by photon correlation spectroscopy, available also are DSC and dielectric measurements collected together in Fig.5. The DSC measurements show two clearly separated glass transitions, $T_g^{\alpha 2}$ =129.1 K and $T_g^{\alpha 1}$ = 245.1 K. There are two widely separated α (or α1) and α′ (or α2)) relaxations in the isothermal dielectric spectra associated with the $T_g^{\alpha 1}$ and $T_g^{\alpha 2}$ respectively, as well as a faster β-relaxation. Since the three processes found in 40%MTHF/oligo MMA can be similar to those in 50%MTHF/PS60K, we compare their dielectric and DSC relaxation times in Fig.6. The temperature dependence of the α′-relaxation times, $\tau_{\alpha'}(T)$ or $\tau_{\alpha 2}(T)$, is Arrhenius in both mixtures. The relaxation times $\tau_\beta(T)$ of the β-relaxation in 40%MTHF/oligo MMA are approximately the same as $\tau_\beta(T)$ in 50%MTHF/PS60K, and thus it is identified as the JG β-relaxation. Another evidence for this is a change of temperature dependence of $\tau_\beta(T)$ near the $T_g^{\alpha 2}$ from either DSC

or dielectric relaxation (green symbols and lines) as shown in Fig.6 and found before in 50%MTHF/PS60K (Fig.4) and shown again for comparison. The dielectric strength $\Delta\varepsilon_{\alpha 2}(T)$ of the confined α2-relaxation in 40%MTHF/oligo MMA increases with decrease of temperature obeying the Curie law of cooperative α-relaxation, while the opposite trend is shown by $\Delta\varepsilon_{\beta}(T)$ which is the characteristic of JG β-relaxation (see left panel of Fig.5).

By considering the relaxation strength of the α′- and β-process at low temperatures, Schramm et al. deduced that apparently not all MTHF molecules in the mixture participate in the fast α′-relaxation. Thus MTHF takes part in both α- and α′-relaxations, as it is found to be the case for MTHF in other binary mixtures. [77], and by NMR in 20%TPP/PS mixture [82,83].

(D) Concentrated toluene solutions of polystyrene

Taniguchi et al. measured the heat capacity C_p on concentrated toluene solutions of polystyrene (PS) using the high precision adiabatic calorimeter [29]. The PS has M_w=7.5×10^5 and polydispersity index of 1.10, and T_{g1}=373 K, while toluene has T_{g2}=117 K [88] and $\Delta T_g = T_{g1} - T_{g2}$ = 256 K. The compositions of the solutions ranges from 20%PS to 70% PS. The C_p curves of PS/toluene solutions exhibit a double-sigmoidal shape. After subtracting the heat capacity due to the lattice vibrations and intramolecular vibrations, the configurational ΔC_p was resolved into two sigmoidal curves. The glass transition temperatures $T_g^{\alpha 1}$ and $T_g^{\alpha 2}$ corresponding to the two sigmoids agree with the dielectric glass transition temperatures, which are defined as the temperatures at which the dielectric relaxation frequencies for the α1 and $\alpha 2$ processes of the PS/toluene systems reaches 10^{-4} Hz. For the 50% PS mixture, $T_g^{\alpha 1}$= 188 K (189 K) and $T_g^{\alpha 2}$=143 K (139 K), where the values not bracketed and in brackets are from adiabatic calorimetry and dielectric relaxation respectively. For the 70% PS mixture, $T_g^{\alpha 1}$= 230 K (243 K) and $T_g^{\alpha 2}$=145 K

(143 K). Thus the PS/toluene systems provide another example of the presence of α1 and $\alpha 2$ processes in highly asymmetric mixtures. The DSC data of the 50 and 70% PS mixtures are shown in Fig.S7 of SI.

Taniguchi et al. also observed a secondary relaxation in the PS/toluene mixtures in their isochronal dielectric loss spectra, in addition to the α1 and $\alpha 2$ relaxations. We found the data from the isochronal loss peak temperature T_f at frequency f in the 20%-50% PS solutions are matching the isothermal JG β-relaxation times $\tau_\beta(T)$ of toluene in order of magnitude to [88]. Therefore the JG β-relaxation coexists with the α1 and $\alpha 2$ relaxations in the PS/toluene mixtures like the THF mixtures with tristyrene, and MTHF mixtures with tristyrene, PS60K, and oligo-PMMA.

3. The JG β-relaxation mistaken as the unresolved confined α2-relaxation

The highly asymmetric mixtures of MTHF or THF in tristyrene, MTHF in PS60k or oligo-PMMA, and concentrated solutions of polystyrene in toluene with large ΔT_g discussed in Section 2 have all the three processes resolved and observed by various spectroscopies, and their properties revealed. The three processes are the α1-relaxation, the JG β-relaxation, and the $\alpha 2$ relaxation which becomes restricted or confined by the relatively immobile higher T_g component at temperatures sufficiently below $T_g^{\alpha 1}$ in mixtures with low concentration c_2 of the low-T_g component. The properties of the three relaxations, and particularly that of the confined $\alpha 2$-relaxation and its relation to the JG β-relaxation are important to be recognized. These properties are useful and critical to uncover the confined $\alpha 2$-relaxation in cases where it is not resolved, to distinguish it from the JG β-relaxation, and to avoid mistaking the resolved JG β-relaxation as

the unresolved confined α2-relaxaiton [24,25, 45-47,56,58,81-85]. A list of these properties are given below.

(1) The glass transition temperature $T_g^{\alpha 2}$ associated with the confined α2-relaxation is detectable by enthalpy (DSC or adiabatic calorimetry), dielectric, TSDC, and mechanical relaxation. The value of $T_g^{\alpha 2}$ is higher and not lower than T_{g2} of the pure low-T_{g2} component. However, in some highly asymmetric mixtures [81-84] and polymer blends [24,25] at low concentration c_2 of the low-T_g component, the confined α2-relaxation was not resolved and directly observed. In these cases, $T_g^{\alpha 2}$ is deduced indirectly via Property 6 to be introduced below.

(2) The temperature dependence of $\tau_{\alpha 2}(T)$ is Arrhenius or close to Arrhenius at temperatures not too far above $T_g^{\alpha 2}$. Its activation energy $E_{\alpha 2}$ is appreciably larger than the activation energy E_β of the JG β-relaxation time $\tau_\beta(T)$, which is at most a few ten times $RT_g^{\alpha 1}$ [112,114]. Consequently the separation between α2-relaxation and the JG β-relaxation decreases on raising temperature above $T_g^{\alpha 2}$, causing the confined α2-relaxation to merge with the JG β-relaxation and making it more difficult to distinguish one from the other

(3) At the same temperature, $\tau_{\alpha 2}(T)$ increases systematically and monotonically with decrease in concentration of the lower-T_{g2} component c_2.

(4) The dielectric strength $\Delta\varepsilon_{\alpha 2}(T)$ of the confined α2-relaxation increases with decrease of temperature, while the opposite trend is exhibited by $\Delta\varepsilon_\beta(T)$ of the JG β-relaxation (see Figs.3 and 4 of 50% MTHF in PS60k and 40%MTHF in oligo-PMMA).

(5) $T_{g\alpha 2}$ increases monotonically with decrease of concentration c_2 of low-T_g component, and does not exhibit a maximum at some low value of c_2.

(6) At or near $T_g^{\alpha 2}$, both $\tau_\beta(T)$ and the dielectric strength $\Delta\varepsilon_\beta(T)$ of the JG β-relaxation change from a weaker temperature dependence below $T_g^{\alpha 2}$ to a stronger one above $T_g^{\alpha 2}$. These changes of $\tau_\beta(T)$ and $\Delta\varepsilon_\beta$ at $T_g^{\alpha 2}$ serve to uncover the presence of the confined α2-relaxation having $\tau_{\alpha 2}(T_g^{\alpha 2}) \approx 100$ s, even if it is not resolved in the dielectric or NMR spectra. The same changes of $\tau_\beta(T)$ and $\Delta\varepsilon_\beta$ occur also at $T_g^{\alpha 1}$ of the α1-relaxation, but stronger.

(7) An observed fast process in mixtures at low value of c_2 is identifiable as the JG β-relaxation if its relaxation time τ_β is in approximate agreement with the primitive relaxation time τ_0 calculated by the CM equation (2) with the values of $\tau_{\alpha 1}$ and n obtained from the fit of the frequency dispersion of the α1-relaxation by the Fourier transform of the Kohlrausch function, $\exp[-(t/\tau_{\alpha 1})^{1-n}]$.

(8) The JG β-relaxation can be identified unequivocally by strong connection it has with the α1-relaxation such as the pressure dependence of its relaxation time $\tau_\beta(P,T)$ at temperatures above $T_{g\alpha 1}$, and the invariance of the ratio $\tau_{\alpha 1}(P,T)/\tau_\beta(P,T)$ to variations of P and T while either $\tau_{\alpha 1}(P,T)$ or $\tau_\beta(P,T)$ is kept constant. This is a remarkable and general property of JG β-relaxation of glass-formers and mixtures and has been justified by the Coupling Model. By contrast, there is no reason to expect the same for the $\tau_{\alpha 2}(T)$ of the confined α2-relaxation.

(9) The variety of nuclear magnetic resonance spectroscopy (NMR) techniques have been proven instrumental in investigating the dynamics of mixtures. The ^{2}H and ^{31}P NMR techniques such as line-shape, spin-lattice relaxation, and 2D exchange were applied to probe the component dynamics of the binary glass-former tripropyl phosphate (TPP)/polystyrene (PS/PS-d_3) [81-83]. Notwithstanding, the interpretation of the NMR data were misguided by the mistake of identifying the observed faster relaxation entirely as the confined α2-

relaxation. The correct interpretation [87] is a combination of the dielectrically resolved JG β-relaxation and the slower but unresolved confined α2-relaxation. This correct interpretation is demonstrated by relating the NMR data to the dielectric data obtained at the same composition of the mixture at 20%TPP [87].

(10) Found by the combination of ^{2}H NMR solid-echo spectra of PS-d_3 [82,83] and dielectric measurements [87] is the participation or coupling of the higher-T_{g1} component PS in the JG β-relaxation, as may be anticipated from the connection of the JG β-relaxation to both the α1-relaxation and the confined α2-relaxation (i.e. Property 6).

(11) At temperatures below $T_g^{\alpha 2}$, the JG β-relaxation time $\tau_\beta(T)$ is not very sensitive to changes in composition of the mixture or blend especially at lower concentrations of the lower-T_{g2} component.

The properties (1)-(11) are experimental facts and should be taken seriously *in toto* when interpreting the dynamics of highly asymmetric mixtures and polymer blends. Apparently B&K were not fully aware of these properties in interpreting the dynamics of 8, 18, 20, and 30%TPP in PS [81-83,85], and also by Pötzschner et al. in interpreting their mixtures of 20 and 34% m-tri-cresyl phosphate (m-TCP, T_{g2} = 206 K) and a spirobichroman derivative (DH379) as the high-T_g component (T_{g1}= 382 K) [84]. Some conflicting evidences were not taken into account. The consequence is the mistake of identifying the resolved JG β-relaxation as the unresolved confined α2-relaxation by them. There are only two relaxations resolved by dielectric and NMR in these mixtures. The slow one, with VFT temperature dependence of its NMR or dielectric relaxation times, is clearly the α1-relaxation dominated by the majority component PS or DH379, and was observed also by DSC at the glass transition temperature $T_g^{\alpha 1}$. The much faster one has approximately Arrhenius temperature dependence over a broad temperature range below

$T_g^{\alpha 1}$, which B&K and Pötzschner et al. interpreted as the α2-relaxation of TPP and m-TCP respectively subjected to confinement, i.e. 'the more mobile (lower-T_g) component relaxes by a liquid-like motion in a matrix formed by the arrested (higher-T_g) component'[81-84]. To show that this is a mistake, we first take from their own published data as evidences. Afterwards we shall bring in our own dielectric relaxation data at ambient and elevated pressures to demonstrate convincingly that the resolved faster relaxation is the JG β-relaxation by utilizing Properties (1)-(9) and (11). Presence of the unresolved α2-relaxation are shown by indirect evidences in accord with Properties (1)-(9). The NMR data from B&K are brought back for reconsideration and shown to be consistent with our identification of the resolved faster process is the JG β-relaxation [87], and the confined α2-relaxation is mostly unresolved albeit present.

3.1 Dielectric data at ambient pressure

8% and 18%TPP mixtures with PS

Kahlau et al. [81] made dielectric measurements of mixtures of tripropyl phosphate (TPP) with polystyrene (PS) with c_2 over the whole range from 100% down to 0%. We consider their data labelled as c_2=20, and 10% (but actually the dielectric measurements were made at 18% and 8% respectively) because the confinement of α2-relaxation is expected more pronounced, the separation between $\tau_{\alpha 2}$ and τ_β larger, and hence easier to distinguish it from the JG β-relaxation. The dielectric spectra of the 18% TPP mixture are reproduced in Fig.7 from Ref.[81,83], where only two relaxations are resolved. The slower one is no doubt the α1-relaxation, but they interpret the faster relaxation as the confined α2-relaxation. It is clear by inspection of the figure that the dielectric strength of the faster process increases with increasing temperature consistent with that of the JG β-relaxation, but at variation with that of the confined α2-relaxation (i.e.

Property 4). Had this been taken into consideration by B&K, perhaps they would hesitate interpret it as the confined α2-relaxation.

The left panel of Fig.8 is the Arrhenius plot of the dielectric relaxation times of the two processes reproduced from Kahlau et al. [81]. We are interested mainly in the data of the mixtures with c_2=20 (actually 18)%, and 10 (actually 8)% in which the slow one is the α1-relaxation and the fast one was interpreted as the confined α2-relaxation [81]. The two lines drawn in the figure are supposedly representing the Arrhenius temperature dependences of $\tau_{\alpha 2}(T)$ of the 18 and 8% mixtures, and the intercepts with the horizontal broken line at 100 s were used to determine the dielectric glass transition temperature $T_g^{\alpha 2}$ of the purported α2-relaxation. The value $T_g^{\alpha 2}$≈137 K at c_2=8% so obtained is shown in Fig.8b, which is also reproduced from Kahlau et al. It is only 2 degrees higher than T_{g2}=135 K of pure TPP, and hence violating Property (5). It is responsible for the existence of a maximum. Therefore this value of $T_g^{\alpha 2}$≈137 K for the purported confined α2-relaxation in mixture with c_2=8% is not consistent with the much higher value of $T_g^{\alpha 2}$ than T_{g2} (Property 5) established in mixtures where the confined α2-relaxation was clearly resolved and identified, i.e., Property (1).

The broadening of the faster process with decreasing temperature can be seen from the spectra of the 20%TPP mixture in Fig.7, which is a well-known property of JG β-relaxation. Notwithstanding, interpreting the fast process as the confined α2-relaxation, Kahlau et al. accounted for the broadening in mixtures with c_2=8 and 18% by a broad distribution of relaxation times represented by a temperature independent distribution of activation energies g(E) so that its mean correlation time $\tau_2(T)$ has an Arrhenius temperature dependence governed by the mean activation energy E_A. The value of E_A for the 8%TPP mixture is 5241 K. Hence E_A

/R≈17 $T_g^{\alpha 1}$ falls within the bounds of the ratio for JG β-relaxations [112,114]. This was recognized by Kahlau et al. but they still interpret the resolved fast process in Figs,7 and 8 as the confined α2-relaxation. By the way, the small value of E_A violates Property (2) of the confined α2-relaxation becasue its activation energy $E_{\alpha 2}$ is appreciably larger than the activation energy E_β of the JG β-relaxation time $\tau_\beta(T)$. The inconsistency with Properties 1 and 2 casts doubt on the interpretation of the resolved fast process as the confined α-2 relaxation by Kahlau et al.

It is natural for Kahlau et al. to fit $\tau_{\alpha 2}(T)$ by the Arrhenius T-dependence in view of the interpretation that $\tau_{\alpha 2}(T)$ are the relaxation times of α2-relaxation confined by the frozen matrix of the high-T_g component PS. However, there is no reason to expect a break from the Arrhenius T-dependence of the confined $\tau_{\alpha 2}(T)$ at any temperature far below $T_g^{\alpha 1}$. By careful examination of the purported $\tau_{\alpha 2}(T)$ data of the 8%TPP mixture (blue circles in Fig.8a), one can find that the temperature dependence actually is not strictly Arrhenius over the entire range. This becomes clearer by selecting the purported $\tau_{\alpha 2}(T)$ data of the 8%TPP from the rest and replotting them together with the $\tau_{\alpha 1}(T)$ data in the left panel of Fig.9. The two straight lines drawn through the $\tau_{\alpha 2}(T)$ data of the 8%TPP mixture with different slopes demonstrate a change from a weaker Arrhenius T-dependence to a stronger one at 238 K far below the dielectric $T_g^{\alpha 1}$=314 K. While this property is not expected from the confined α2-relaxation, it manifestly belongs to that of the JG β-relaxation (i.e., Property 6) at or near the glass transition temperature $T_g^{\alpha 2}$(8%)=238 K. Thus the resolved fast process in the 8%TPP mixture is the JG β-relaxation and not the confined α2-relaxation mistakenly identified as such by Kahlau et al. Incidentally, the presence of the confined α2-relaxation in the 8%TPP mixture is revealed by this Property (6) of the JG β-

relaxation, and hence we have an estimate of $\tau_{\alpha 2}(T)$ of the unresolved α2-relaxation is about 100 s at $T= T_g^{\alpha 2}$=238 K, i.e., the dielectric α2 glass transition temperature $T_g^{\alpha 2}$ is 238 K.

The value 238 K of the dielectric α2-glass transition temperature $T_g^{\alpha 2}$(8%) for the 8%TPP mixture is entered into the plot of $T_g^{\alpha 2}$ and $T_g^{\alpha 1}$ versus c_2 or $c_{\rm TPP}$ in the right panel of Fig.9. This helps to restore the monotonic increase of both the dielectric $T_g^{\alpha 2}$ and $T_g^{\alpha 1}$ with decreasing c_2 at small c_2 (i.e. Property 5), and replace the maximum of $T_g^{\alpha 2}$ not found by anyone else except in Refs.[81-85]. In these papers, included are the $T_g^{\alpha 2}$ supposedly determined from DSC data of the 20%TPP and 10%TPP mixtures to support the presence of the maximum. Although the DSC traces of these mixtures were published, they were not analyzed to support the DSC values of $T_g^{\alpha 2}$ in Figs.8 and 9. If the features of the DSC traces of these mixtures at low temperatures were used by B&K to suggest the purported values of the DSC $T_g^{\alpha 2}$, it is worthwhile to point out similar feature is present in the pure PS used (see Fig.1a in Ref.[81]). Also even if the weak feature in the DSC trace truly reflects an enthalpy relaxation, it can very well be associated with the JG β-relaxation [99].

The inset of the left panel of Fig.9 is a reproduction of the master curve of the dielectric loss spectra of the α1-relaxation taken at several temperatures close to $T_g^{\alpha 1}$ together with the fit by the Fourier transform of the Kohlrausch function with n=0.73 performed by Kahlau et al. [81]. The open inverted triangles in the main figure are the values of the primitive relaxation times $\tau_0(T)$ calculated by the CM equation (2) from $\tau_{\alpha 1}(T)$ with n=0.73 and t_c=2 ps. The value of $\tau_0(T)$ at $T= T_g^{\alpha 1}$ is in agreement with the extrapolation of the Arrhenius T-dependence of the $\tau_\beta(T)$ data for $T> T_g^{\alpha 2}$ to $T_g^{\alpha 1}$, which further supports the resolved fast relaxation is the JG β-relaxation according to Property 7. Also the stronger T-dependence of $\tau_0(T) \approx \tau_\beta(T)$ for $T> T_g^{\alpha 1}$ together

with the weaker *T*-dependence of $\tau_\beta(T)$ for $T< T_g^{\alpha 1}$ indicates another change of *T*-dependence of $\tau_\beta(T)$ at $T_g^{\alpha 1}$. In accord with Property 6. These results further confirm the confined α2-relaxation alleged by B&K is actually the JG β-relaxation.

The relaxation strength of $\Delta\varepsilon_2$ of the purported confined α2-process in the 18%TPP mixture obtained by Kahlau et al. is shown as a function of temperature in the left panel of Fig.10. It increases with increase of temperature at odds with the opposite trend of genuine confined α2-process according to Property 4, but consistent with the behavior of the dielectric strength of the JG β-relaxation. The broken line in Fig.10 was drawn by Kahlau et al. [81] to show that there is change of *T*-dependence of $\Delta\varepsilon_2$ at 273 K identified with $T_g^{\alpha 1}$. No doubt this is correct because 273 K is the $T_g^{\alpha 1}$ determined by DSC, We pointed out there is yet another change at *T*-dependence of $\Delta\varepsilon_2$ at 232 K we identified with $T_g^{\alpha 2}$ for the 18%TPP mixture. It is 8 degrees lower than $T_g^{\alpha 2}$=238 K for the 8%TPP mixture as can be expected due to higher concentration of TPP. Thus for the 18%TPP mixture, the dielectric glass transition temperature $T_g^{\alpha 2}$ of the truly confined α2-relaxation time is 232 K, and $\tau_{\alpha 2}(T)$ is about 100 s at $T=T_g^{\alpha 2}$=232 K. These changes of $\Delta\varepsilon_2$ at $T_g^{\alpha 2}$ and $T_g^{\alpha 1}$ are another support of the resolved fast process is the JG β-relaxation (from Property 6), and not the confined α2-relaxation misinterpreted by Kahlau et al. The value $T_g^{\alpha 2}$=232 K of the 18%TPP mixture is represented by the red ellipsoid in the right panel of Fig.10. On replacing the false dielectric $\hat{T}_g^{\alpha 2}$≈137 K from Ref.[81] by $T_g^{\alpha 2}$≈232 K of the confined α2-relaxation, we restore the monotonic increase of $T_g^{\alpha 2}$ with decrease in c_2 (i.e., Property 1), and dismiss the purported maximum at c_2 near 36% of B&K. The monotonic increase of $T_g^{\alpha 2}$ on decreasing c_2 at low values equal to 18 and 8%TPP is demonstrated in Fig.10.

20%TPP mixtures with PS

We made our own dielectric relaxation measurements at ambient and elevated pressures of a truly 20%TPP mixture [87] with the same PS as used in the study of B&K [81-83]. The data from 140 K to 260 K at ambient pressure showing the α1-relaxation and the JG β-relaxation are presented in Fig.11. Data at ambient pressure and temperatures higher than 260 K are shown in the two panels of Fig.12 together with some data taken at elevated pressures to be discussed later. The relaxation times $\tau_{\alpha 1}$(T) and $\tau_{\beta}(T)$ at ambient pressure are shown by black open and closed squares respectively in Fig.13, and the dielectric glass transition temperature $T_g^{\alpha 1}$ = 268 K is determined by $\tau_{\alpha 1}(T_g^{\alpha 1})$ = 100 s. The α1-loss peak can be well fit by the imaginary part of the Fourier transform of the KWW function with (1-*n*)=0.25, but the low frequency flank of the JG β-loss peak is indeterminate. Therefore the loss from the α2-relaxation cannot be deduced by subtracting the sum of the α1 and JG β losses from the measured loss spectra. The best one can do is to use the frequency of the measured loss minimum as an approximate guide to the location of the unresolved α2-relaxation and its peak frequency $f_{\alpha 2}(T)$. The approximate α2-relaxation times $\tau_{\alpha 2}(T)$ corresponding to $f_{\alpha 2}(T)$ at four temperatures, 260, 268, 280, and 289 K are shown by the black diamonds in Fig.13. (T)

From the spectra at ambient pressure of the JG β-relaxation in Fig.11, we determined the *T*-dependence of its $\Delta\varepsilon_{\beta}$ and the results are presented in Fig.14. There is a clear change of $\Delta\varepsilon_{\beta}(T)$ within the neighborhood of 265 K, close to $T_g^{\alpha 1}$=268 K of the α1-relaxation dominated by the majority PS component. A weaker change of $\Delta\varepsilon_{\beta}(T)$ at about 223 K is assigned to the $T_g^{\alpha 2}$ of the truly confined α2-relaxation from the minority TPP component. This assignment is represented by the upper black closed diamond in the relaxation map (Fig.13) by assuming at $T_g^{\alpha 2}$=223 K

that $\tau_{\alpha 2}=10^2$ s. The line is the Arrhenius fit of the approximate $\tau_{\alpha 2}(T)$ at four temperatures to include the value of $\tau_{\alpha 2}(T_g^{\alpha 2})$=100 s at $T_g^{\alpha 2}$=223 K. The Arrhenius *T*-dependence of $\tau_{\alpha 2}(T)$ of the confined α2-relaxation is expected from Property (2), and it is evidently stronger than that of $\tau_\beta(T)$, causing the two to merge at higher temperatures. The $\tau_{\alpha 1}(T)$ and $\tau_{\alpha 2}(T)$ increase monotonically with decrease in concentration of TPP in the three mixtures (i.e. Property 3), while $\tau_\beta(T)$ changes little (i.e. Property 11). This is like 8%, 12%, 50%, and 70% of MTHF in 3styrene (Fig.2) and 10%, 20%, and 33% THF in 3styrene, where the confined α2-relaxation was resolved in the dielectric spectra [77,78].

Altogether, the data of $\tau_{\alpha 1}$, the approximate $\tau_{\alpha 2}$, and τ_β and their relations in the 20% TPP mixture in Fig.13 resemble that found in 50% MTHF in PS60k by Blochowicz et al. [79] shown in Figs.4, and 6. Included in the relaxation map (Fig.13) are the values of $\tau_{\alpha 2}=10^2$ s at the glass transition temperatures $T_g^{\alpha 2}$=238 K (red diamond) and 233 K (blue diamond) of the true α2-relaxation in the 8% and 18% TPP mixtures respectively. As the reader may recall, the value of 238 K of $T_g^{\alpha 2}$ for the 8%TPP mixture was deduced from the temperature at which $\tau_\beta(T)$ changes its *T*-dependence (Fig.9), while the $T_g^{\alpha 2}$ value of 232 K for the 18%TPP mixture was deduced from the temperature at which $\Delta\varepsilon_\beta(T)$ changes its *T*-dependence (Fig.10). Shown in the relaxation map (Fig.13) are the dielectric $\tau_{\alpha 1}(T)$ and $\tau_\beta(T)$ of the 8% (red) and 18% (blue) TPP mixtures from Kahlau et al. [81]. The primitive relaxation times $\tau_0(T)$ calculated by the CM equation (2) from $\tau_{\alpha 1}(T)$ and 1-*n*=0.27 determined from the Kohlrausch fit to the frequency dispersion and represented by inverted triangles in Fig.13 are consistent with the data of $\tau_\beta(T)$ obtained at lower temperatures. Thereby Property (7) is also verified.

The method of obtaining approximate $\tau_{\alpha 2}(T)$ from the dielectric spectra of the 20%TPP mixture was applied to the 8%TPP and 18%TPP mixtures published by B&K [81-83]. The approximate $\tau_{\alpha 2}(T)$ for the 8%TPP at 290 K and 298 K, and $\tau_{\alpha 2}(T)$ for the 18%TPP mixtures at 317 K are presented in Fig.S8 in SI`. These values of $\tau_{\alpha 2}(T)$ together with $\tau_{\alpha 2}(T_g^{\alpha 2})$=100 s at $T_g^{\alpha 2}$=238 K and 232 K for the 8%TPP and 18%TPP mixtures respectively were fit to the Arrhenius *T*-dependences according to Property (2) and are represented by the red and blue lines in Fig.S8.

3.2 Mixtures of TCP with DH379

Pötzschner et al. [84] studied the component dynamics of the highly asymmetric mixtures of m-tri-cresyl phosphate (TCP) (T_g=206 K) with a spirobichroman derivative (DH379) (T_g=382 K) at concentrations of 34% and 20%. They observed two relaxations by dielectric spectroscopy. Dominated by the majority DH379 component, the temperature dependence of the slower α1-relaxation time $\tau_{\alpha 1}(T)$ was used to determine $T_{g\alpha 1}$ in Fig.15a. Following the example of B&K, Pötzschner et al. interpreted the faster process as the confined α2-relaxation in the immobile matrix of DH379. The Arrhenius *T*-dependence fit to the relaxation times of the faster relaxation were extrapolated to 100 s to determine $T_g^{\alpha 2}$ of the purported confined α2-relaxation as shown in Fig.15a. The values of the alleged $T_g^{\alpha 2}$ of the 34% and 20% TCP mixtures produce a maximum when considered together with those determined at higher c_2 in Fig.15b. The presence of the maximum is based solely on the dielectric data since no NMR or calorimetric data were presented for these two mixtures. This maximum, instead of monotonic increase of $T_g^{\alpha 2}$ with decreasing c_2, is the consequence of misidentifying the faster relaxation as the confined α2-relaxation, which is actually the JG β-relaxation as we demonstrate below. The mistake can be

perceived from the 20% TCP mixture having the alleged $T_g^{\alpha 2}$ the same as T_g of 100% TCP, violating Property (1). This is also surprising and impossible because the environment of the TCP in the two cases are drastically different. It also violates Property 2. We demonstrate the mistake made by producing more evidences from the experimental data of Pötzschner et al.

Firstly, the isothermal dielectric loss spectra of the mixture with 34% TCP show the frequency dispersion of the α2-process narrows and the relaxation strength increases with increasing temperature (see Fig.S9), which is the signature of the JG β-relaxation.

Secondly, this identification of the resolved faster process in the 34%TCP mixture as the JG β-relaxation is supported by its relaxation times changing at near $T_g^{\alpha 1}$≈285 K from a non-Arrhenius high-temperature dependence to an Arrhenius dependence at lower temperatures, i.e. Property 6 (see left panel of Fig.16).

Thirdly, the frequency dispersion of the dielectric α1-loss peak at 320 K in the 20%TCP mixture published by Pötzschner et al.[84] is fitted by the Fourier transform of the Kohlrausch function (Eq.1) with (1-*n*)=0.44 and shown in the upper right panel of Fig.16. If the broadening of the α1-loss peak by concentration fluctuations in this mixture is negligible, the value of (1-*n*)=0.44 can be used to calculate τ_0 by the CM Eq.(2), which gives an estimate of the JG τ_β. Indicated by the tip of the vertical arrow and marked by × in the left panel of Fig.16, the order of magnitude of the calculated τ_0 at 320 K is in agreement with the observed relaxation time of the faster relaxation at the same temperature. This is another support of identifying the faster process with the JG β-relaxation (i.e. Property 7), like demonstrated before in Figs. 2, 4, and 6 for mixtures of 10% and 20% TPP with PS respectively.

Fourthly, by examining closely the temperature dependence of the relaxation time of the faster process at lower temperatures in the left panel of Fig.16, there is a change to a weaker

temperature dependence at above ≈ 250 K. With the faster process now correctly interpreted as the JG β-relaxation, this change is evidence of the presence of the truly confined α2-relaxation having its glass transition temperature $T_{g\alpha 2}$ ≈250 K (i.e. Property 6). This correct value of $T_g^{\alpha 2}$ of the 20%TCP mixture is entered into the lower right panel of Fig.16 to replace the erroneous value of ≈206 K obtained by Pötzschner et al. in extrapolating the Arrhenius *T*-dependence of $\tau_\beta(T)$ to 100 s (Fig.15). The replacement restore the monotonic increase of $T_{g\alpha 2}$ with decrease of $c_{\text{m-TCP}}$.

3.3 Dielectric data of 20%TPP mixture at elevated pressures

In order to make quantitative comparison with the rich NMR data and DSC data of Bock et al. [82,83], we made our own dielectric relaxation measurements at elevated pressures on a mixture with exactly the same composition of 20%TPP [87]. The TPP and PS used were obtained from the same source as B&K. Only two relaxations are resolved in all experiments including ours at elevated pressures, with the slower one being definitely the α1-relaxation. By observing the change of the dynamics of the faster relaxation with applied pressure and how its relaxation time τ_f is related to that of the slower α1-relaxation, we shall be able to ascertain its identity. Significant changes of the fast relaxation times τ_f were observed on elevating pressure and are shown in Fig,S10 in SI. The sensitive pressure dependence of the faster relaxation is consistent with our interpretation of it as the JG β-relaxation, i.e. Property (8). Furthermore, at temperatures above $T_g^{\alpha 1}$ we can check if the ratio $\tau_{\alpha 1}(P,T)/\tau_f(P,T)$ is invariant to changes of pressure *P* and temperature *T* while either $\tau_{\alpha 1}(P,T)$ or $\tau_f(P,T)$ is kept constant. The latter is a general relation between the α-relaxation time τ_α and the relaxation time τ_β of the JG β-relaxation [70-76,91,97-103], which is derived from the same relation between τ_α and τ_0 of the CM Eq.(1) and the

relation $\tau_\beta \approx \tau_0$ or the CM Eq.(2). If these properties are found to be true between $\tau_{\alpha 1}$ and τ_f, we have strong evidence for identifying the faster process as the JG β-relaxation. Indeed the results from the experiment at elevated pressure have borne this out as shown before in Fig.12. Consequently, the confined α2-process lying in between the α1-relaxation and the JG β-relaxation is not resolved in dielectric relaxation and NMR experiments.

The relaxation times $\tau_{\alpha 1}(P)$ and $\tau_f(P)$ (or τ_β) at three different fixed temperatures T_{fix} of 294, 310, and 319 K were determined from the respective loss peak frequencies and plotted against pressure in the left panel of Fig.17. The α1 glass transition pressure $P_g^{\alpha 1}$ is determined by $\tau_{\alpha 1}(P_g^{\alpha 1})$ =100 s in the figure. For pressures below $P_g^{\alpha 1}$, for each fixed temperature $\tau_{\alpha 1}(P)$ is well described by $\tau_{\alpha 1}(P) = \tau_\infty \exp\left[D_P P_0/(P - P_0)\right]$, and above $P_g^{\alpha 1}$ the isothermal $\tau_f(P, T_{fix})$ or $\tau_\beta(P, T_{fix})$ has the pressure dependence of $\tau'_\infty \exp\left(V^{\#} P/RT_{fix}\right)$, where $V^{\#}$ is the activation volume. At pressures higher than 200 MPa and up to the highest pressure of 400 MPa in Fig.17, the data of $\tau_f(P,T)$ at T=294 K were taken way above $P_g^{\alpha 1}$ or deep inside the frozen PS matrix, and yet the pressure dependence of $\tau_f(P,T$=294 K) is significant, as found for $\tau_\beta(P)$ of JG β-relaxation in other mixtures [70-76] and pure glass-formers [91,97-103]. The same can be concluded from the right panel of Fig.17 where at any temperature way below $T_g^{\alpha 1}$ that $\tau_f(P,T)$ increase by about 2 orders of magnitude with pressure increase from 0.1 MPa to 190 MPa. It is not clear if $\tau_{\alpha 2}$ of the unresolved confined α2-relaxation has similar pressure dependence. To check this out, it would be worthwhile to make high pressure dielectric measurements on the mixture of 50%MTHF in PS60k by Blochowicz et al. to investigate the pressure dependences of the truly confined α2-relaxation and the JG β-relaxation, as well as possible relation between the P and T dependences of these two relaxations. The suggested study is feasible since these two relaxations are resolved

and have large dielectric strength (see Figs.4 and 5), although the lower temperatures may be challenging to perform dielectric relaxation measurement at high pressures.

Measurements at pressure below $P_g^{\alpha 1}$ were made in the equilibrium liquid state, and a change to a steeper pressure dependence of $\tau_f(P)$ is observed in the left panel of Fig.17 on crossing $P_g^{\alpha 1}$, which is another known property of $\tau_\beta(P)$. Our isobaric data of α_2-process taken at 294 K are of higher quality and measured up to higher pressures than those at 310 and 319 K. The data show at $P_g^{\alpha 1}$ that $\tau_f(P_g^{\alpha 1})=10^{-7}$ s at T=294 K. The right panel of Fig.17 shows similarly at $T_g^{\alpha 1}$ that $\tau_f(T_g^{\alpha 1})=10^{-7}$ s for P=0.1 MPa and 190 MPa. Since $\tau_{\alpha 1}(P_g^{\alpha 1}) = \tau_{\alpha 1}(T_g^{\alpha 1})$=100 s. Combining these results from the isothermal and isobaric data, we have the remarkable property that τ_f=10^{-7} s of the fast process is always the same if $\tau_{\alpha 1}$=100 s, independent of the pressure and temperature combinations. The property is no surprise if the fast process or at least the short time part of it is identified with the JG β-relaxation, which is seen before in other systems [70-76, 91,97-103]. However, a priori, there is no reason to expect it to hold if the α2-process originates from TPP confined by the frozen PS matrix. Substituting these values of $\tau_{\alpha 1}$ and τ_f now identified as τ_β at $T_g^{\alpha 1}$ or $P_g^{\alpha 1}$ into the CM Eq.(2), we obtain the value of 0.66 for coupling parameter n of the α1-relaxation. This is just slightly larger than the value of n≡(1-β_K)=0.63, where β_K=0.37 is the exponent of the Kohlrausch function used by Bock et al. to fit the ^{2}H NMR reorientational correlation functions $C_2(T)$ of the 20% TPP mixture. This rather good agreement is another support of identifying the fast process as the JG β-relaxation via Property (7).

The strong relation between α1-relaxation and the fast relaxation or the JG β-relaxation also can be shown by comparing the spectra taken at various combinations of P and T while keeping the peak frequency $f_{\alpha 1}$ or the relaxation time $\tau_{\alpha 1}$ constant. Performed in Fig.18, the

invariance of $\tau_{\alpha 1}(P,T)/\tau_f(P,T)$ to several different combinations of P and T at constant $\tau_{\alpha 1}(P,T)$ (i.e., Property 8) are substantiated. Again this is a property of JG β-relaxation, and hence the fast relaxation should be identified as such. Fig.12 also shows that the frequency dispersion of α1 is also invariant. This property of α1 was also found in pure glass-formers [89,91,97,99,100], in mixtures [70-76] and polymer blends [97]. However in the present case of 20%TPP, concentration fluctuations may contribute some broadening of the dispersion. The Kohlrausch function used to fit the frequency dispersion of α1 in Fig.12 has exponent β_K=0.25. This value of β_K is the same as that of the 18% TPP mixture of B&K, and thus it suggests that the actual coupling parameter $n\equiv(1-\beta_K)$ of the α1-relaxation in the 20%TPP mixture is smaller than $(1-\beta_K)$=0.75 obtained from the fit to the frequency dispersion of its dielectric loss peak. In fact it is 0.66 or β_K=0.34 from applying Eq.(2), and β_K=0.37 is the exponent of the Kohlrausch function used by Bock et al. to fit the ^{2}H NMR reorientational correlation functions $C_2(T)$.

3.4 ^{2}H NMR and ^{31}P NMR data of 10% and 20% TPP mixtures

The studies by Bock et al. [82,83] using several NMR techniques are potentially critical to elucidate the nature of the two resolved processes in 10% and 20%TPP mixtures. Unfortunately in interpreting their own NMR data, they were committed in identifying the faster process as the confined α2-relaxation, same as in the dielectric study of Kahlau et al. [81] This is a mistake as we have shown convincingly in previous sections that the dielectrically resolved fast process is the JG β-relaxation and the confined α2-relaxation is unresolved, albeit it is present spectrally in between the JG β-relaxation and the slow α1-relaxation. Therefore it is pertinent to reconsider the NMR data to show consistency with our interpretation that the faster process is

composed of the prominent JG β-relaxation followed in time by the unresolved confined α2-relaxation.

By probing the polystyrene component in the slower α1-relaxation by ^{2}H NMR, and the TPP component in the faster process by ^{31}P NMR stimulated echo decay, the relaxation times $\tau_{\alpha 1}(T)$ and $\tau_f(T)$ in mixtures with 10 and 20% TPP are replotted in Fig.19. For the 10% TPP mixture, $T_g^{\alpha 1}$≈300 K from both DSC and ^{2}H NMR, while for the 20% TPP mixture, $T_g^{\alpha 1}$≈275 K from DSC, and ≈280 K from ^{2}H NMR. The values of the NMR $\tau_f(T)$ have been determined (closed red circles and blue squares in Fig.19 by fitting reorientation correlation function from ^{31}P NMR at temperatures above and below the $T_g^{\alpha 1}$ defined by the NMR $\tau_{\alpha 1}(T_g^{\alpha 1})$ is equal to 100 s or from DSC. Observed by Bock et al. [82,83] in the 10 and 20% TPP mixtures and shown in Fig.19 is the change of temperature dependence of the NMR $\tau_{\alpha 2}(T)$ from Arrhenius dependence below $T_g^{\alpha 1}$ to a stronger dependence above $T_g^{\alpha 1}$. This behavior of the NMR $\tau_{\alpha 2}(T)$ of the α2-process is consistent with that of the JG β-relaxation (i.e., Property 6), and generally found in other mixtures. Bock et al. fitted the reorientational correlation functions $C_2(t)$ measured by ^{2}H NMR by the Kohlrausch function to obtain $\tau_{\alpha 1}(T)$ and β_K for the α1-relaxation in the mixtures. The ^{2}H NMR α1-relaxation times $\tau_{\alpha 1}(T)$ of the 10% and 20% TPP mixtures are shown in Fig.19 by the open red circles and the blue squares respectively. The value of n_1 obtained from $\beta_K \equiv (1-n_1)$ corresponds exactly to the coupling parameter of the CM if and only if concentration fluctuations do not broaden the dispersion of the α1-relaxation. In the mixture with 10% TPP, the effect from concentration fluctuations can be neglected, and the value of n_1=0.61 corresponding to $\beta_K \equiv (1-n_1)$=0.39 determined by Bock et al. can be taken to be the coupling parameter of the α1-relaxation. The smaller coupling parameter n_1=0.61 for 10% TPP mixture of

the NMR correlation function $C_2(t)$ than n_1=0.73 for the 8% TPP mixture from the frequency dispersion of dielectric susceptibility is consistent with the 2 per cent lower TPP content in the latter. It follows from Eq.(2) that this difference in coupling parameters is also consistent with the shorter NMR $\tau_{\alpha 1}(T)$ than the dielectric $\tau_{\alpha 1}(T)$ found experimentally (compare Fig.13 with Fig.19), as well as the weaker T_g-scaled temperature dependence (or smaller fragility index m) of the former than the latter [115].

The primitive $\tau_0(T)$ of the CM calculated from the NMR $\tau_{\alpha 1}(T)$ of the 10%TPP mixture via Eq.(2) with n=0.61, are shown in Fig.19 by the red open inverted triangles. Remarkably, the calculated $\tau_0(T)$ are in good agreement with the NMR $\tau_f(T)$ at the $T= T_g^{\alpha 1}$ and temperatures above it. By Property (7), this indicates that the NMR faster process is the JG β-relaxation and thus $\tau_f(T) = \tau_{JG}(T)$. Also the NMR $\tau_f(T)$ changes from the stronger temperature to the weaker Arrhenius dependence on crossing the NMR $T_g^{\alpha 1}$ from below, which is Property (6) of the JG β-relaxation time $\tau_{JG}(T)$. This feature of the NMR $\tau_f(T)$ of was also highlighted in Fig.9 of Ref.[82] or Fig.S11 in SI by the two arrows at $1000/T_g^{\alpha 1}$ put by Bock et al. to indicate it is the location where the change occurs for the 10% and 20% mixtures.

2D ^{31}P NMR spectra

^{31}P stimulated echo decay is a technique able to pick up not only the contribution to the faster process at shorter times by the JG β-relaxation, but also at longer times the unresolved confined α_2-relaxation. The decomposition of the faster process into these two relaxations have support from the two-dimensional (2D) NMR exchange spectra of the TPP/PS sample with c_2= 20% at 200 K for mixing times t_m=0.05 ms, 500 ms and 5000 ms, and at 296.5 K for mixing times t_m=0.1 ms, 10 ms, 100 ms, and 3000 ms. This is elucidated at 200 K in Fig.19, where the

horizontal lines indicate t_m=0.05 ms, 500 ms and 5000 ms. For very short t_m=0.05 ms, the entire intensity essentially was found along the diagonal, i.e. no isotropic reorientation occurs on this time scale, and consistent with our identification of the faster relaxation as the JG β-relaxation with restricted orientation, and having $\tau_{JG}(T=200\text{ K}) = \tau_{\alpha 2}(T=200\text{ K}) \approx t_m$=0.05 ms. For the long mixing times t_m=500 or 5000 ms, the signal in the plane gains much intensity, clearly indicating spatially unrestricted (isotropic) reorientation, consistent with the unresolved confined α_2-relaxation principally coming from the TPP component and having such long relaxation times at 200 K (see Fig.19).

^{2}H NMR solid-echo spectra

^{2}H NMR solid-echo spectra of PS-d_3 were measured for mixture with 20% TPP at temperatures well below $T_g^{\alpha 1}$ [82,83]. By prolonging the inter-pulse delay t_p of the solid-echo pulse sequence, spatially highly restricted motion is probed. On crossing the time scale of the solid or Hahn-echo experiment, a spatially restricted relaxation process shows up as a minimum in the line shape parameter $R(T)$. Measured on the mixtures with 10% and 20% TPP with long t_p = 200 μs, $R(T)$ exhibits a minimum first around 120 K due to the non-JG secondary process of TPP and another minimum at around T = 225 K (for c_{TPP} = 20%) and T = 250 K (for c_{TPP} = 10%). The time constants $\tau_{se}(T)$ at 225 K and 250 K of spatially restricted relaxation of PS determined were included in Fig. 9 of Bock et al. [82] and also in Fig.19 herein as the red and blue crosses respectively. It can be seen by inspection of Fig.19 that the solid echo times τ_{se} coincides with τ_f of the NMR faster process, which we have identified in the above as the JG β-relaxation, and $\tau_f(T)=\tau_{JG}(T)$. This leads to $\tau_{JG}(T)=\tau_f(T)=\tau_{se}(T)$ at 225 K (c_2 = 20%) and 250 K (c_2 =10%), and from which we conclude that the JG β-relaxation has participation from the PS in

performing a spatially highly restricted reorientational motion on the same timescale. Also note that at T=225 K and 250 K, the values of $\tau_{JG}(T)=\tau_{\alpha 2}(T)=\tau_{se}(T)$ is close to the mixing time t_m=0.05 ms of (2D) ^{31}P NMR spectra of the mixture with c_{TPP}= 20% at 200 K. It can be seen from Fig.19 herein or Fig.10 of Bock et al.[82] for t_m=0.05 ms that essentially the entire intensity is found on the diagonal, and hence no reorientation occurs on this time scale. Thus, the observation of a spatially highly restricted reorientational motion of PS on the same timescale as $\tau_{JG}(T)=\tau_{\alpha 2}(T)=\tau_{se}(T) \approx t_m$ =0.05 ms is consistent with our interpretation of the faster process as the JG β-relaxation, in which both TPP and PS participate (from ^{2}H NMR solid-echo spectra of PS-d_3), and naturally also in its successors, the α1 and the confined α2 relaxations. On the other hand, the observation poses a problem to identifying the faster process by Bock et al. entirely as the isotropic α2-process of the TPP.

Consistency of the interpretations of dielectric and NMR data

The dielectric relaxation data we obtained are in the mixture with 20% TPP exactly the same as that studied by various NMR techniques by Bock et al. This allows quantitative inter-comparison of our dielectric spectra and interpretations given with that of the NMR data. Valenti et al.[87] have demonstrated in detail that the dielectric data and our interpretations are fully consistent with the NMR data. For a detailed comparison we refer the reader to Ref.[87]..

4. JG β-relaxation mistaken as confined α2-relaxation in polymer blends

We have convincingly shown in mixtures of molecular glass-formers with oligo-polymers and polymers that the resolved faster relaxation is the JG β-relaxation but was misidentified as the confined α2-relaxation. The mistake was made by others in polymer blends, and it is necessary to rectify this problem by presenting experimental evidences.

4.1 Ambient pressure dielectric relaxation data of *x*PVME-(1-*x*)PS blends

Bock et al, Kahlau et al.[81-83], and Pötzschner et al.[84] all mentioned the studies of binary polymer blends of poly(vinyl methylether) (PVME, T_g=250 K) and PS (T_g=373 K) with large ΔT_g= 123 K of the two components by Lorthioir et al. [24,58]. DSC measurements detected only one transition in blends at all c_{PVME}, which is the upper glass transition temperature $T_g^{\alpha 1}$ = 337 K of the α1-relaxation. The isochronal dielectric loss data at 1 Hz for blends with various values of c_{PVME} are reproduced from Ref.25 in Fig.20. Two relaxations were resolved in blends with c_{PVME} ≤ 30%. For the blends with c_{PVME} =20%, the orange-color arrow at 228 K serves to indicate the locations of the fast relaxation at 1 Hz, and the other arrow at 331 K indicates the α1 relaxation at 1 Hz consistently with $T_g^{\alpha 1}$ = 337 K by DSC at a lower frequency. The dielectric strength of the faster relaxation at 228 K is significantly stronger than the slower one at 337 K. From the isothermal dielectric spectra of the fast relaxation in blends with c_{PVME} ≤ 30% (to be shown later), the temperature dependence of its relaxation times $\tau_f(T)$ changes to more like Arrhenius at low temperatures. Based on these dielectric properties, Lorthioir et al. interpreted the fast relaxation in blends of 10, 20, and 30% PVME with PS as coming from confined PVME in the frozen matrix of PS, and this interpretation was maintained in two reviews [58,86], and neutron scattering studies [45-47,56]. However, we have shown the fast relaxation, identified by Lorthioir et al. as the confined PVME relaxation, is actually the JG β-relaxation in the blends of 10, 20, and 30% PVME with PS [80]. Notwithstanding in a recent review [86], Allegria and Colmenero (AC) cited the paper by Pötzschner et al. [84] in the mixtures of TCP with DH379, which we have discussed before in Section 3, and shown to have given a wrong assignment to the fast process. The interpretation of the fast dielectric relaxation as TCP confined by frozen DH379 given by Pötzschner et al. [84] is similar to that of Lorthioir et al., and AC used it as

another support in reaffirming their interpretation of the fast relaxation in 10, 20, and 30% PVME blends with PS as the confined PVME relaxation [24,25]. Thus there is a need to revisit the experimental data of the PVME blends with PS to demonstrate unequivocally that the resolved fast relaxation is the JG β-relaxation as well as to uncover the confined α2-relaxation of PVME and its properties, which has not been done before.

In this section we analyze the data of Lorthioir et al. in conjunction with the data of Urakawa et al. [31] obtained in the same blends, and demonstrate from the properties of the resolved fast relaxation that it is not the confined PVME relaxation, but instead it is the JG β-relaxation. Although dielectrically unresolved, the confined PVME α2-relaxation in the 20% PVME blend was detected by thermally stimulated depolarization current (TSDC) by Leroy et al. [26] and the value of its $T_g^{\alpha 2}$=293 K determined directly, while $T_g^{\alpha 1}$=337 K was obtained by DSC. These values of $T_g^{\alpha 2}$ by TSDC and $T_g^{\alpha 1}$ by DSC of all blends are presented in Fig.21, where the data are taken from Ref.[26]. The values of $T_g^{\alpha 2}$ and $T_g^{\alpha 1}$ are entered into the relaxation map of <log τ(s)> in Fig.22b. Also shown are the averaged relaxation times <log $\tau_f(T)$> of the fast relaxation (filled green circles) taken from Ref.[58], which are related to $\tau_f(T)$ in Fig.22d deduced from isothermal dielectric spectra of the fast relaxation in Fig.22c. The data in Figs.22c and 22d were taken from Lorthioir et al. and redrawn. This fast relaxation was interpreted by Lorthioir et al. as the PVME all confined by the frozen PS chains. The activation energy E_a of the $\tau_f(T)$ for the 20%PVME blend in Fig.22d is 7869 K in temperature units, and the ratios, $E_a/T_g^{\alpha 2}$=26.9 and $E_a/T_g^{\alpha 1}$=23.3, all fall within the bounds of the values for JG β-relaxation in pure glass-formers [112,114]. On decreasing temperature, the data of <log $\tau_f(T)$> in Fig.22b as well as $\tau_f(T)$ in Fig.22d exhibit a crossover from a VFT-like T-dependence to an Arrhenius T-dependence after crossing a temperature nearly the same as $T_g^{\alpha 2}$=293 K. This is reminiscent of

Property 6 on the temperature dependence of the JG β-relaxation time $\tau_{JG}(T)$, and hence we label the $<\log \tau_f(T)>$ and the $\tau_f(T)$ data by JG β-relaxation in Figs.22b and 22d respectively, and the crossover temperature is identifiable with the glass transition temperature $T_g^{\alpha 2}$=293 K of the confined α2-relaxation. By contrast, according to Lorthioir et al., *all* PVME are confined by the frozen PS chains at low enough temperatures and contribute *entirely* to the fast relaxation observed (filled circles). Their proposal was already contradicted by the detection of the $T_g^{\alpha 2}$=293 K from TSDC measurements by Leroy et al. in Fig.21 and Fig.22b. This is because at $T_g^{\alpha 2}$=293 K there is another faction of PVME having relaxation time of the order of 100 s, in addition to the faction contributing to the fast relaxation with relaxation time τ_f=10^{-4} s at the same temperature. Thus the interpretation by Lorthioir et al. of the fast relaxation originating from PVME all confined by the immobile PS chains is clearly invalid.

On the other hand, the experimental data in Figs.21 and Fig.22(b) are fully consistent with our interpretation of presence of two separate relaxations at temperature below $T_g^{\alpha 1}$=337 K, namely the JG β-relaxation to account for the fast relaxation and the confined α2-relaxation for the glass transition at $T_g^{\alpha 2}$=293 K. Notwithstanding, validity of the interpretation by Lorthioir et al. is still maintained by the authors to the present times [86], and were referred to by others [81-85] despite the publication in 2013 [80] pointing out the mistake. Therefore we need to go deeper into the discussion of the experimental data of Lorthioir et al. and the complementary data of Urakawa et al. [31] to show that the entire data sets are inconsistent with the interpretation of Lorthioir et al. but consistent with ours. We also present in the next section data of other polymer blends with large difference in ΔT_g of the two components to demonstrate consistency with our interpretation in all these cases.

We start by considering the dielectric loss data at 1 kHz, $\varepsilon''(T,1\text{ kHz})$, of the blends of PVME with PS for widely different values of c_{PVME} in Fig.22a from Urakawa et al. [31]. The low temperature peaks with maxima at about 130 K with peak intensity roughly proportional to c_{PVME} is the intramolecular γ-relaxation of PVME, and it is unimportant and of no interest to us. The 1 kHz isochronal loss peak at about 280 K of the blend with c_{PVME}=20% from Urakawa et al. is consistent with the 1 kHz peak frequency of isothermal loss spectra of the fast relaxation of the blend in Fig.22c, and also the temperature dependence of $\tau_f(T)$ in Fig.22d. So is the 1 Hz isochronal loss peak at 228 K of Lorthioir et al., shown before in Fig.20, when compared with $\tau_f(T)$ in Fig.22d. This fast relaxation is identifiable with the JG β-relaxation from Property 6 since on increasing temperature $\tau_f(T)$ changes its temperature dependence from Arrhenius to a stronger dependence on crossing $T_g^{\alpha 2}$=293 K. This behaviour can be seen from $<\log \tau_f(T)>$ in Fig.22b and better from $\log \tau_f(T)$ in Fig.22d where more data of $\tau_f(T)$ are presented. Having identified the broadly resolved loss peak in the 1 kHz $\varepsilon''(T)$ data of the 20% PVME blend in Fig.22a unequivocally as the JG β-relaxation, naturally the broad loss peaks in the 10%, 6%, and 4% PVME blends with reduced intensity are also the JG β-relaxation, although the shift of the loss peak to lower temperature in the 6% and 4% PVME blends remains to be explained.

In Fig.22b, the broken horizontal line indicates the relaxation time of $10^{-3.8}$ s corresponding to 1 kHz. The open green circle on the line corresponds to the JG β-loss peak temperature at 280 K in Fig.22a, and it can be seen that it lies close to the data of $<\log \tau_f>$ or $<\log \tau_{JG}>$ at temperatures nearby. The temperature at which the confined α2-relaxation time is equal to $10^{-3.8}$ s, corresponding to 1 kHz, has to be higher than 280 K because at $T=T_g^{\alpha 2}$=293 K $\tau_{\alpha 2}(T)$ is already the order of 100 s. Determined by the onset of the shoulder of the 1 kHz

isochronal $\varepsilon''(T)$ data in Fig.22a and indicated by the red arrow, it is approximately 320 K, and thus $\tau_{\alpha 2}(T$=320 K) $\approx 10^{-3.8}$ s. The red line in Fig.22b connecting the two data points, $\tau_{\alpha 2}(T$=320 K) = $10^{-3.8}$ s and $\tau_{\alpha 2}(T_g^{\alpha 2}$=293K) $\approx 10^2$ s, should approximately represent the supposedly Arrhenius T-dependence of the confined $\tau_{\alpha 2}(T)$ according to Property 2. The second shoulder with onset at $T\approx$354 K is the temperature at which $\tau_{\alpha 1}(T$=354 K) =$10^{-3.8}$ s. It is located in Fig.22b by the open blue diamond. The two data points, $\tau_{\alpha 1}(T$=354 K) =$10^{-3.8}$ s and $\tau_{\alpha 1}(T_g^{\alpha 1}$=337 K) $\approx 10^2$ s of the α1-relaxation are supposedly connected by a VFT temperature dependence, which is not provided.

Summarizing the above, we are able to show the presence of three relaxations, and identify the fast one as the ubiquitous JG β-relaxation, the slower one as the confined α2-relaxation, and the slowest one as the α1-relaxation in the 20% PVME blend with PS. The success is made possible by considering and analyzing the combined experimental data of $T_g^{\alpha 2}$ by TSDC and $T_g^{\alpha 1}$ by DSC by Leroy et al., the isothermal and the 1 Hz isochronal dielectric spectra of Lorthioir et al. and the 1 kHz isochronal spectra of Urakawa et al. The results in the PVME/PS blends are isomorphic to the other mixtures with large difference in the glass transition temperatures of the two components.

4.2 Dielectric relaxation of 25%PVME-75%PS blend at elevated pressures

Dielectric relaxation measurements were made by Schwartz et al. [55] at ambient and elevated pressures on the 25% PVME/75% PS blend. As already been demonstrated in the above and in Figs.20-22 using data from similar blends studied by Lorthioir *et al.*, the dielectrically resolved fast relaxation that Schwartz et al. observed in the 25% PVME blend is not from the confined α2-relaxation, but from the JG β-relaxation in the blend contributed in its dielectric strength from the PVME component. This can be confirmed by putting the ambient pressure data of $\log \tau_f(T)$ in

the 25% PVME blend from Schwartz et al. together with the 30% and 20% PVME blends of Lorthioir et al. in Fig22d. This is done in Fig.23 to show the good correspondence between the data from blends of similar compositions from two sources. Moreover, the relaxation time $\tau_f(T)$ of the 25% PVME blend of Schwartz et al. changes its temperature dependence from Arrhenius below some temperature ≈289 K to a stronger *T*-dependence above it, which we can identify as $T_g^{\alpha 2}$ of the confined α2-relaxation from Property 6. This identification is supported by the actual value of $T_g^{\alpha 2}$ obtained from the interpolation curve given by Leroy *et al.* of their TSDC data (see Fig.21), and is consistent with the larger value of 293-295 K for $T_g^{\alpha 2}$ of the 20% PVME blend.

The entire data of $\log \tau_f(T)$ for the 25%PVME blend from Schwartz *et al.* at ambient and elevated pressures are reproduced here as Fig.24 with illustrations added to make the following points clear. In this figure, the vertical dashed orange and the thinner orange continuous arrows indicate at ambient pressure the location of $1000/T_g^{\alpha 2}$ with $T_g^{\alpha 2}$≈ 289 K, obtained by interpolation of the TSDC data of Leroy et al.[26], and $1000/T_g^{\alpha 1}$ with $T_g^{\alpha 1}$ ≈ 321 K from DSC of the blend (see Fig.21). While there is a marked change in *T*-dependence of $\tau_{JG}(T)$ at the $T_g^{\alpha 2}$ ≈ 289 K of the PVME component, the change at $T_g^{\alpha 1}$ ≈ 321 K is more subtle. Nevertheless its presence is indicated by the VFT fit of $\tau_{JG}(T)$ at higher temperatures (orange curve) starting to deviate from the data at temperature near $T_g^{\alpha 1}$ ≈ 321 K. This behavior reminds us of Property 6 and the same observation in the mixtures of mixture of 50%MTHF with PS60k in Figs.4 and 6, and in the mixture of 8% and 18% TPP in PS in Figs.9 and 13. It is an evidence of the connections of the JG β-relaxation to both the α1-relaxation and the α2-relaxation in the blend, and hence it brings out the fundamental importance of the JG β-relaxation in the blend.

The same Property 6 also can be observed from the data of $\tau_{JG}(P, T)$ at elevated pressures. In Fig.24, lines are drawn to connect points at lower temperatures to show the change of

temperature dependence at $T_g^{\alpha 2}(P)$, the α2 glass transition temperature at pressure *P*. Aided by these lines, the crossover seems to occur uniformly at the same value of the relaxation time, $\tau_\beta(P, T) \approx 10^{-4.8}$ s, independent of *P*, which is indicated by open symbols in the figure. This behavior is the same as $\tau_\beta(P, T)$ of the 20% TPP in mixture with PS shown before in Figs.17 and 18, which is Property 8 showing once more the connection of the JG β-relaxation to the α2-relaxation. Moreover, this relaxation time at the crossover of 25% PVME for all *P* is close to $\tau_\beta \approx 10^{-5}$ s for the crossover at ambient pressure of the 20% PVME blend at $T_g^{\alpha 2} \approx 293$ K shown previously in Fig.22d, The property of $\tau_\beta(P,T)$ found by Schwartz *et al.* is another proof that the observed process is the JG *β*-relaxation of the blend. The constancy of $\tau_\beta(P, T)$ at the crossover temperature, $T_\times(P) \approx T_g^{\alpha 2}(P)$, is remarkable. Same as found in the 20%TPP mixture with PS, this property of the 25% PVME blend is shown explicitly by the inset of Fig.24, where the $\tau_\beta(P,T)$ data at different pressures are collapsed into a master-curve by plotting $\tau_\beta(P,T)$ against scaled reciprocal temperature, $T_\times(P)/T$. The colored vertical arrows in Fig.24 mark the positions where the α1-relaxation enters into the glassy state, as determined by PVT data [116]. Note the approximate agreement between this location and $1000/T_g^{\alpha 1}$ from DSC at ambient pressure. The data of $\tau_\beta(P,T)$ at higher pressures are too sparse to consider the constancy of $\tau_\beta(P,T)$ at the crossover temperature, $T_\times(P) \approx T_g^{\alpha 1}(P)$.

The valuable information coming from our analysis of the dielectric data at elevated pressure of Schwartz et al. in Fig.24 is the monotonic increase of $T_g^{\alpha 2}(P)$ with increase of pressure from 289 K at 0.1 MPa to about 351 K at 300 MPa. The increase in $T_g^{\alpha 2}(P)$ of the confined α2-relaxation with pressure indicates correspondingly large increase of $\tau_{\alpha 2}(P,T)$ with pressure. This property of $\tau_{\alpha 2}(P,T)$ is not expected a priori from the idea of confinement of

PVME by the frozen PS matrix by LAC. However, it can be reconciled by the cooperative nature of the α2-relaxation, as revealed by the detection of glass transition at $T_g^{\alpha 2}$ by DSC in other highly asymmetric mixtures and blends [16,39,54,65,78,79], and the change of the temperature dependence of $\tau_\beta(T)$ on crossing $T_g^{\alpha 2}$.

5. Corroborating evidences from other polymer blends

Solid evidences have been given to demonstrate the mistakes made by others in identifying the resolved fast relaxation as the confined α2-relaxation, instead of the JG β-relaxation, in highly asymmetric blends [24,25,45-47,56,58,86] and mixtures [81-85] with large ΔT_g. In these systems, the propensity of the high-T_g component makes it easy to detect the higher glass transition temperature $T_g^{\alpha 1}$ by DSC, but not $T_g^{\alpha 2}$. The situation led others to assume that the low-T_{g2} component are *entirely* confined by the frozen high-T_{g1} component at temperatures sufficiently far below $T_g^{\alpha 1}$, and resulting in a *single* localized relaxation with Arrhenius temperature dependence for its relaxation times $\tau_{\alpha 2}$. Thus, a critical evidence to expose the mistake is the presence of a slower relaxation also originating from the low-T_{g2} component coexisting with the resolved fast relaxation at temperatures sufficiently below $T_g^{\alpha 1}$. It comes from the detection of a second glass transition temperature $T_g^{\alpha 2}$ lower than $T_g^{\alpha 1}$ by TSDC [26], dielectric relaxation [29], adiabatic calorimetry [88], or conventional DSC [16,39,54,65,78,79], indicating the presence of another process below $T_g^{\alpha 1}$ with relaxation time of the order of 100 s or longer. This process is distinctly different from the resolved fast relaxation since the value of its relaxation time $\tau_f(T)$ at $T=T_g^{\alpha 2}$ is many orders of magnitude shorter than 100 s (see Fig.22b). The fact that at $T_g^{\alpha 2}$ we have two relaxations with widely different relaxation times clearly contradicts a single

relaxation from the hypothesis of the low-T_g component is *entirely* confined by the frozen high-T_g component [24,25,45-47,56,58,86]. In the following we present experimental observation of $T_g^{\alpha 2}$ in other polymer blends, and in some cases the concurrent presence of the JG β-relaxation, for the purpose of showing the generality of our interpretation.

5.1 *x*PEO-(1-*x*)PMMA blends

These blends were studied by many different groups, and the various results are collected together in this section to bring out the facts *in toto*. We start with the DSC measurements of Floudas and coworkers [39] Lodge and coworkers [54], and Goulart Silva et al. [16], all of them detected two glass transitions at $T_g^{\alpha 2}$ and $T_g^{\alpha 1}$. Shown in Fig.25a is the derivative dC_p/dT of the specific heat taken from Ref.[39] whereby detected are the two glass transitions at $T_g^{\alpha 2}$ and $T_g^{\alpha 1}$ for two blends with c_{PEO}=30 and 20%. These values together with those for other compositions are plotted against c_{PEO} in Fig.25b. In the relaxation map of Fig.26, the magenta star placed at 100 s is supposed to represent the α2-relaxation time $\tau_{\alpha 2}$ of the PEO component at 1000/$T_g^{\alpha 2}$ with $T_g^{\alpha 2}$=245 K in the 20% PEO–80% PMMA blend. The α2-relaxation of the PEO component was not resolved in the dielectric studies of Runt and coworkers [21,22] because it is obscured by the dielectric loss over broad frequency range from the JG β-relaxation of the PMMA component. However, it was observed in blends of perdeuteriopoly(ethylene oxide) (d4PEO) and PMMA using deuteron NMR over the concentration range from 0.5 to 100% d4PEO with Larmor frequencies ranging from 31 to 76 MHz [23,27,28] discussed before and shown in Fig.S6. The α2-relaxation times $\tau_{\alpha 2}$ of the 20%PEO-80%PMMA blends from deuteron NMR are shown again in Fig.26, together with QENS data of Sakai et al. [51,52]. The closed and open red circles are the faster and the slower α2-relaxation times found in QENS experiment of Sakai et

al. at Q = 1.3 Å^{-1} [48]. The faster α2-relaxation is identifiable with the primitive relaxation of the CM [80,97], and its relaxation time is related to the slower α2-relaxation by the CM Eq.(2), like that between τ_0 and τ_α. In the inset, in addition to the same symbols and line in the main figure, we show by asterisks the QENS data for PEO in the 25/75 blend from QENS at Q=1.02 Å^{-1} by Genix et al. (appear in Fig.6 of Ref.[52]), and the other symbols are other QENS data of Sakai et al. [48].

Absence are the dielectric data of $\tau_{\alpha 2}$ over the range $10^{-10} < \tau_{\alpha 2} < 10^2$ s. Although a VFT function can be found to fit the deuteron NMR data and for it to reach $\tau_{\alpha 2}(T_g^{\alpha 2})$=100 s at $T_g^{\alpha 2}$=245 K from DSC as shown by the pale blue line [80], the high value of about 140 for the fragility index m is not expected for the confined α2-relaxation in the frozen PMMA matrix. Also from Property 2, the temperature dependence of confined $\tau_{\alpha 2}(T)$ is Arrhenius-like at temperatures not too far above $T_g^{\alpha 2}$. So the blue line in Fig.26 may better represent $\tau_{\alpha 2}(T)$ in the range of $10^{-10} << \tau_{\alpha 2} < 10^2$ s, similar to the Arrhenius T-dependence of $\tau_{\alpha'}(T)$ of 50%MTHF in PS60k in Fig.6. Dielectric relaxation measurements of the 20% PEO blend with PMMA made by Runt and coworkers [21,22] observed a secondary relaxation having practically the same relaxation times as in pure PEO, and identifiable as the JG β-relaxation of PEO in the blend. Most of its relaxation times, τ_β, were obtained at temperatures lower than the range in Fig.26. The full set of data of τ_β are shown in Fig.S12 in the SI. Notwithstanding, by showing some values of τ_{JG} at higher temperatures in Fig.26, the presence of the three major processes, the α1-relaxation, the confined α2-relaxation, and the JG β-relaxation, is clear, as well as Property 2.

We have discussed in Section 2.1(B), and in Fig.10 of Ref.[46] or Fig.S4 in SI, that Tyagi et al. suggested Arrhenius temperature dependence of $\tau_{\alpha 2}(T)$ in 20% PEO in PVAc as well as

25%PEO in PMMA (from Genix et al.[45]) based on two data points (labeled τ^*) shorter than 100 ps in each case, and used the Arrhenius dependence as microscopic evidence for the dynamic confinement effects. The joint fit of τ^* for PEO in PVAc and PMMA to an Arrhenius law leads to a prefactor of 3.4×10^{-15} s and an activation energy of 0.26 eV [46].

The QENS data of Sakai et al. [48,51,52] are more substantial than Genix et al., and their data show the presence of a faster and a slower relaxation (see Fig.26). The relaxation times of the slower relaxation for the scattering vector Q = 1.3 Å^{-1} are consistent the VFT dependence of deuteron NMR, and also the two data points of Genix et al. The faster one is the primitive relaxation of the CM [80]. The deuteron NMR data and the QENS data of Garcia-Sakai et al. are all showing VFT dependence [80], and rule out the Arrhenius dependence deduced from two data points by Tyagi et al. to surmise that the dynamics of PEO is already confined at relaxation times shorter than 100 ps.

The detection of a fast relaxation with exp(-t/τ_0) time dependence changing over to exp $[-(t/\tau_\alpha)^{1-n}]$ at t_c=1 ps of PEO in blends with PMMA by Garcia–Sakai is verification of the crux of the CM [104-109], in addition to other QENS experiments and simulations in other polymers [110,111] and van der Waals glass-formers [97]. By the way, the CM was used [28] to explain the insensitivity of the NMR relaxation time $\tau_{\alpha 2}(T)$ to composition of the blend that range from 3% to 30% PEO [27]. These experimental results from QENS and deuteron NMR studies of the x%PEO-(1-x)PMMA blends and relations to the CM had been discussed before in Refs.[28,80], and there is no need to repeat them here.

Urakawa and coworkers [113] studied viscoelastic and dielectric relaxation behavior of poly(ethylene oxide)/poly(vinyl acetate)/ (x%PEO-(1-x)PVAc) and x%PEO-(1-x)PMMA blends and determine the effective glass transition temperature $T_{g,eff}$ of the PEO component, equivalent

to our $T_g^{\alpha 2}$, down to low values of x. Their results in Fig.27 show monotonic increase of $T_{\mathrm{g,eff}}$ down to low concentrations of PEO, and contradict the existence of a maximum suggested by Kahlau et al. [81], Bock et al. [82,83,85], and Pötzschner et al.[84].

5.2 *x*PI-(1-*x*)PtBS blends

Zhao et al. [60] studied the miscible blends of polyisoprene (PI) and poly(4-tert-butylstyrene) (P4tBS) very large ΔT_g ~215 K over a broad composition range. Two distinct calorimetric glass transitions were observed in blends of with concentration of PI as low as 25% by both conventional and temperature-modulated DSC, and the values of $T_g^{\alpha 1}$ and $T_g^{\alpha 2}$ are shown in Fig.28a. The fits of the component T_g values to the Lodge-McLeish model [18] gives a value of 0.63 for the self-concentration φ_{self} for the PI in this blend significantly larger than values reported for PI in other blends with smaller ΔT_g, but comparable to reported values for PEO in blends with PMMA also having large ΔT_g [27,32,54]. The difficulty of reconciling the large value of φ_{self} found in blends of large ΔT_g led Zhao et al. to interpret their results as due to confinement of the fast PI component below the $T_g^{\alpha 1}$ of the slow component in P4tBS in the 25% PI blend. The change from VFT-dependence to Arrhenius T-dependence of the relaxation time $\tau_{\mathrm{B}}(T)$ or $\tau_2(T)$ of the confined PI with molecular weight of 10 k at temperatures sufficiently below $T_g^{\alpha 1}$was suggested by Zhao et al. and reproduced in Fig.28b, which is modified from their Fig.6. The T_{g2} of pure PI and two JG β-relaxation times $\tau_{\mathrm{JG}}(T)$ are added to the figure. The latter are determined from the dielectric spectra of PI with molecular weight of 21 k [89] in Fig.28c, and assumed to be the same in the blend based on Property 11. The presence of the α1, α2, and JG β-relaxation in the blend is clear. The activation energy ≈ 1.4 eV of the confined α2-relaxation from Zhao et al. in Fig.28b is much larger than that of the JG β-relaxation, and thus it

preempts mistaking the latter as the former. It is an order of magnitude larger than 0.26 eV, the activation energy of the purported confined PEO in blends with PVAc and PMMA, obtained from two QENS data points by Tyagi et al. [46] in their Fig.10, or Fig.S4 in SI.

Arrese-Igor et al. [65] also studied miscible blends of polyisoprene (PI) with T_{g2}=204 K and poly(tert-butylstyrene) (PtBS) with T_{g1}=330 K and 373 K for PtBS1300 and PtBS2300 respectively over the entire composition range by DSC and dielectric relaxation. The dielectric loss of PI is almost 2 orders of magnitude larger than that of PtBS, and therefore the dielectric measurements of the PI/PtBS blends sense principally the PI component dynamics in the blend. The difference, ΔT_g, between T_{g1} and T_{g2} of the two blends is 126 K and 169 K, respectively comparable to or larger than 120 K in the case of the blends of PVME with PS. Since ΔT_g of the PI/PtBS blends is even larger than the PVME/PS blends, the localized motions with Arrhenius *T*-dependence of its relaxation time with low activation energy proposed by Lorthioir et al. should be found in 20%PI-80%PtBS blend if the proposal is correct. The dielectric relaxation times of the PI component in the 20%PI-80%PtBS and 35%PI-65%PtBS blends from the study by Arrese-Igor et al. are shown in Fig.29 and Fig.30 constructed by us. The inset in each figure show calorimetric measurements showing the presence of two glass transitions from the PI component at $T_g^{\alpha 2}$ and the PtBS components at $T_g^{\alpha 1}$. The value of $T_g^{\alpha 2}$ from DSC are compatible with dielectric $T_g^{\alpha 2}$ estimated from the dielectric α2-relaxation time $\tau_{\alpha 2}(T)$ at 100 s (see Figs.29 and 30), and thus the calorimetric and dielectric measurements are complementary. The temperature dependence of $\tau_{\alpha 2}(T)$, whether VFT-like or returning to Arrhenius at lower temperatures before reaching $T_g^{\alpha 2}$, is much stronger than the Arrhenius activation energy of localized motion of PI confined in frozen PtBS chains according to the proposal of Lorthioir et al. The reader may recall the value of the activation energy E_a of the $\tau_f(T)$ for the 20%PVME

blend with PS in Fig.22d, interpreted as the confined PVME relaxation by frozen PS, is 7869 K in temperature units, and the ratios, $E_a/T_g^{\alpha 2}$=26.9 and $E_a/T_g^{\alpha 1}$=23.3 is typical of JG β-relaxation. On the other hand, the activation energy E_a of $\tau_{\alpha 2}(T)$ in 20%PI blend with PtBS in Figs.29 and 30 is estimated to be 5 to 7 times higher, and the ratios $E_a/T_g^{\alpha 1}$ and $E_a/T_g^{\alpha 2}$ are much larger than expected for localized relaxation. From other experimental studies of PI [102], we know the JG β-relaxation has low dielectric strength and broad frequency dispersion, and is barely resolved in dielectric measurements. Its dielectric strength is much reduced in the 20%PI-80%PtBS, and understandably it is not easy to resolve it. Nevertheless, it has to be present because the α1 and α2 relaxations would not transpire without it acting as the precursor.

6. Conclusions

The much larger difference in the glass transition temperatures of the two components, $\Delta T_g = T_{g1} - T_{g2}$, in highly asymmetric miscible mixtures and polymer blends is definitely the major factor determining the dynamics and thermodynamic properties. In mixtures and blends where the ΔT_g is not too large (e.g. less than 100 K), usually observed is a single glass transition temperature coming from a single structural α-relaxation accompanied by a secondary relaxation having with various strong connections in properies to the former, and hence belong to the class called the Johari-Goldstein (JG) β-relaxations [92,93]. Satisfactory explanation of the dynamics of the α- and the JG β-relaxation and how it changes with composition was given by the Coupling Model. The dynamics and thermodynamics in highly asymmetric mixtures and blends where ΔT_g is large (e.g., 200 K or more) are more complex particularly at low concentration c_2 of the lower-T_{g2} component. The results obtained experimentally by various spectroscopies in different highly asymmetric mixtures and blends are not uniformly the same. In some mixtures and blends at low

concentrations c_2 of the low-T_{g2} component, only the α1-relaxation and its associated glass transition at $T_g^{\alpha 1}$ (contributed mainly from the high-T_{g1} component) were found together with a fast relaxation having approximately an Arrhenius temperature dependence for its relaxation time at low temperatures. This scenario led other to propose that it is the α2-relaxation of the low-T_{g2} component drastically modified due to confinement by the frozen high-T_{g1} component, and transforming it to local relaxation within the confined spaces. Moreover, they identified the confined local relaxation with the observed fast relaxation. On the other hand, two α-relaxations, α1 and the α2, and the corresponding glass transition temperatures, $T_g^{\alpha 1}$ and $T_g^{\alpha 2}$, were found in some highly asymmetric mixtures and blends, with and without the presence of the JG β-relaxation. The confusing experimental situations are clarified in this paper by considering the results from the most comprehensive experimental studies of highly asymmetric mixtures by Blochowicz and coworkers using dielectric, photon correlation, and neutron scattering spectroscopies in conjunction with calorimetry. Covering over 14 orders of magnitude of relaxation time and wide temperature range in the studies, they were able to find all three relaxations, α1, α2, and JG β. Moreover, the properties of the three relaxations were delineated, and the strong connections of the JG β-relaxation with each of the two α-relaxations were found and verified in accord with the Coupling Model. The results enable us to formulate 11 properties of the dynamics and thermodynamics of the components in highly asymmetric mixtures and polymer blends at low concentration of the low-T_{g2} component. Using these properties we revisit several highly asymmetric mixtures and polymer blends and show the following general results. (1) All the three relaxations, α1, confined α2, and JG β-relaxation are present although either the confined α2-relaxation or the JG β-relaxation may not be resolved. (2) The glass transition temperatures $T_g^{\alpha 2}$ associated with the low-T_{g2} component is present indicating that the confined

α2-relaxation is cooperative, although it is not always possible to detect $T_g^{\alpha 2}$ by calorimetry. (3) The relaxation time $\tau_{\alpha 2}$ of the confined α2-relaxation has approximately Arrhenius temperature dependence for temperatures not far above $T_g^{\alpha 2}$. (4) The JG β-relaxation is strongly connected in its properties with the α1-relaxation as well as with the confined α2-relaxation, and the connections are as predicted by the Coupling Model. (5) The value of $T_g^{\alpha 2}$ is found to increase with pressure and hence also $\tau_{\alpha 2}$ of the confined α2-relaxation, which is somewhat a surprise in view of it is described as confined, but consistent with the fact that it is a cooperative process. (6) The last but not the least, we show that a mistake was made by others in identifying the resolved JG β-relaxation as the unresolved confined α2-relaxation in mixtures and polymer blends where only the α1-relaxation and a fast relaxation were resolved. The mistake led to a wrong interpretation of the dynamics in mixtures and polymer blends, and the error of finding a maximum in the temperature dependence of $T_g^{\alpha 2}$ as a function of c_2 instead of a monotonic dependence.

References

[1] D.J. Plazek, E. Riande, H. Markovitz, N. Raghupathi, J. Polym. Sci. Poly. Phys. 17 (1979) 2189.

[2] R. H. Colby, Polymer 30 (1989) 1275.

[3] A. Zetsche, W. Jung, F. Kremer, H. Schulze, Polymer 31 (1990) 1883.

[4] C. M. Roland, K. L. Ngai, Macromolecules 24 (1991) 2261.

[5] C. M. Roland, K. L. Ngai, Macromolecules, 25 (1992) 363.

[6] A.K. Rizos, R. *M.* Johnsen, W. Brown and K.L. Ngai, Macromolecules, 28 (1996) 5450.

[7] G.-C. Chung, J.A. Kornfield, S.D. Smith, Macromolecules 27 (1994) 964.

[8] G.-C. Chung, J.A. Kornfield, S.D. Smith, Macromolecules 27 (1994) 5729.

[9] K.L. Ngai, C.M. Roland, Macromolecules,28 (1995) 4033.

[10] A, Alegria, J. Colmenero, K.L. Ngai, C. M. Roland, Macromolecules, 27 (1994) 4486.

[11] S. K. Kumar, R.H. Colby, S.H. Anastasiadis, G. Fytas, J. Chem. Phys. 105 (1996) 3777.

[12] S. Kamath, R. H. Colby, S.K. Kumar, K. Karatasos, G. Floudas, G. Fytas, and J. E. L. Roovers, J. Chem. Phys. 111 (1999) 6121.

[13] S. Kamath, R.H. Colby, S.K. Kumar et al., J. Chem. Phys. 111 (1999) 6121.

[14] E. von Meerwall, E.J. Feick, R. Ozisik, W.L. Mattice, J. Chem. Phys. 111 (1999) 750.

[15] A. Arbe, A. Alegria, J. Colmenero, S. Hoffmann, L. Willner, D. Richter, Macromolecules, 32 (1999) 7572.

[16] G. Goulart Silva, J. C. Machado, M. Song, D.J. Hourston, J. Appl. Polym. Sci. 77 (2000) 2034.

[17] C.M. Roland, K.L. Ngai, Macromolecules 33 (2000) 3184.

[18] T. P. Lodge, T. C. B. McLeish, Macromolecules 33 (2000) 5278.

[19] O. Urakawa, Y. Fuse, H. Hori, Q. Tran-Cong, O. Yano, Polymer, 42 (2001) 765.

[20] Paul, D. R.; Bucknall, C. B. Polymer Blends; Wiley-Interscience: New York, (2000).

[21] S. Zhang, X. Jin, P.C. Painter, J. Runt, Macromolecules 35 (2002) 3636.

[22] Jin, X.; Zhang, S.; Runt, J. Polymer 43 (2002) 6247.; J. Macromolecules 37 (2004) 8110.

[23] C. Lartigue, A. Guillermo, J. P. Cohen-Addad, J. Polym. Sci. Part B: Polym. Phys. 35 (1997) 1095.

[24] C. Lorthioir, A. Alegrıa, J. Colmenero, Phys. Rev. E 68 (2003) 031805.

[25] C. Lorthioir, A. Alegrıa, J. Colmenero, Eur. Phys. J. E 12 (2003) S127.

[26] E. Leroy, A. Alegrı´a, J. Colmenero, Macromolecules 35 (2002) 5587.

[27] T.R. Lutz, Y.Y. He, M.D. Ediger, H.H. Cao, G.X. Lin, A.A. Jones, Macromolecules 36 (2003) 1724.

[28] K.L. Ngai, C.M. Roland, Macromolecules 37 (2004) 2817.

[29] N. Taniguchi, O. Urakawa, K. Adachi, Macromolecules 37 (2004) 7832.

[30] K.L. Ngai, S. Capaccioli, J. Phys. Chem. B 108 (2004) 11118.

[31] O. Urakawa, T. Sugihara, K. Adachi, Polym. Appl. (Japan) 51 (2002) 10.

[32] J. C. Haley, T. P. Lodge, J. Chem. Phys. 122 (2005) 234914.

[33] D. Bedrov, G.D. Smith, Macromolecules 38 (2005) 10314.

[34] D. Bedrov, G.D. Smith, Macromolecules 39 (2006) 8526.

[35] K. L. Ngai, S. Capaccioli, C. M. Roland, Macromolecules, 39 (2006) 8543.

[36] K.L. Ngai, S. Capaccioli, J. Phys. Condens. Matter 19 (2007) 205114.

[37] K.L. Ngai, S. Capaccioli, J. Phys. Chem. B 108 (2004) 11118.

[38] G.D. Smith, D. Bedrov, J. Polym. Sci. B 45 (2007) 627.

[39] K. Mpoukouvalas, G. Floudas, Macromolecules, 41 (2008) 1552.

[40] Y. Y. He, T. R. Lutz, M. D. Ediger, Macromolecules, 37 (2004) 9889.

[41] K. L. Ngai, C. M. Roland, Rubber Chem. Technol. 77 (2004) 579.

[42] Y. Y. He, T. R. Lutz, M. D. Ediger, M. Pitsikalis, N. Hadjichristidis, E. A. von Meerwall, Macromolecules 38 (2005) 6216.

[43] J. C. Haley, T. P. Lodge, Y. Y. He, M. D. Ediger, E. D. von Meerwall, J. Mijovic, Macromolecules, 36 (2003) 6142.

[44] R.H. Colby, J.E.G. Lipson, Macromolecules 38 (2005) 4919.

[45] A. C. Genix, A. Arbe, F. Alvarez, J. Colmenero, L. Willner, D. Richter, Phys. Rev. E, 72 (2005) 031808.

[46] M. Tyagi, A. Arbe, J. Colmenero, B. Frick, J. R. Stewart, Macromolecules 39 (2006) 3007.

[47] A.-C. Genix, A. Arbe, S. Arrese-Igor, J. Colmenero, D. Richter, B. Frick, P. P. Deen, J. Chem. Phys. 128 (2008) 184901.

[48] Garcia Sakai, V.; Chen, C.; Maranas, J. K.; Chowdhuri, Z. Macromolecules 37 (2004) 9975.

[49] A. Neelakantan, J. K. Maranas, J. Chem. Phys. 120 (2004) 465.

[50] A. Neelakantan, J. K. Maranas, Chem. Phys. 120 (2004) 1617.

[51] V.G. Sakai, J.K. Maranas, Z. Chowdhuri, I. Peral, J.R.D. Copley, J. Polym. Sci. B Polym. Phys. 43 (2005) 2914.

[52] V.G. Sakai, J.K. Maranas, I. Peral, J.R.D. Copley, Macromolecules 41 (2008) 3701.

[53] S. Capaccioli, K L Ngai, J. Phys. Chem. B 109 (2005) 9727.

[54] T. P. Lodge, E. R. Wood, J. C. Haley, J. Polym. Sci.: Part B: Polym. Phys., 44 (2006) 756.

[55] G. A. Schwartz, J. Colmenero, A. Alegrı´a, Macromolecules 40 (2007) 3246.

[56] M. Tyagi, A. Arbe, A. Alegrı´a, J. Colmenero, B. Frick, Macromolecules 40 (2007) 4568.

[57] J. Maranas, Curr. Opin. Colloid Interface Sci. 12 (2007) 29.

[58] J. Colmenero, A. Arbe, Soft Matter 3 (2007) 1474.

[59] Junshu Zhao, Liang Zhang, M. D. Ediger, Macromolecules, 8030 (2008) 41.

[60] Junshu Zhao, M. D. Ediger, Ye Sun, Lian Yu, Macromolecules 42 (2009) 6777.

[61] H. Y. Watanabe, J. Matsumiya, H. Takada, Y. Sasaki, A. Matsushima, A. Kuriyama, T. Inoue, K. H. Ahn, W. Yu, R. Krishnamoorti, Macromolecules 40 (2007) 5389.

[62] Hiroshi Watanabe, Osamu Urakawa, Component dynamics in miscible polymer blends: A review of recent findings, Korea-Australia Rheology Journal 21 (2009) 235.

[63] K. L. Ngai, J. Non-Cryst. Solids 353 (2007) 709.

[64] D. Bedrov, W. Liu, R.H. Colby, Philos. Mag. 88 (2008) 3979.

[65] S. Arrese-Igor, A. Alegrıa, J. Colmenero, Macromolecules 43 (2010) 6406.

[66] I. Zeroni, S. Ozair, T. P. Lodge, Macromolecules 41 (2008) 5033.

[67] V. Harmandaris, K. Kremer, G. Floudas, Phys.Rev.Lett. 110, 165701 (2013)

[68] T. Blochowicz, E. A. Rossler, Phys. Rev. Lett. 92 (2004) 225701.

[69] T. Blochowicz, *Broadband Dielectric Spectroscopy in Neat and Binary Molecular Glass Formers* (Logos Verlag, Berlin, 2003), ISBN: 3-8325-0320-X.

[70] K. Kessairi, S. Capaccioli, D. Prevosto, M. Lucchesi, S. Sharifi, P. A. Rolla, J. Phys. Chem. B 112 (2008) 4470.

[71] K. Kessairi, S. Capaccioli, D. Prevosto, M. Lucchesi, P. A. Rolla, J. Chem. Phys. 127 (2007) 174502.

[72] M. Mierzwa, S. Pawlus, M. Paluch, E. Kaminska, K.L. Ngai, J. Chem. Phys. 128 (2008) 044512.

[73] S. Capaccioli, M. Paluch, D. Prevosto, Li-Min Wang, K. L. Ngai, J. Phys. Chem. Lett. 3 (2012) 375.

[74] M. Shahin Thayyil, K. L. Ngai, S. Capaccioli, D. Prevosto, J. Non-Cryst.Solids 407 (2015) 98.

[75] S. Capaccioli, K.Kessairi, M. Shahin Thayyil, D. Prevosto, M. Lucchesi, J. Non-Cryst. Solids 357 (2011) 251.

[76] S. Capaccioli, M. Paluch, D. Prevosto, L.-M.Wang, and K. L. Ngai, J. Phys. Chem. Lett. 3 (2012) 735.

[77] T. Blochowicz, S. Lusceac, S. Schramm, P. Gutfreund, B. Stühn, J. Phys. Chem. B 115 (2011) 1623.

[78] Sebastian Schramm, Thomas Blochowicz, Emmanuel Gouirand, Robert Wipf, Bernd Stühn, Yuriy Chushkin, J. Chem. Phys. 132 (2010) 224505.

[79] T. Blochowicz, S. Schramm, S. Lusceac, M. Vogel, B. Stühn, P. Gutfreund, B. Frick, Phys. Rev. Lett. 109 (2012) 035702.

[80] K. L. Ngai, S. Capaccioli, J. Chem. Phys. 138 (2013) 054903.

[81] R. Kahlau, D. Bock, B. Schmidtke, E. A. Rössler, J. Chem. Phys. 140 (2014) 044509.

[82] D. Bock, R. Kahlau, B. Pötzschner, T.Körber, E.Wagner, E. A. Rössler, J. Chem. Phys. 140 (2014) 094505.

[83] D. Bock, N. Petzold, R. Kahlau, S. Gradmann, B. Schmidtke, N. Benoit, E. A. Rössler, J. Non-Cryst. Solids 407 (2015) 88.

[84] B. Pötzschner, F. Mohamed, A. Lichtinger, D. Bock, E.A. Rössler, J. Chem. Phys. 143 (2015) 154506.

[85] D. Bock, Th. Körber, F. Mohamed, B. Pötzschner, E. A. Rössler, *Dynamic Heterogeneities in Binary Glass-Forming Systems*, in *Scaling of Relaxation Processes*, Friedrich Kremer and Alois Loidl, Eds. pp.177-201, Springer (2018) https://doi.org/10.1007/978-3-319-72706-6.

[86] Angel Alegria, Juan Colmenero, Soft Matter, 12 (2016) 7709.

[87] S. Valenti, S. Capaccioli, K. L. Ngai, J. Chem. Phys. 148 (2018) 054504.

[88] Minoru Hatase, Minoru Hanaya, Takaaki Hikima, Masaharu Oguni, J. Non-Cryst.Solids, 307-310 (2002) 257.

[89] K. L. Ngai, R. Casalini, S. Capaccioli, M. Paluch, and C. M. Roland, J.Phys.Chem. Lett. 109 (2005) 17356.

[90] S. Capaccioli, D. Prevosto, M. Lucchesi, P.A. Rolla, R. Casalini, K.L. Ngai, J. Non-Cryst. Solids, 351 (2005) 2643.

[91] D. Bedrov, and G. D. Smith, , J. Non-Cryst. Solids, 357 (2011) 258.

[92] K.L. Ngai, J. Chem. Phys. 109 (1998) 6982.

[93] K.L. Ngai, M. Paluch, , J. Chem. Phys. 120 (2004) 857.

[94] G. P. Johari, M. Goldstein, J. Chem. Phys. 53 (1970) 2372.

[95] M. Goldstein, J. Non-Cryst. Solids 357 (2010) 249.

[96] S. Capaccioli, M. Shahin Thayyil, K. L. Ngai, J. Phys. Chem. B 112 (2008) 16035.

[97] K.L. Ngai, *Relaxation and Diffusion in Complex Systems,* Springer (New York) 2011.

[98] K. L. Ngai, M. Paluch, J.Non-Cryst.Solids, 478 (2017) 1.

[99] K. L. Ngai, S. Capaccioli, D. Prevosto, Li-Min Wang, J. Phys. Chem. B, 119 (2015) 12502.

[100] K. L. Ngai, J. Habasaki, D. Prevosto, S. Capaccioli, M. Paluch, J. Chem. Phys., 137 (2012) 034511.

[101] W.Tu, S. Valenti, K.L.Ngai, S. Capaccioli, Y. D. Liu, L. M. Wang, , J. Phys. Chem. Lett., 8 (2017) 4341.

[102] Sławomir Kołodziej, Sebastian Pawlus, K. L. Ngai, Marian Paluch, Macromolecules, 51 (2018) 4435.

[103] K. L. Ngai, S. Capaccioli, J. Phys. Chem. B, 119 (2015) 5677.

[104] K.L. Ngai, Comment Solid State Phys. 9 (1979) 127.

[105] K.Y. Tsang, K.L. Ngai, Phys. Rev. E, 56 (1997) R17-R21.

[106] K.L. Ngai, S.L. Peng, K.Y. Tsang, Physica A, 191 (1992) 523.

[107] R.W. Rendell, Phys. Rev. E, 48 (1993) R17.

[108] K.Y. Tsang, K.L. Ngai, Phys. Rev. E 54 (1996) R3067.

[109] K.L. Ngai, K.Y. Tsang, Phys. Rev. E 60 (1999) 4511.

[110] J. Colmenero, A. Alegria, A. Arbe, B. Frick, Phys. Rev. Lett. 69 (1992) 478.

[111] J. Colmenero, A. Arbe, G. Coddens, B. Frick, C. Mijangos, H. Reinecke, Phys. Rev. Lett. 78 (1977) 1928.

[112] K.L. Ngai, S. Capaccioli, Phys.Rev.E 69 (2004) 031501.

[113] Osamu Urakawa, Takahiro Ujii, Keiichiro Adachi, J. Non-Cryst. Solids 352 (2006) 5042.

[114] A. Kudlik, C. Tschirwitz, S. Benkhof, T. Blochowicz, E. Rössler, Europhys. Lett. 40 (1997) 649.

[115] R. Böhmer, K. L. Ngai, C. A. Angell, D. J. Plazek, J. Chem. Phys. 99 (1993) 4201.

[116] P. Zoller and D. J. Walsh, *Standard Pressure-Volume Temperature Data for Polymers* (Technomic Publishing Company, Lancaster, PA, 1995).

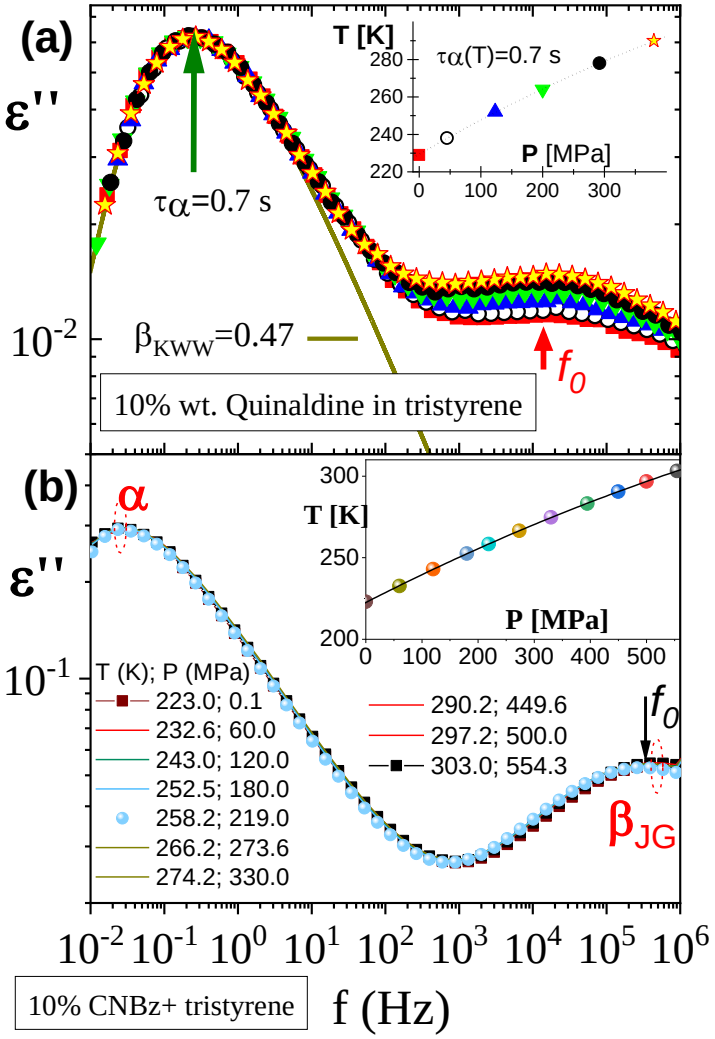

Figure 1 (a) (b). T-P superposition of isochronal loss spectra for (a) 10% wt. quinaldine in tyistyrene and (b) 10% molar fraction of cyanobenzene in trystyrene. Different pressure and temperature combinations keeping the same structural relaxation time are shown in the inset,

same symbols are used for loss spectra. The vertical arrow indicates f_0, the characteristic frequency of the primitive relaxation predicted by coupling model.

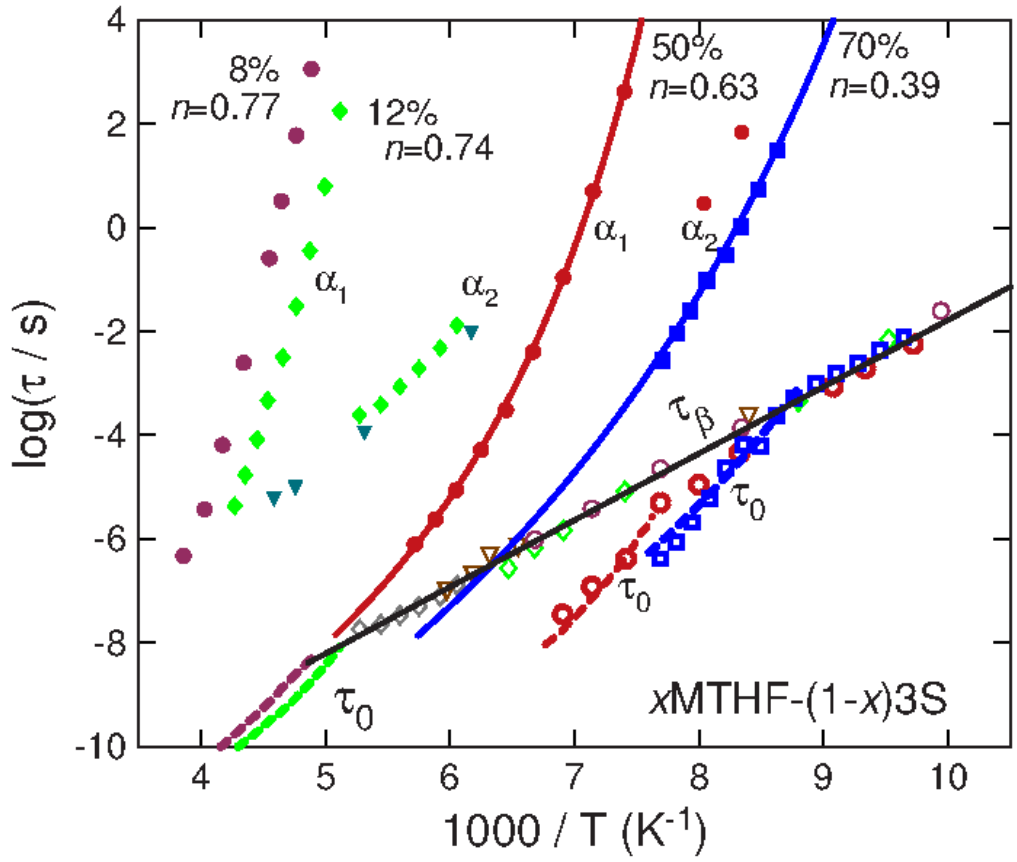

Figure 2. Relaxation times for α-process (τ_α, closed symbols) and β-process (τ_β, open symbols with the same color) at 8% (purple circles), 12% (green diamonds), 50% (red circles) and 70% (blue squares) of MTHF in tristyrene. Lines through the data points are VFT fits. The dashed lines are the primitive relaxation times, τ_0, calculated with coupling parameters *n* given in the figure (the color of each line is the same as that of τ_α and τ_β for each mixture). The thicker black line represents approximately the common Arrhenius dependence of τ_β in all four mixtures. The α_2 or α′-relaxation times, $\tau_{\alpha'}$, are represented by closed dark grey symbols: inverted triangles (6% MTHF), diamonds (12% MTHF), and circles (50% MTHF). The dark grey open diamonds lying closely on the Arrhenius line of τ_β are calculated from $\tau_{\alpha'}$ of the 12% MTHF mixture. The irrelevant δ-relaxation times in mixtures and in neat MTHF are not shown.

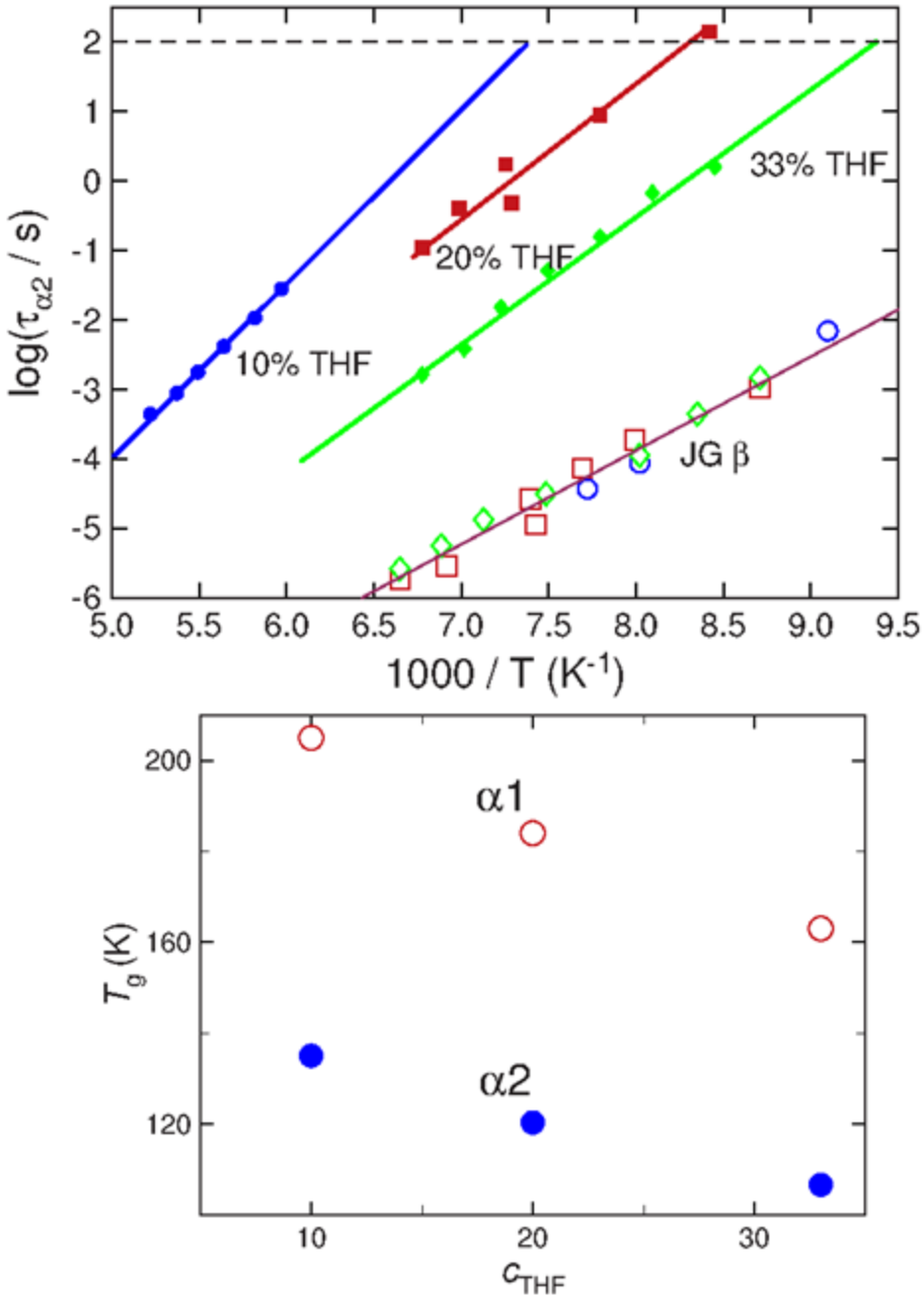

Figure 3. (Upper panel) relaxation map of α_2 or α'- and JG-relaxation time vs reciprocal temperature of THF mixtures [78]; (Lower panel) $T_g^{\alpha 1}$ and $T_g^{\alpha 2}$ as a function of THF concentration.

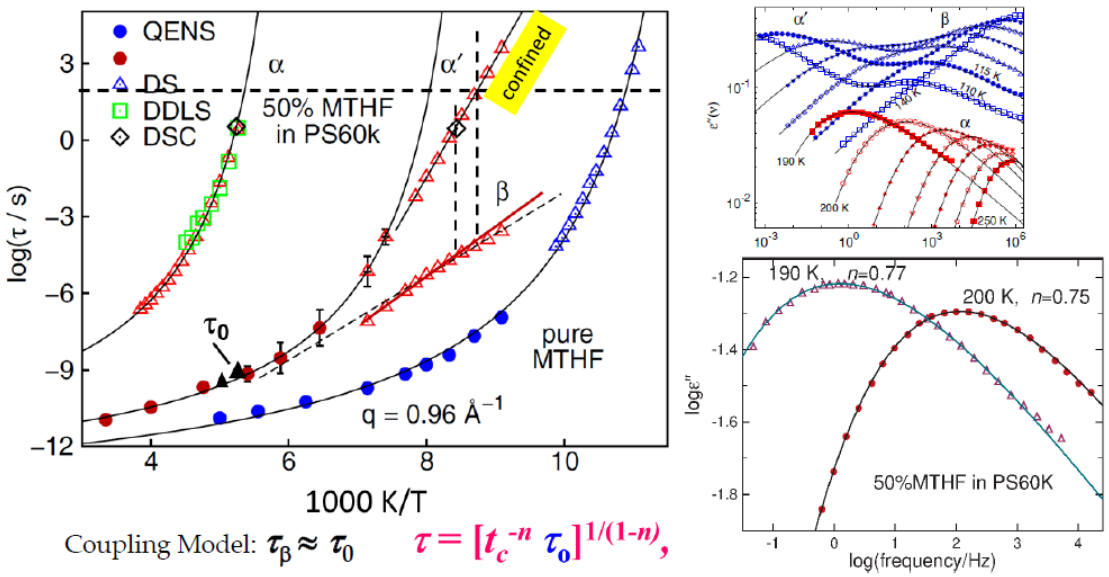

Figure 4. (Left panel): relaxation map for $\tau_{\alpha 2}(T)$, $\tau_{\alpha 2}(T)$, and $\tau_{\beta}(T)$ of the 50%wt. MTHF-PS60K mixture [79]. Thinner and thicker vertical dashed lines indicate $T_g^{\alpha 2}$ determined respectively by DSC and dielectric spectroscopy. Horizontal dashed line shows T_g defined when τ =100s. Figure modified from [79]. (Upper right panel): Loss spectra for MTHF-PS60K mixture showing all three processes. Figure reproduced from [79] with permission from APS. (Lower right panel): Fit of the loss α-peak using Fourier transform of the Kohlrausch function.

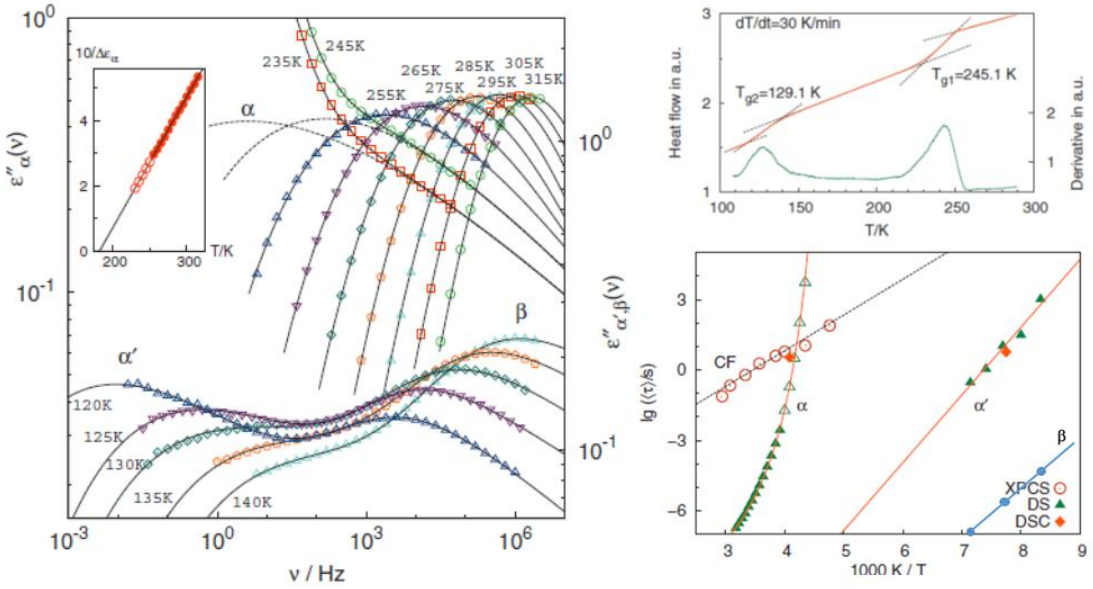

Figure 5. Data for the mixture of 40%MTHF/oligo-MMA. Figures are reproduced from ref.[78] with permission of AIP, J.Chem.Phys. (Left panel): Dielectric loss spectra at different temperatures, inset: reciprocal of dielectric strength of α-relaxation vs. temperature. (Upper right panel): DSC thermogram (red line) and its derivative (green line). ((Lower right panel): Relaxation map for α-, α'-, β-, and concentration fluctuation processes obtained with different techniques.

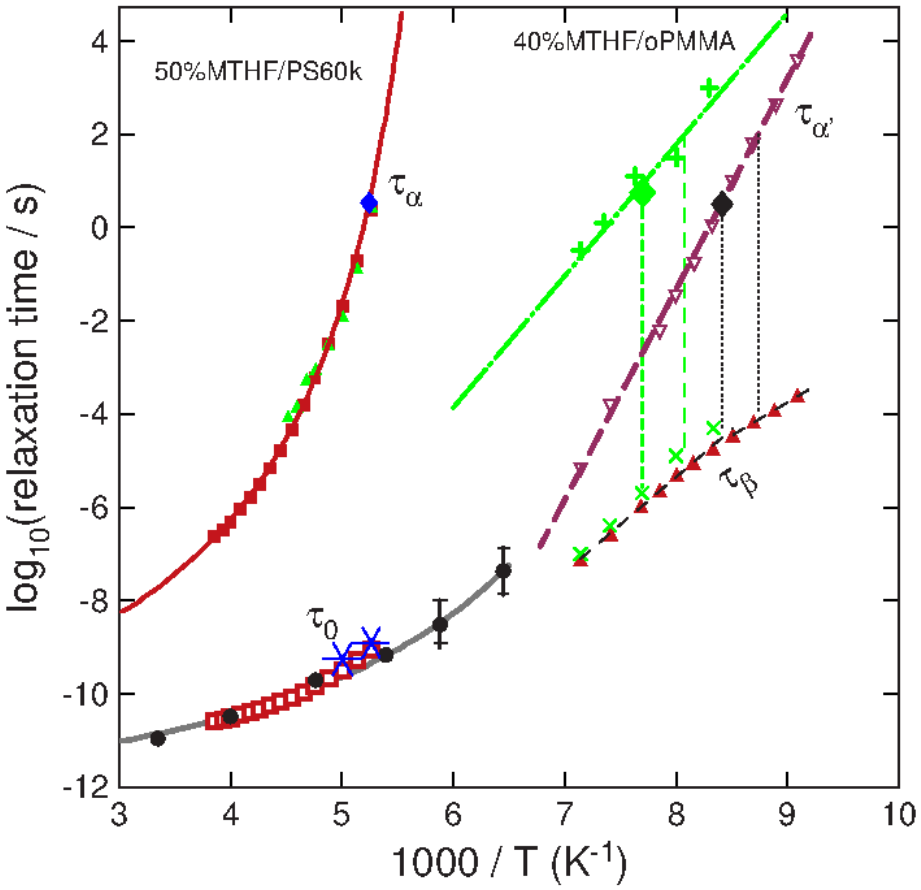

Figure 6. Relaxation map for 40%MTHF/o-MMA mixture (green symbols and lines) [78] and 50%MTHF/PS60K mixture (red symbols and lines) [79]. DSC data are represented by large solid diamonds. Dielectric relaxation data for 40%MTHF/o-MMA are green triangles for α-relaxation, green crosses for α′-relaxation, green × for *β*-relaxation; dielectric relaxation data for 50%MTHF/PS60K are shown as red solid squares for α-relaxation, red open inverted triangles for α′-relaxation, red solid triangles for *β*-relaxation. Black solid circles are QENS data for 50%MTHF/PS60K mixture. Red open squares and blue asterisks indicate the primitive relaxation time by CM obtained from dielectric and calorimetric data respectively.

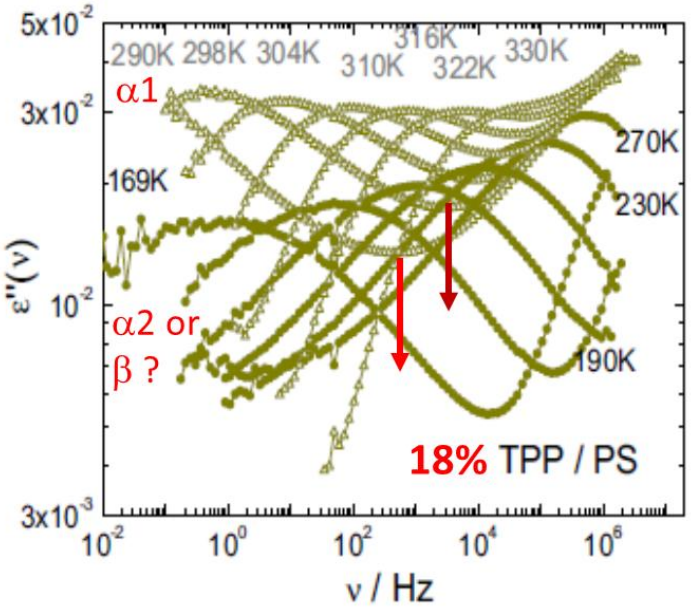

Figure 7. Dielectric loss spectra of the 18% TPP/PS mixture at different temperatures. Figure from Ref.[81] is reproduced with permission from AIP. Remarks in red are added (see text).

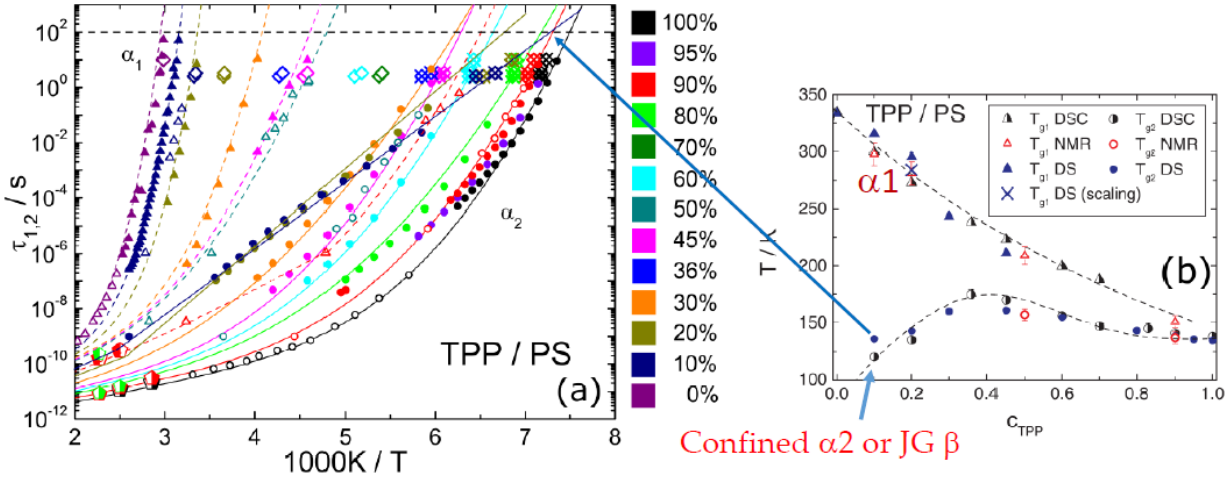

Figure 8. Left panel: Arrhenius plot of the dielectric relaxation times of the two processes in TPP/PS mixture at different TPP concentration. Right panel: T_g as obtained from DSC experiments or by extrapolating to 100 s the relaxation time obtained by different techniques. Figures reproduced from Kahlau et al [81] with permission from AIP.

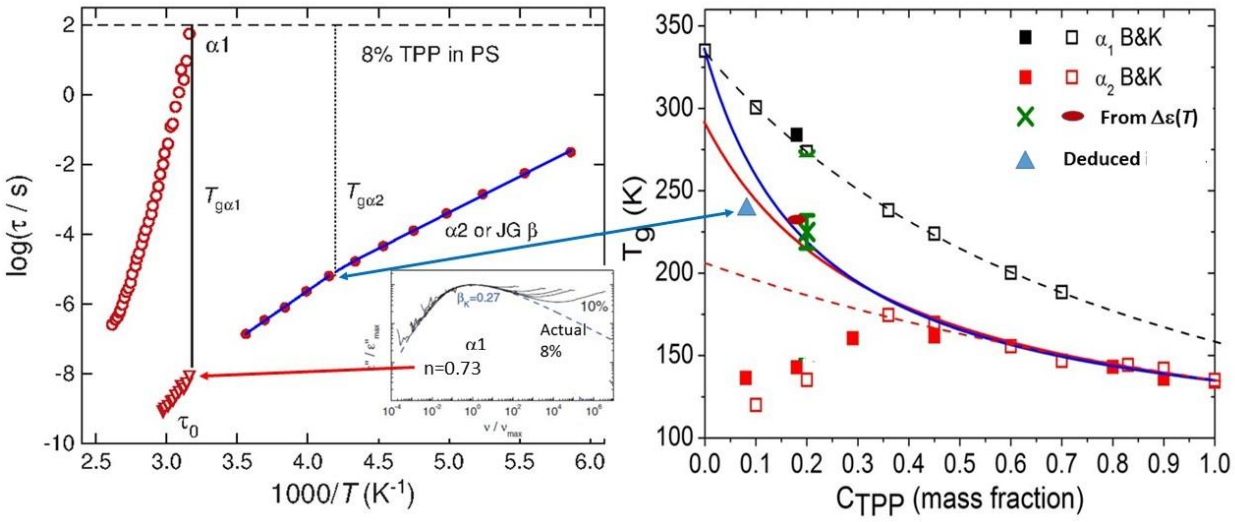

Figure 9. Left panel: relaxation map of 8%TPP in PS. Red open circles represent α1-relaxation times, red open inverted triangles represent the primitive relaxation times from CM. Red solid circles indicate α2- or JG β- relaxation times. The vertical solid line indicates $T_{g\alpha1}$ while the vertical dotted line indicate $T_{g\alpha2}$. Inset shows the superposition of α2-loss peaks fitted with Fourier transformed KWW function (n=0.73). Right panel: $T_{g\alpha1}$ and $T_{g\alpha2}$ plotted versus concentration of TPP. The data represented by the black and red symbols are reproduced from Ref. [81]. Blue triangle indicates the T_g value estimated by the change in T-dependence of $\tau_{JG\beta}$ shown in left panel. T_g values estimated from dielectric strength crossovers are: green multiplication signs obtained in ref.[87] for c_{TPP}=0.20 with (upper ×) $T_g^{\alpha1}$=268 K of α1-relaxation and (middle ×) $T_{g\alpha2}$ or $T_g^{\alpha2}$=225 K of the true α2-relaxation; red ellipse symbol indicate $T_g^{\alpha2}$=232 K of the true α2-relaxation for c_{TPP}=0.20 [81]. The blue and red lines are Gordon-Taylor fits of $T_g^{\alpha2}$ using the value of the pure fast component as $T_{g,2}$ = 135 K (that of pure TPP) and that of the slow pure component as $T_{g,1}$ = 335 K (that of pure PS 2 kg/mol) or T_{g1} = 291 K (T_g of the nano-confined PS with molecular mass=2000 g/mol), respectively.

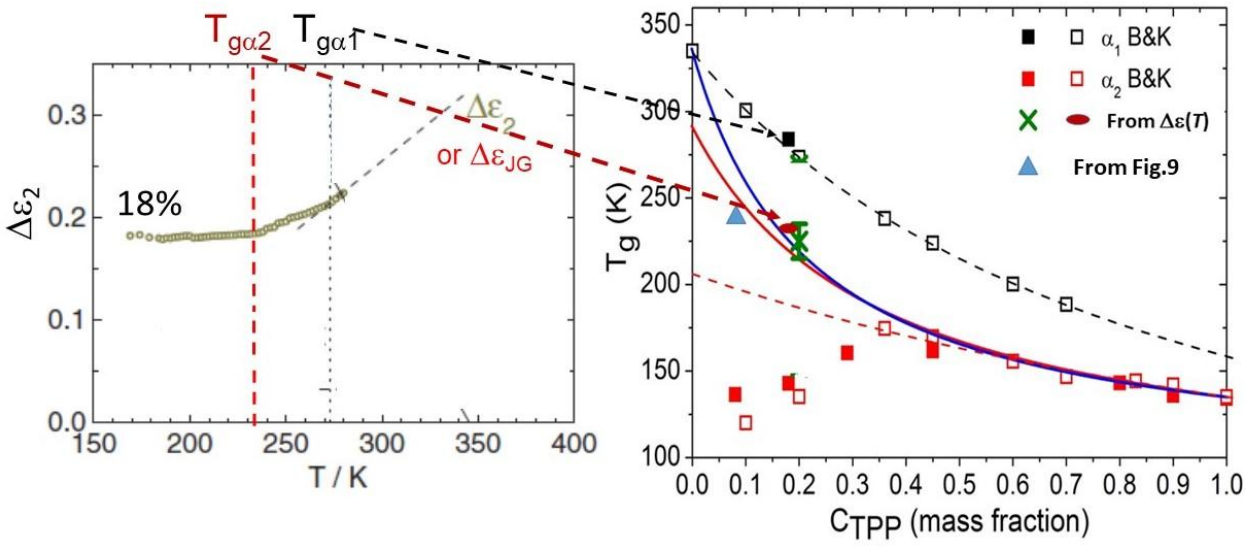

Figure 10. Left panel: Dielectric strength $\Delta\varepsilon_2$ of the purported confined α2-process shown as a function of temperature in the 18%TPP in PS mixture obtained by Kahlau et al [81]. The broken black line indicates change of *T*-dependence of $\Delta\varepsilon_{JG\beta}$ at 273 K identified with $T_g^{\alpha 1}$. The red dash-dotted line indicates a change at *T*-dependence of $\Delta\varepsilon_{JG\beta}$ at 232 K identified with $T_g^{\alpha 2}$. Figure reproduced from Ref.[81] with permission from AIP. Right panel: $T_{g\alpha 1}$ and $T_{g\alpha 2}$ plotted versus concentration of TPP, symbols are the same as in Figure 9.

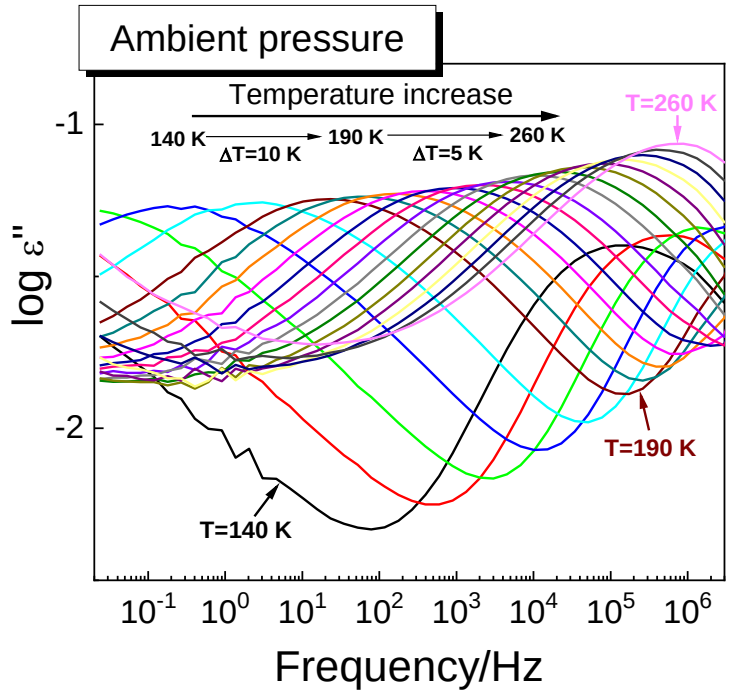

Figure 11. Dielectric loss spectra of the 20%TPP in PS mixture [87] at different temperatures from the liquid down to the glassy state.

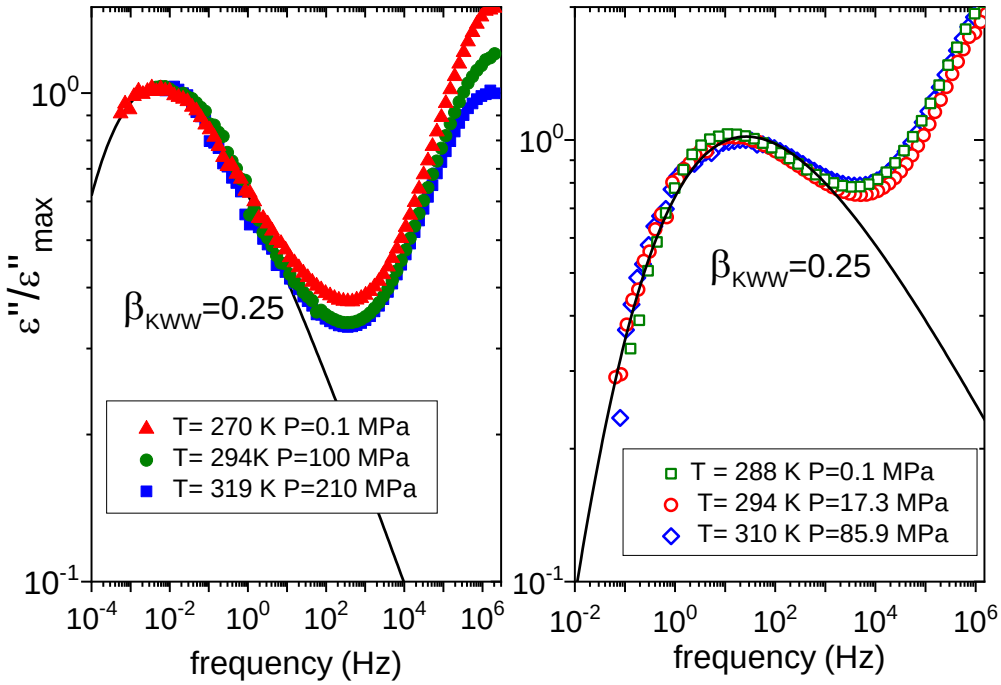

Figure 12. Superposition of spectra at different pressures and temperatures, for two different frequencies of the maximum of the peak, for the 20%TPP in PS mixture [87]. The conductivity has been subtracted in both cases. Solid black lines are fits by the Fourier transform of the KWW function.

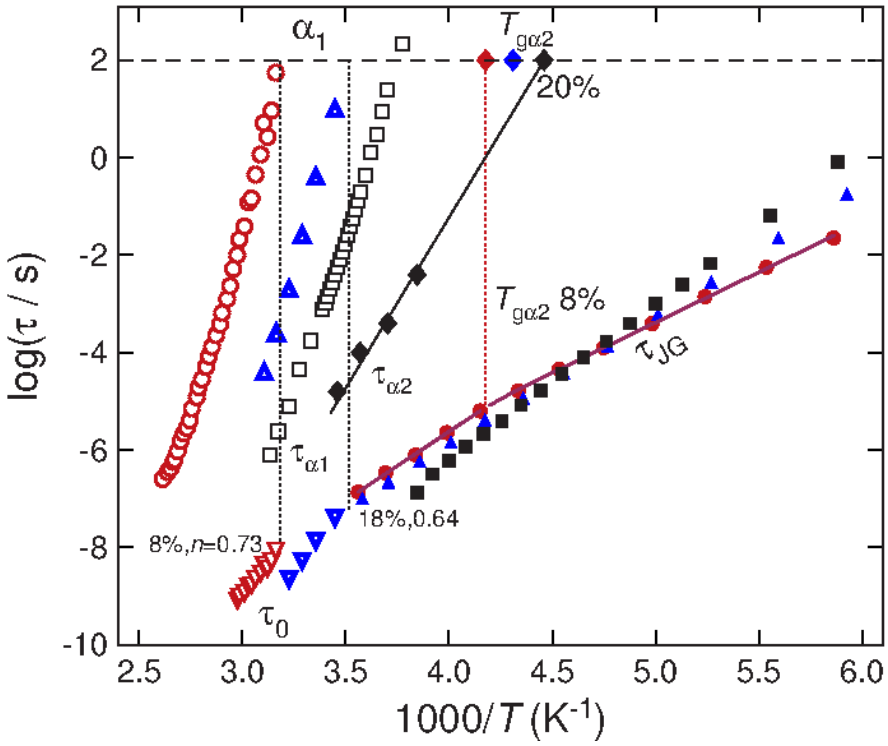

Figure 13. Relaxation map for the data of 8% (red symbols), 18% (blue symbols) and 20% (black symbols) TPP in PS mixture relaxation times: $\tau_{\alpha 1}$ are shown as open circles, open triangles and open squares, respectively. The $\tau_{\alpha 2}$ for 8%, 18% and 20%TPP are shown by red, blue and black diamonds. The τ_{β}s are shown by solid circles, triangles and squares, respectively. The inverted open triangles indicate the primitive relaxation time of the CM. The vertical dotted lines indicate $T_g^{\alpha 1}$ or $T_g^{\alpha 2}$.

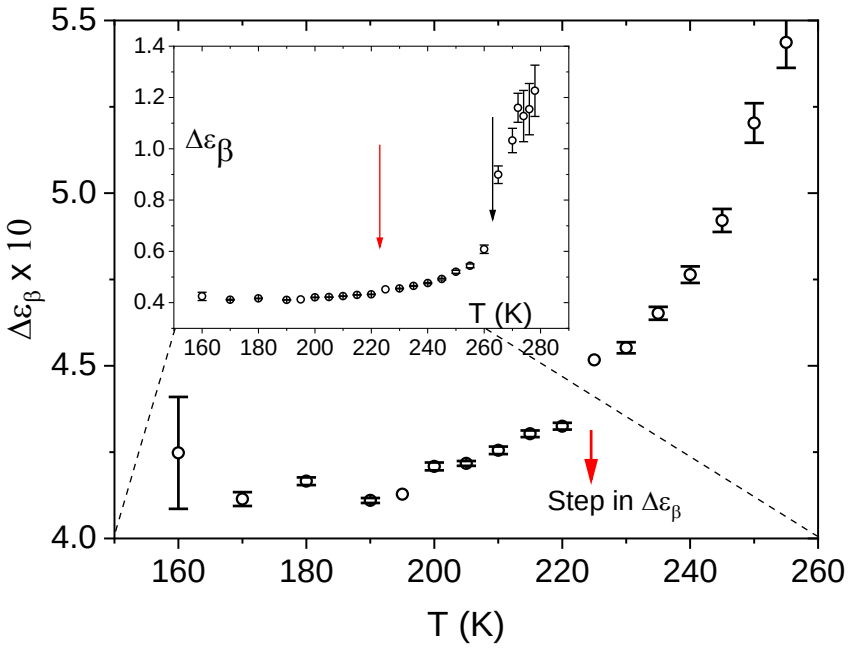

Figure 14. $\Delta\varepsilon_{JG\beta}$ or $\Delta\varepsilon_{\alpha 2}$ of 20%TPP in PS mixture as a function of temperature, zoom of the inset, which shows the whole set of temperatures. The inset shows a wider *T*-range where a sharp rise can be noticed in the neighborhood of 265 K close to $T_g^{\alpha 1}$=268 K of the α1-relaxation (black arrow), and another milder change is observable for $\Delta\varepsilon_{\beta}$ at about 223 K (red arrow) which we assigned to the $T_g^{\alpha 2}$ of the truly confined α2-relaxation from the minority TPP component.

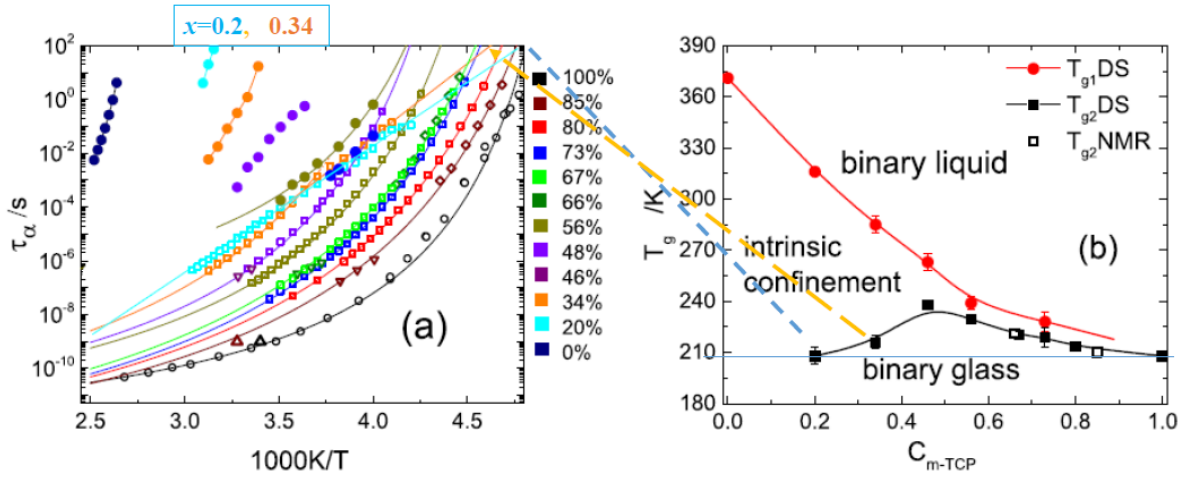

Figure 15. (a) Arrhenius plot of the dielectric relaxation times of the two processes in TCP/ DH379 mixture at different TCP concentration. Solid and open symbols represent $\tau_{\alpha 1}$ and $\tau_{\alpha 2}$ (labelled as the relaxations dominated by the majority DH379 and TCP component), respectively. (b): T_g as obtained from dielectric spectroscopy or NMR experiments by extrapolating to 100 s the relaxation time. Figures reproduced from Pötzschner et al. [84] with permission from AIP.

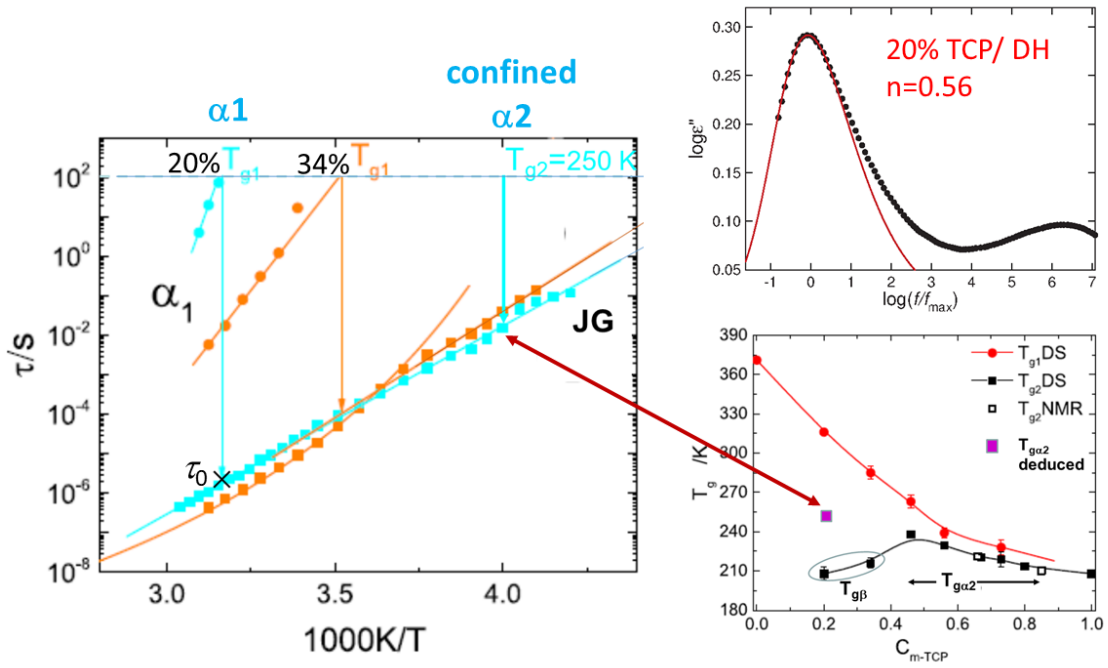

Figure 16. Left panel: Arrhenius plot of the α1 and JG β-relaxation times of TCP/ mixture at 20% (cyan symbols) and 34% (orange symbols) TCP concentration [84]. Solid and open symbols represent $\tau_{\alpha 1}$ and $\tau_{\alpha 2}$ (labelled as the relaxations dominated by the majority DH379 and TCP component), respectively. The black cross represents the primitive relaxation time predicted by CM. (upper right panel): Logarithm of dielectric susceptibility at 320 K for the $c_{\text{m-TCP}}$ = 20% sample plotted against log($f/f_{\max}$) taken from Ref.[84]. The line is the fit of the α1-relaxation by the Fourier transform of the Kohlrausch function with n=0.56. (lower right panel): T_g as obtained from dielectric spectroscopy or NMR experiments by extrapolating to 100 s the relaxation time. Figures reproduced from Pötzschner et al. [84] with permission from AIP.

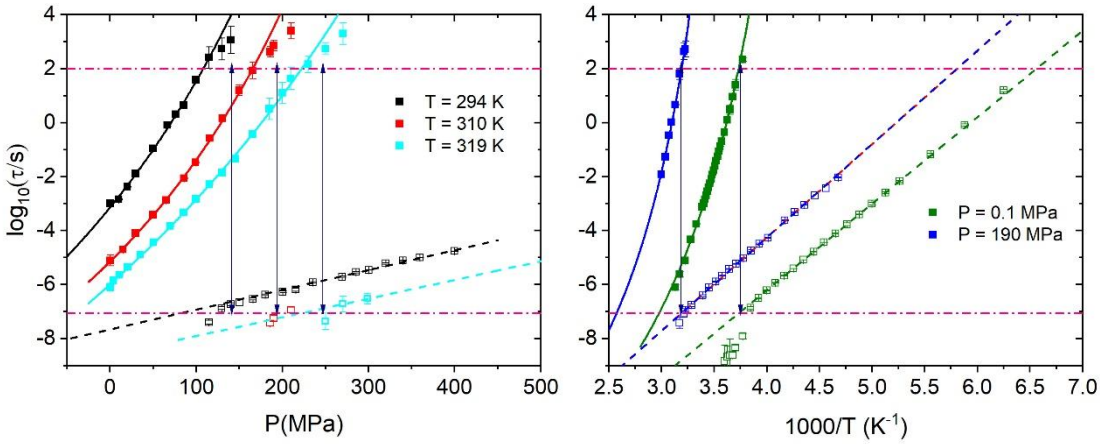

Figure 17. Relaxation map for 20%TPP in PS mixture: isotherms are shown on the left panel, while isobars on the right. Solid points represent relaxation times of the α1-relaxation, while open points of the JG β-relaxation. Also shown are the fits of the α1-relaxation with the Vogel-Fulcher-Tammann equation (solid lines), while the JG β-relaxation times have been fitted with an Arrhenius law.

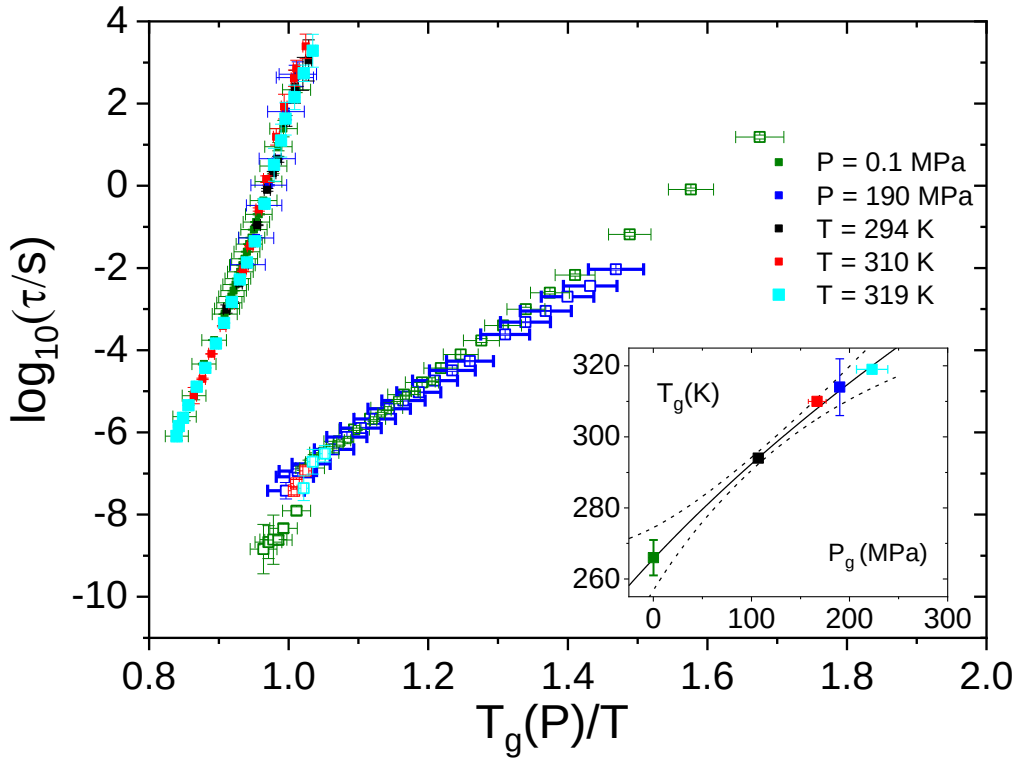

Figure 18. Master plot of the relaxation times for all temperatures and pressures data shown in Fig.17, with temperature rescaled by $T_g(P)$. Inset shows the dependence of $T_g(P)$, the solid line is the fit by the Andersson - Andersson function, dashed lines mark the confidence bands.

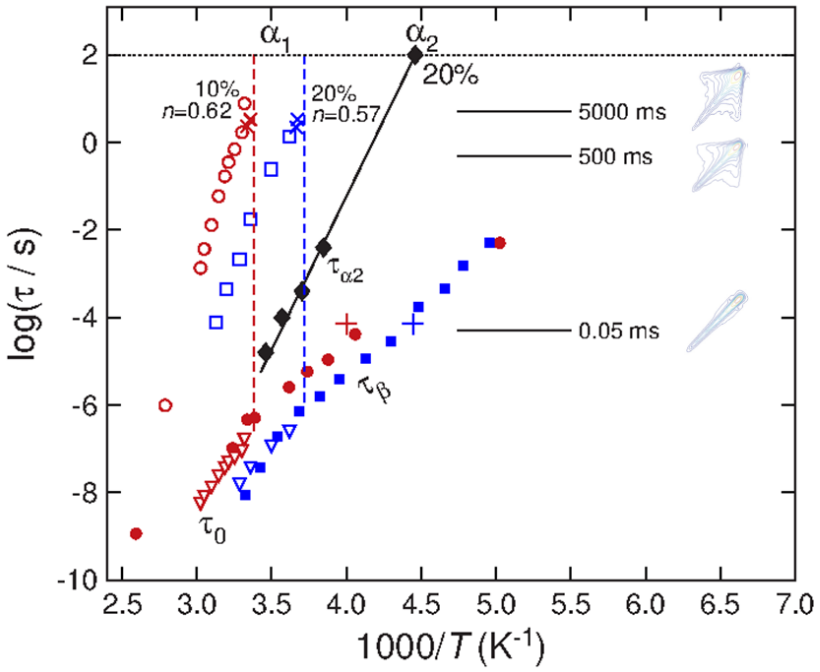

Figure 19. Relaxation map from NMR data [82, 83] for 10% and 20% TPP in mixture with PS, represented by red and blue symbols respectively. Open and solid symbols indicate α1 and JG β relaxation times, respectively. α2 relaxation times of the minority TPP component for 20%TPP mixture are represented by solid black diamonds. The inverted triangles are the calculated primitive relaxation by CM. The red and blue (×) crosses are data form DSC and the red and blue (+) crosses are from solid echo for 10% and 20% TPP concentration respectively. On the right side of the figure are the 2D ^{31}P NMR spectra of TPP for mixture with *cTPP* = 20% with mixing times indicated, reproduced with permission from Bock *et al.*, J. Non-Cryst. Solids **407**, 88–97 (2015). Copyright (2015) Elsevier.

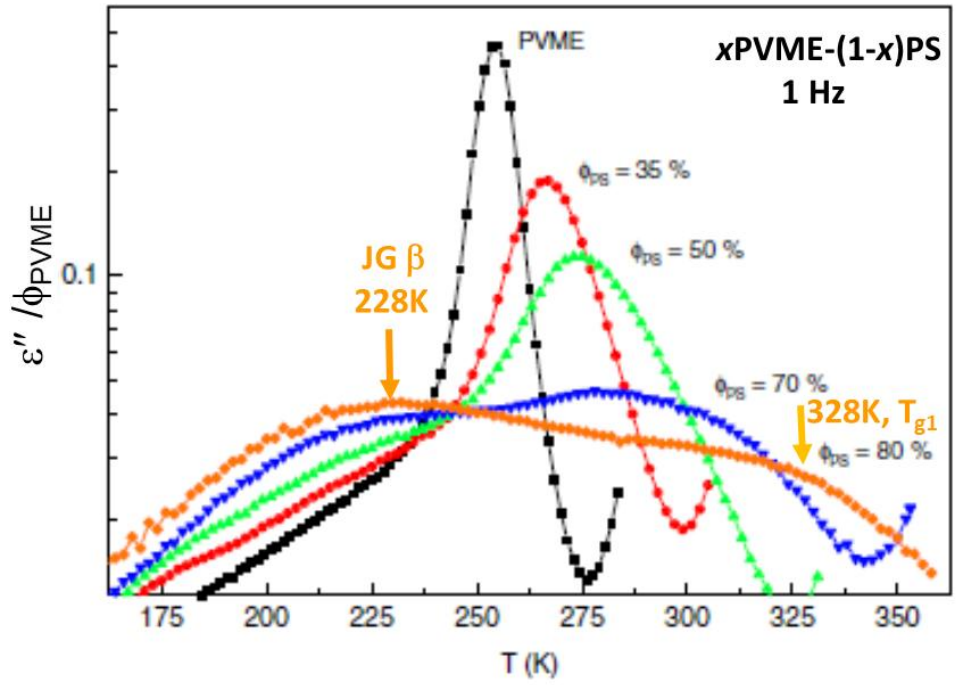

Figure 20. Isochronal dielectric losses measured at frequency *f*=1 Hz plotted as a function of temperature for blends of PVME and PS at different compositions. For the blends with c_{PVME} =20%, the orange-color arrow at 228 K serves to indicate the locations of the fast relaxation at 1 Hz which we identified as the JG β-relaxation, and the other arrow at 328 K indicates the α1 relaxation at 1 Hz. Figure reproduced from Ref.25 with permission.

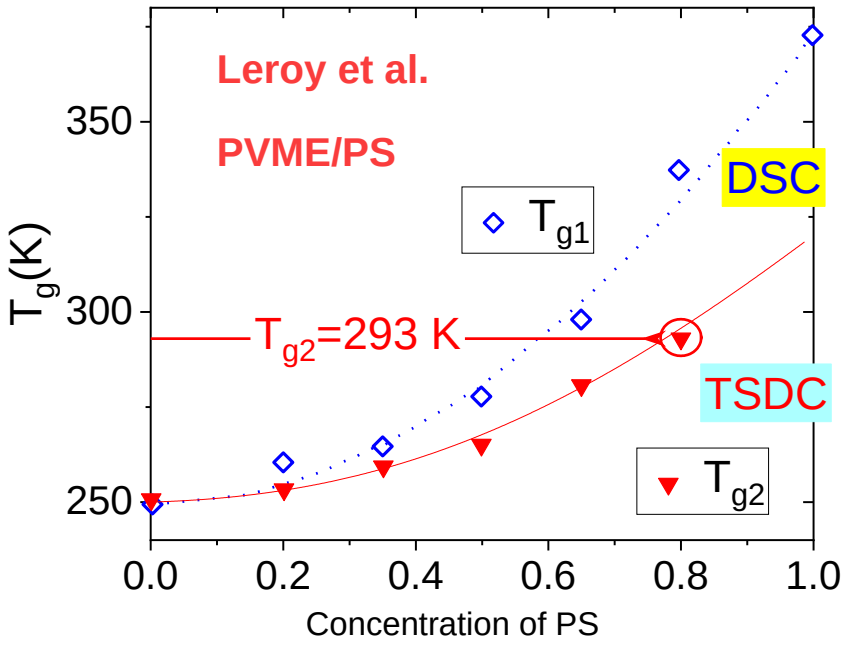

Figure 21. T_g values for the PVME/PS blends as a function of PS concentration obtained from DSC (blue diamonds) and thermally stimulated depolarization current (TSDC) (red triangles) [26]. For the blend with 0.8 PS, the values of $T_g^{\alpha 2}$=293 K and $T_g^{\alpha 1}$=337 K are obtained by TSDC and DSC.

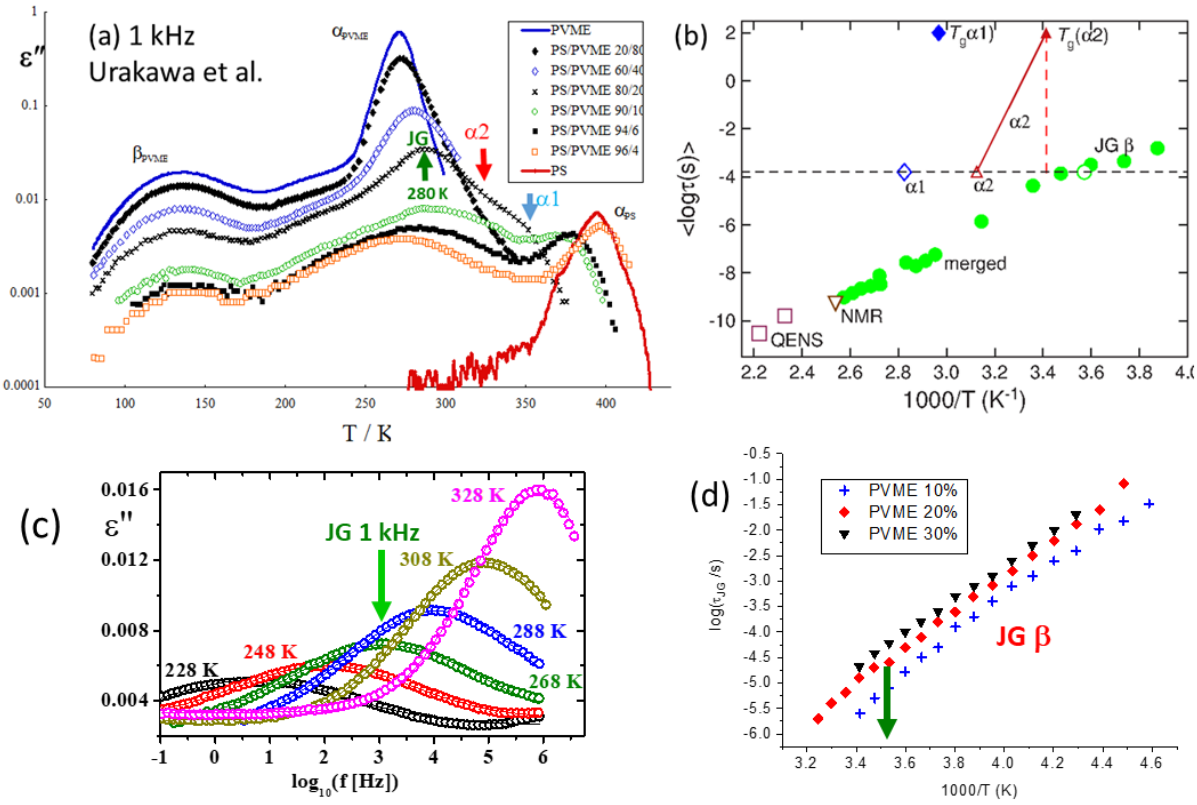

Figure 22.(a) Isochronal plot of dielectric losses measured at 1 kHz for PVME/PS blends at different composition [31]. Arrows indicate the characteristic temperatures for JG β-, α2- and α1-relaxation for the 20%PVME blend. **(b)** Relaxation map of <log τ(s)> for the 20%PVME blend together with the values of $T_g^{\alpha 2}$ and $T_g^{\alpha 1}$ obtained in Figure 21. Also shown are the averaged relaxation times <log $\tau_f(T)$> of the fast relaxation (filled green circles) taken from Ref.[58], which are related to $\tau_f(T)$ in Fig.22d deduced from isothermal dielectric spectra of the fast relaxation in Fig.22c. **(c).** Dielectric loss spectra for the 20%PVME blend at different temperatures [24, 25]. **(d).** Relaxation map for the fast relaxation time τ_f shown in panel (c), for 10%, 20% and 30% PVME/PS blends.

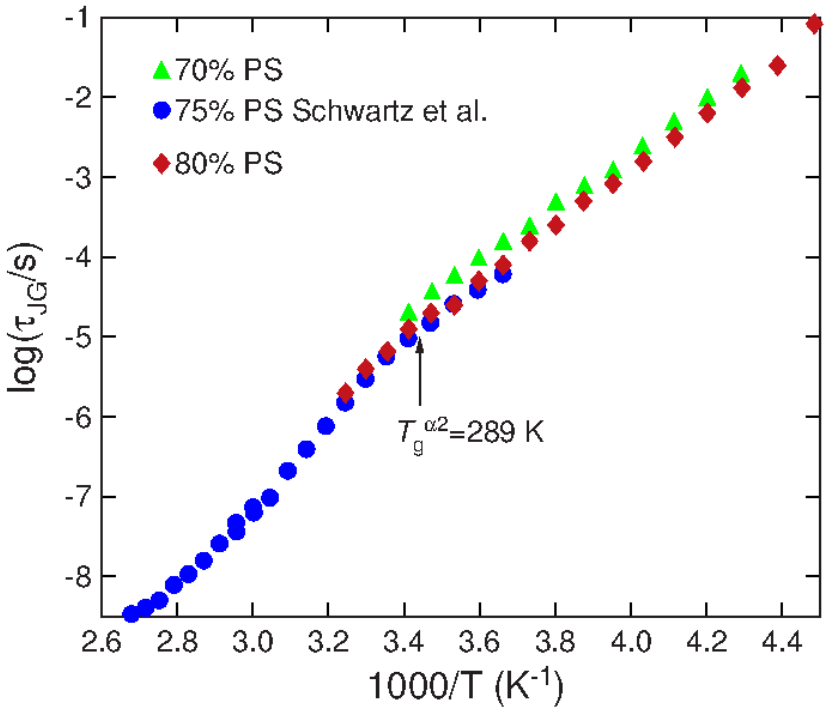

Figure 23. Relaxation map for the ambient pressure data of fast relaxation time log $\tau_f(T)$ (JG β-relaxation for us or confined α2-relaxation according to LAC) for quite similar composition of the PVME/PS blends: 70% PS (green triangles) are from ref.[24, 25], 75% (blue circles) are from ref.[55], 80% PS (red diamonds) are from [24].

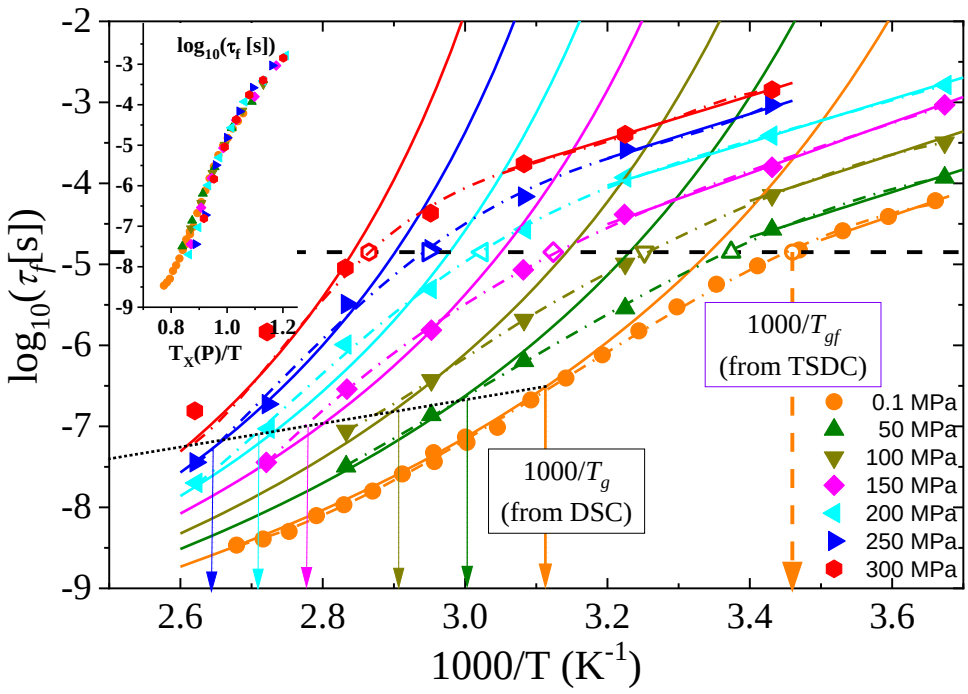

Figure 24 Logarithm of the fast relaxation time τf vs reciprocal temperature at different pressures (from bottom to top: P = 0.1, 50, 100, 150, 200, 250, and 300 MPa) for PVME in PS (25/75). Data from Schwartz *et al.*[55] in which they interpret the observed as α-relaxation with VFT dependence and crossover to Arrhenius dependence due to confinement by the PS matrix. Solid curved lines represent the VFT fits of the experimental data at higher temperatures. The vertical dashed orange and the thinner orange continuous arrows indicate at ambient pressure the locations of $1000/T_g^{\alpha 2}$, with $T_g^{\alpha 2} \approx 289$ K of the PVME component and $1000/T_g^{\alpha 1}$, with $T_g^{\alpha 1} \approx 321$ K of the blend obtained by interpolation of TSDC and DSC data from Leroy *et al.* The horizontal black dashed line marks the $\tau_{JG}(P, T) \approx 10^{-4.8}$ s. The dotted-dashed color lines are polynomial fits drawn to suggest the crossover of temperature dependence of $\tau_{JG}(P, T)$ at $T_x(P)$ where $\tau_{JG}(P, T_x(P)) \approx 10^{-4.8}$ s independent of P. The open symbols mark $T_x(P)$ of the crossover, which occurs at the same values of $\tau_{JG}(P, T_x(P))$ for all $T_x(P)$. Inset shows the master-curve obtained by plotting $\tau_{JG}(P, T)$ versus $T_x(P)/T$. The colored vertical arrows mark the positions where the α1-relaxation enters into the glassy state, as determined by PVT data [116]. Note the approximate agreement between this location and $1000/T_g^{\alpha 1}$ from DSC at ambient pressure.

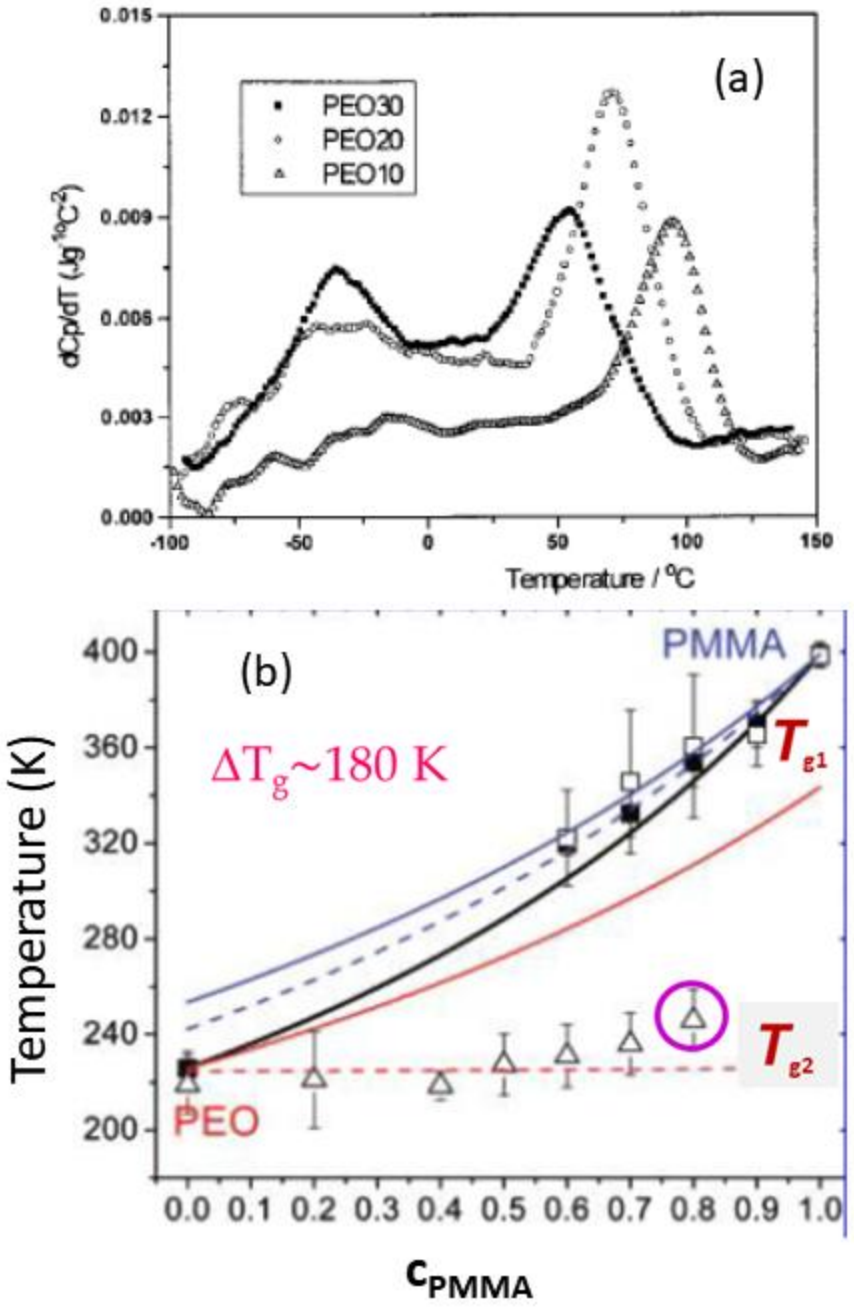

Figure 25.(a) the derivative dC_p/dT of the specific heat obtained from DSC curve for PEO/PMMA blends with PEO concentration c_{PEO}=30%, 20% and 10%. **(b).** Values of the two glass transitions $T_g^{\alpha 2}$ and $T_g^{\alpha 1}$ for all compositions plotted against c_{PEO} . Figures are reproduced from Ref.[39] with permission from ACS.

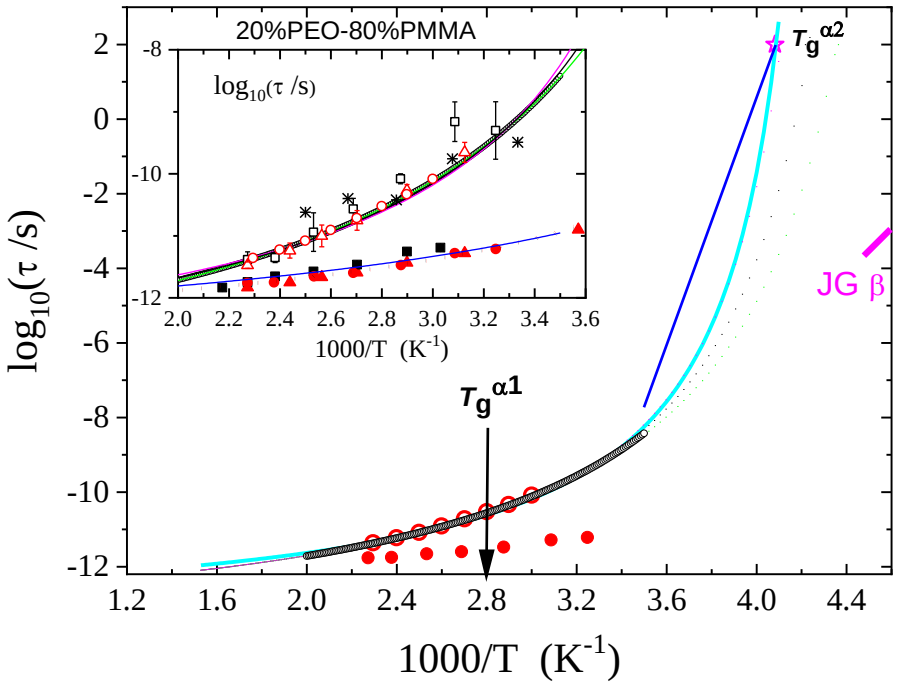

Figure 26. In the main figure, the line defined by open black circles is the fit of ^{2}H NMR data of segmental α-relaxation time of the PEO component from Lutz et al. [27] in 20% PEO–80% PMMA blend. The magenta star is placed at 100 s to represent the α2-relaxation time $\tau_{\alpha 2}$ of the PEO component at $T_g^{\alpha 2}$=245 K in the 20% PEO–80% PMMA blend. The closed and open red circles are the fast and slow α2-relaxation times found in QENS experiment of Garcia-Sakai et al. at Q = 1.3 Å^{-1} [51, 52]. The vertical black arrow locates the position of $T_g^{\alpha 1}$=356 K for the PMMA component in the blend. The pale blue line is the VFT fit of the NMR data of the PEO component in 20% PEO–80% PMMA blend and requiring it to reach $\tau_{\alpha 2}(T)$=100 s at $T_g^{\alpha 2}$=245 K, which is not acceptable (see text). The blue line is the Arrhenius T-dependence of the confined α2-relaxation suggested to interpolate $\tau_{\alpha 2}(T)$=100 s at T=$T_g^{\alpha 2}$ and the deuteron NMR data (open black circles). The short and thick magenta line represents the relaxation times of the JG β-relaxation. In the inset, in addition to the same symbols and line in the main figure, it shows QENS data for PEO in the 25/75 blend from QENS at Q=1.02 Å^{-1} [52] (asterisks). Also from QENS data at Q=1.02 Å^{-1} [48] are open black squares indicating the slow relaxation, and the closed black squares the fast relaxation for the PEO component in 20%PEO-80%PMMA blend. The red closed and open triangles are the same for the 30%PEO-70%PMMA blend. The blue line is the primitive relaxation time of PEO obtained from NMR data of pure PEO.

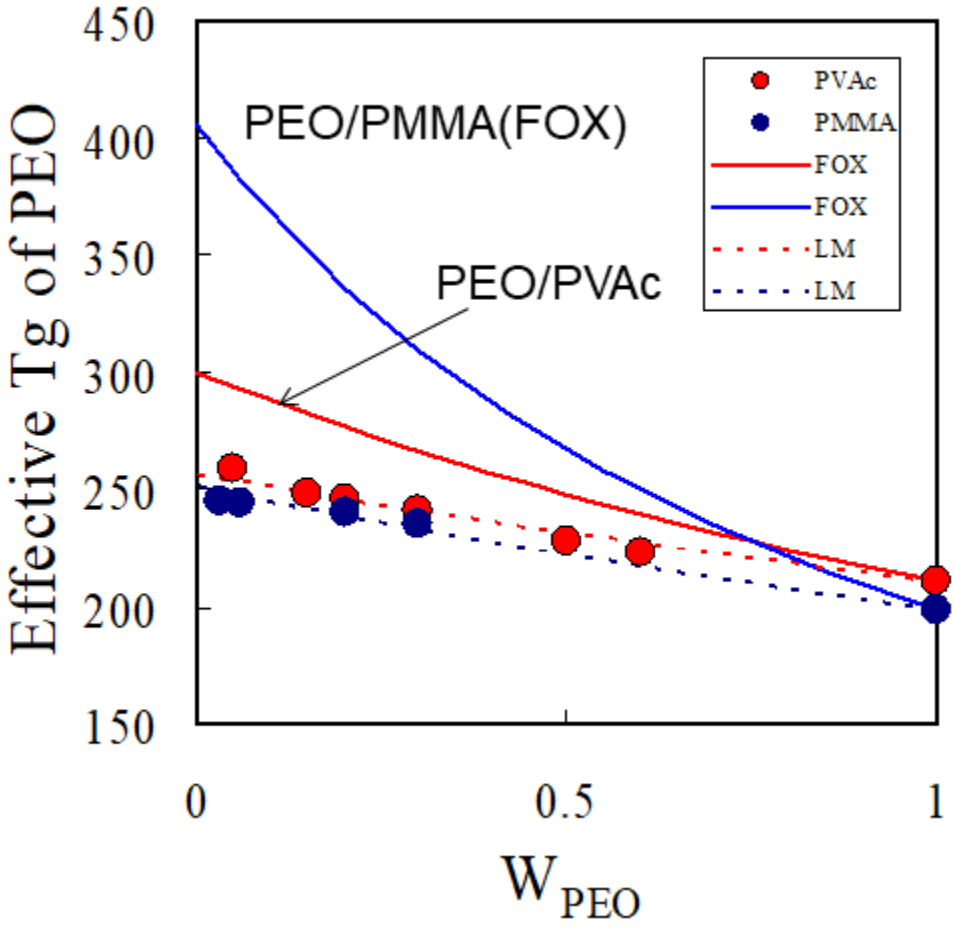

Figure 27. Effective glass transition temperature $T_{g,eff}$ of the PEO component (that is $T_g^{\alpha 2}$) for poly(ethylene oxide)/poly(vinyl acetate)/ (*x*%PEO-(1-*x*)PVAc) and *x*%PEO-(1-*x*)PMMA blends plotted as a function of PEO fraction [113]. Continuous and dashed lines are from Fox-Flory and Lodge-McLeish model predictions. Figure reproduced from Ref.113 with permission from Elsevier.

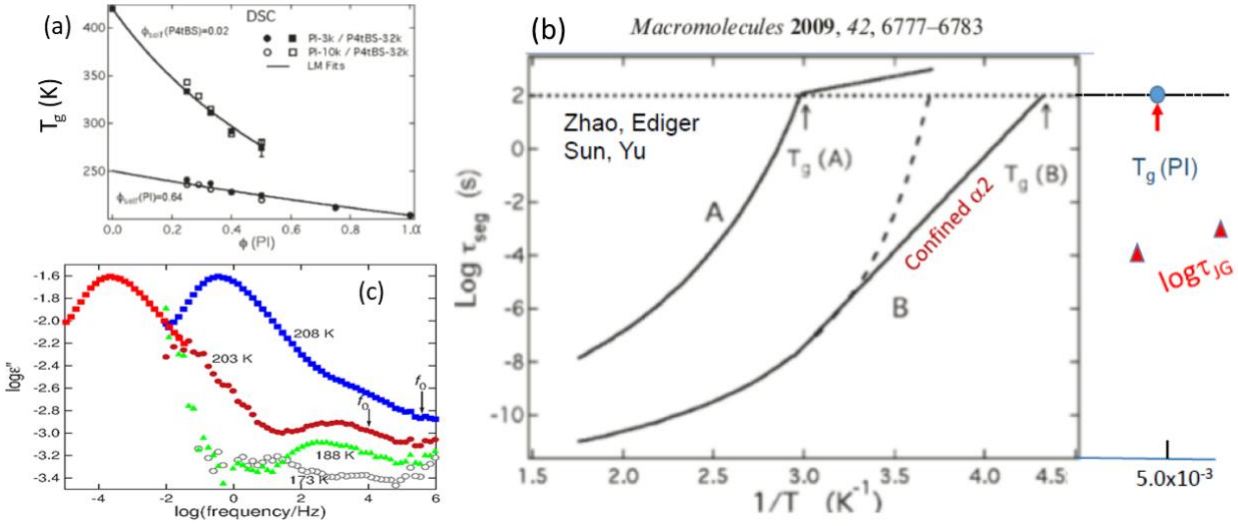

Figure 28. (a) Values of $T_g^{\alpha 1}$ and $T_g^{\alpha 2}$ obtained by conventional and temperature-modulated DSC for miscible blends of polyisoprene (PI) and poly(4-tert-butylstyrene) (P4tBS) over a broad composition range [60]. Lines are fits to the Lodge-McLeish model [18]. Figure reproduced from ref.[60] by permission. **(b)** Sketch of the segmental dynamics of the slow (A) and fast (B) components in a miscible A/B polymer blend, reproduced from ref.[60] by permission and modified. The dotted line represents a segmental relaxation time of 100 s, and effective glass transition temperatures of the components are indicated. For component B, below the effective T_g of A, the dashed curve represents the VTF extension of its high-temperature dynamics, while the thick solid line represents the enhanced dynamics that result from the vitrification of the blend. The T_{g2} of pure PI and two JG β-relaxation times $\tau_{JG}(T)$ are also shown. **(c)**. Dielectric spectra of PI with molecular weight of 21 k [89].

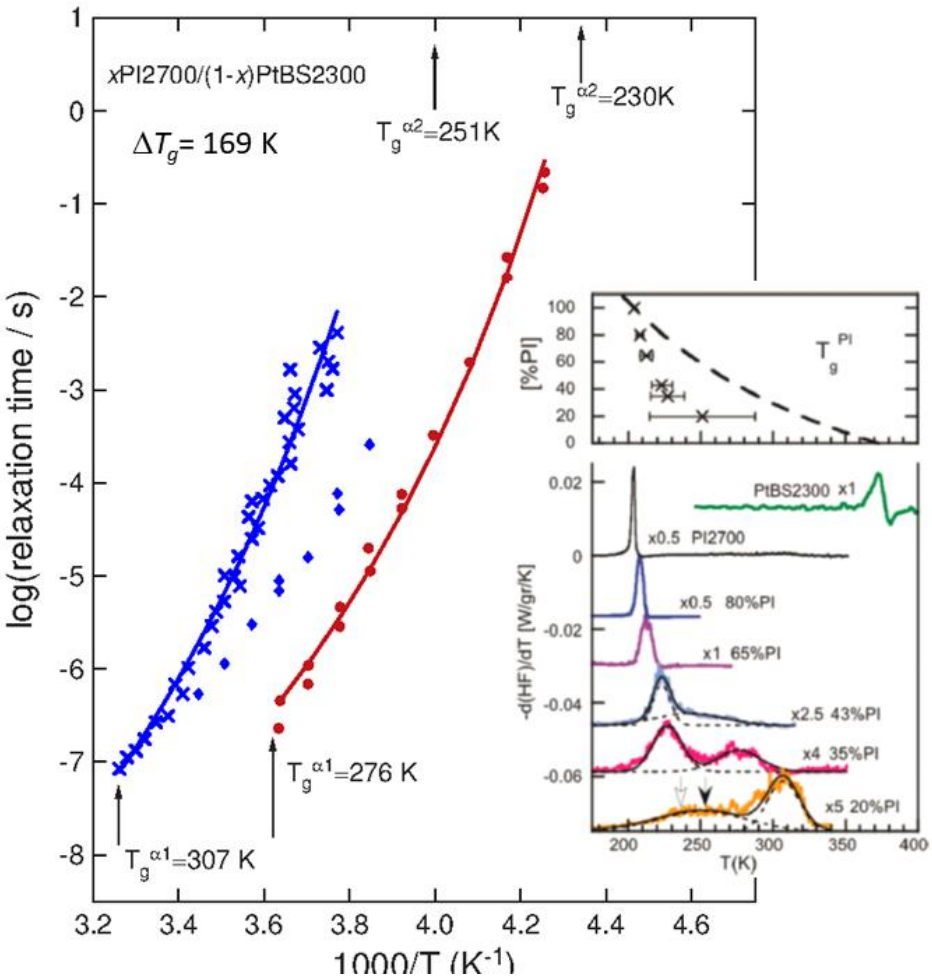

Figure 29. The segmental α-relaxation time $\tau_{\alpha 2}$ (closed symbols) of PI27 in 35%PI27 blend (red circles), and 20%PI27 blend (blue diamonds) with PtBS2300. Data from Refs.[65], and replotted as a new figure. The blue × symbols represent $\tau_{\alpha 2}$ obtained from isochronal representation of the data for 20% PI blends. The locations of the $1000/T_g^{\alpha 2}$ and $1000/T_g^{\alpha 1}$ in each of the two blends are indicated by the arrows accompanied by the value. Right inset is reproduced from Ref.[65] with permission. Lower part shows the derivative of the heat flow with respect to T for PI2700 and PtBS2300 homopolymers and their blends at different compositions. The intensity of the curves was multiplied by 0.5, 0.5, 2.5, 4, and 5, for 100, 80, 43, 35, and 20% samples, respectively. In addition, curves have been shifted in the y axis for clearness. Continuous black lines represent fits to two Gaussian functions and dashed lines individual components of the fitting. Upper panel: Glass transition temperature of PI component in the blend as a function of

PI content (crosses); horizontal bars represent full width at half-maximum of the Gaussian fits; dashed line represents the expected global glass transition temperature for the blend according to a simple mixing rule.

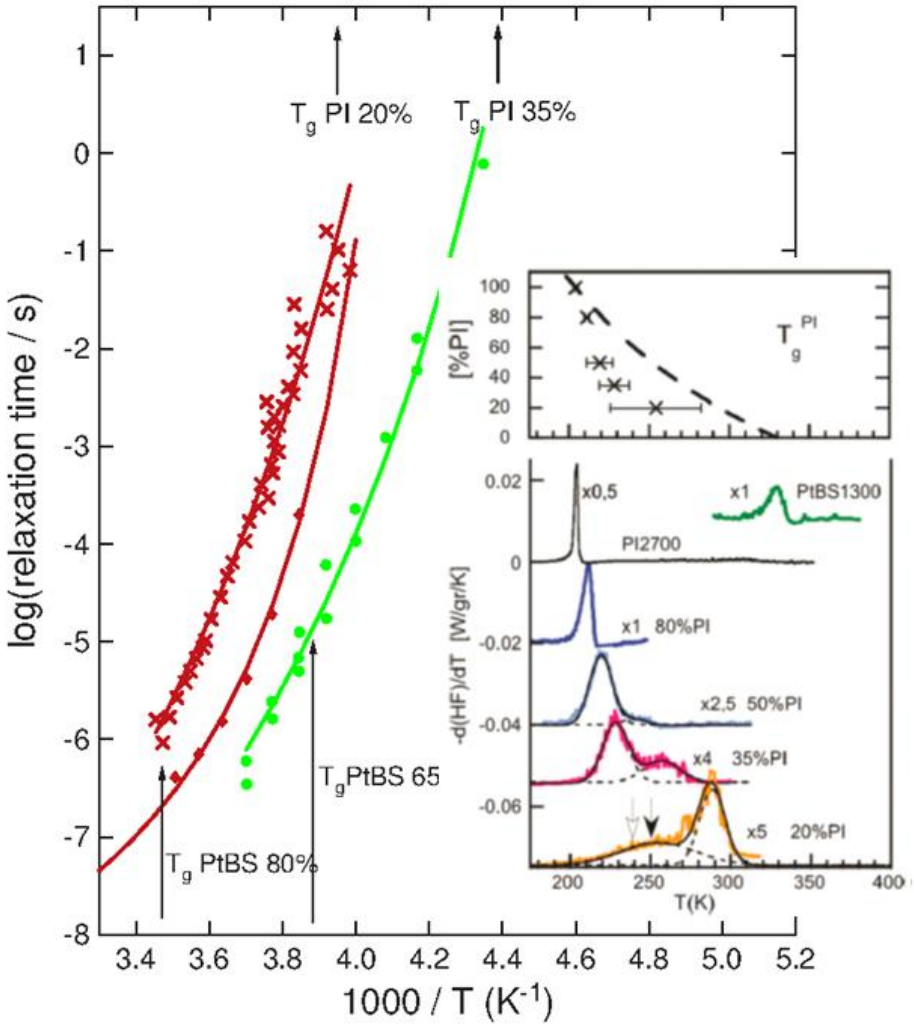

Figure 30. The segmental α-relaxation time $\tau_{\alpha 2}$ (closed symbols) of PI27 in 35%PI27 blend (green circles), and 20%PI27 blend (red diamonds) with PtBS1300. Data from Refs.[65], and replotted as a new figure. The red × symbols represent $\tau_{\alpha 2}$ obtained from isochronal representation of the data for 20% PI blends. The locations of the $1000/T_g^{\alpha 2}$ and $1000/T_g^{\alpha 1}$ in each of the two blends are indicated by the arrows accompanied by the value. Right inset has the same information as in Figure 29 and is reproduced from Ref.[65] with permission from ACS.

Figure 1

Click here to download high resolution image

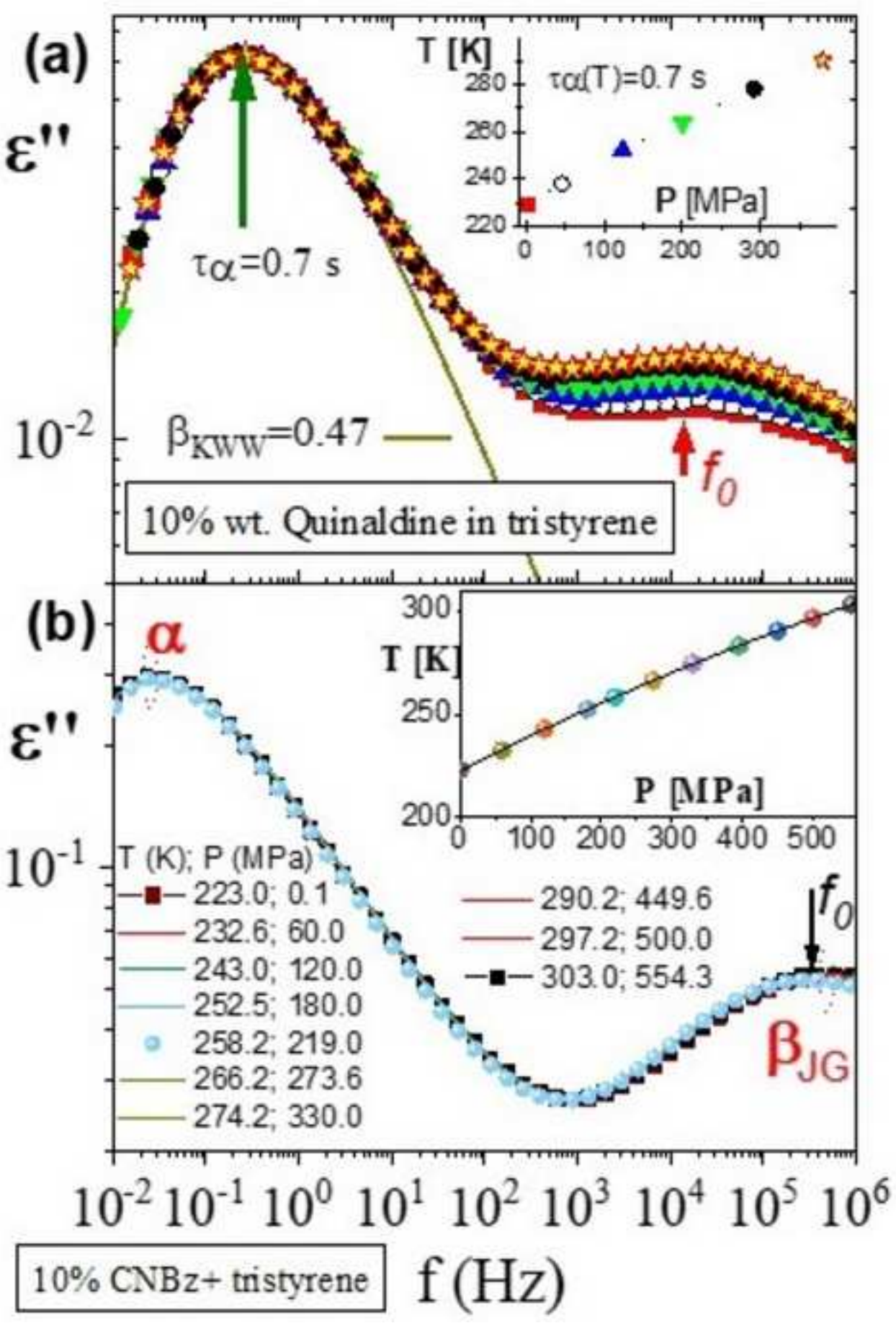

Figure 2

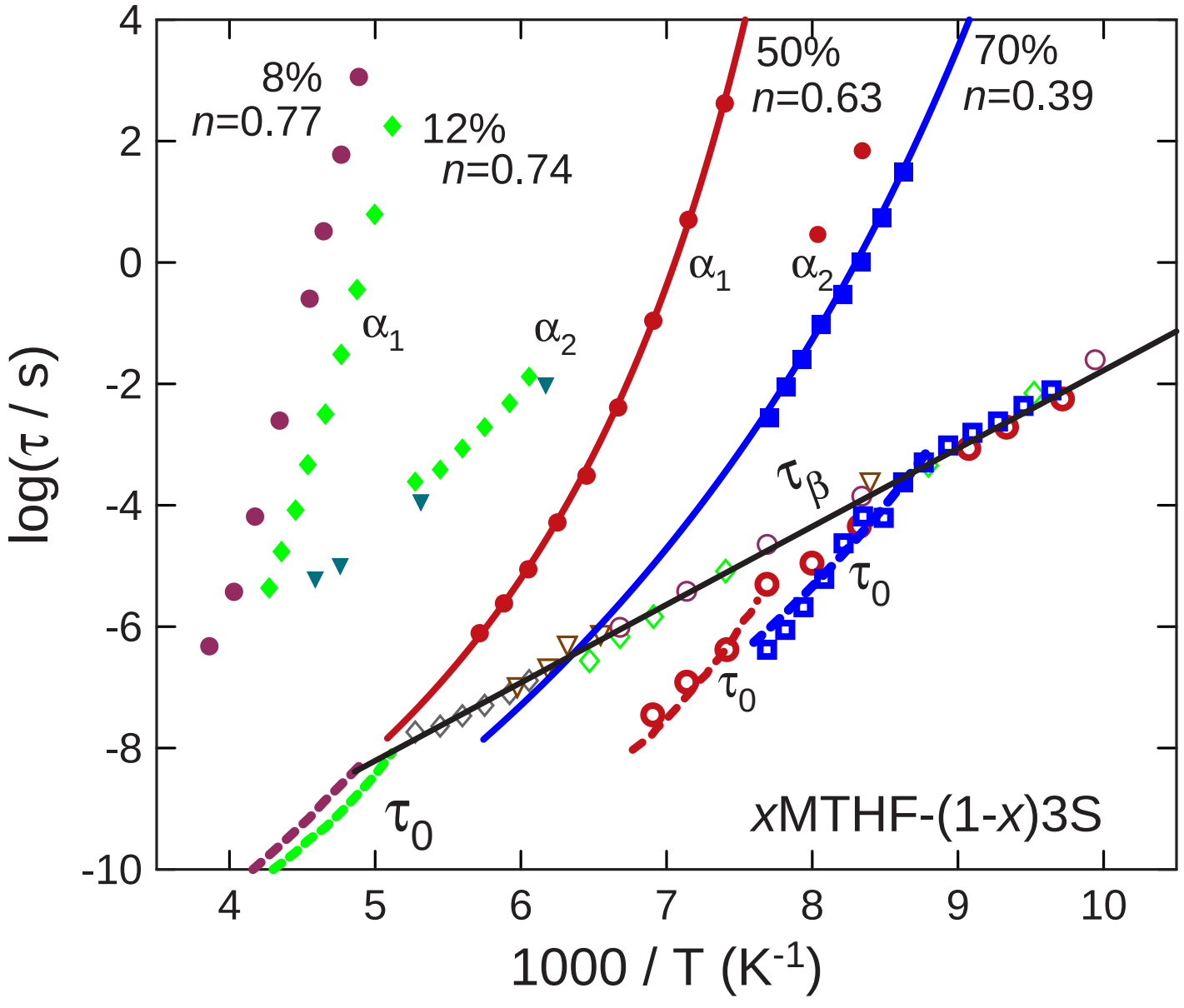
8%
n=0.77
12%
n=0.74
50%
n=0.63
70%
n=0.39
α1
α2
α1
α2
τβ
τ0
τ0
τ0
xMTHF-(1-x)3S
log(τ / s)
1000 / T (K-1)
4
2
0
-2
-4
-6
-8
-10
4
5
6
7
8
9
10

Figure 3

Click here to download high resolution image

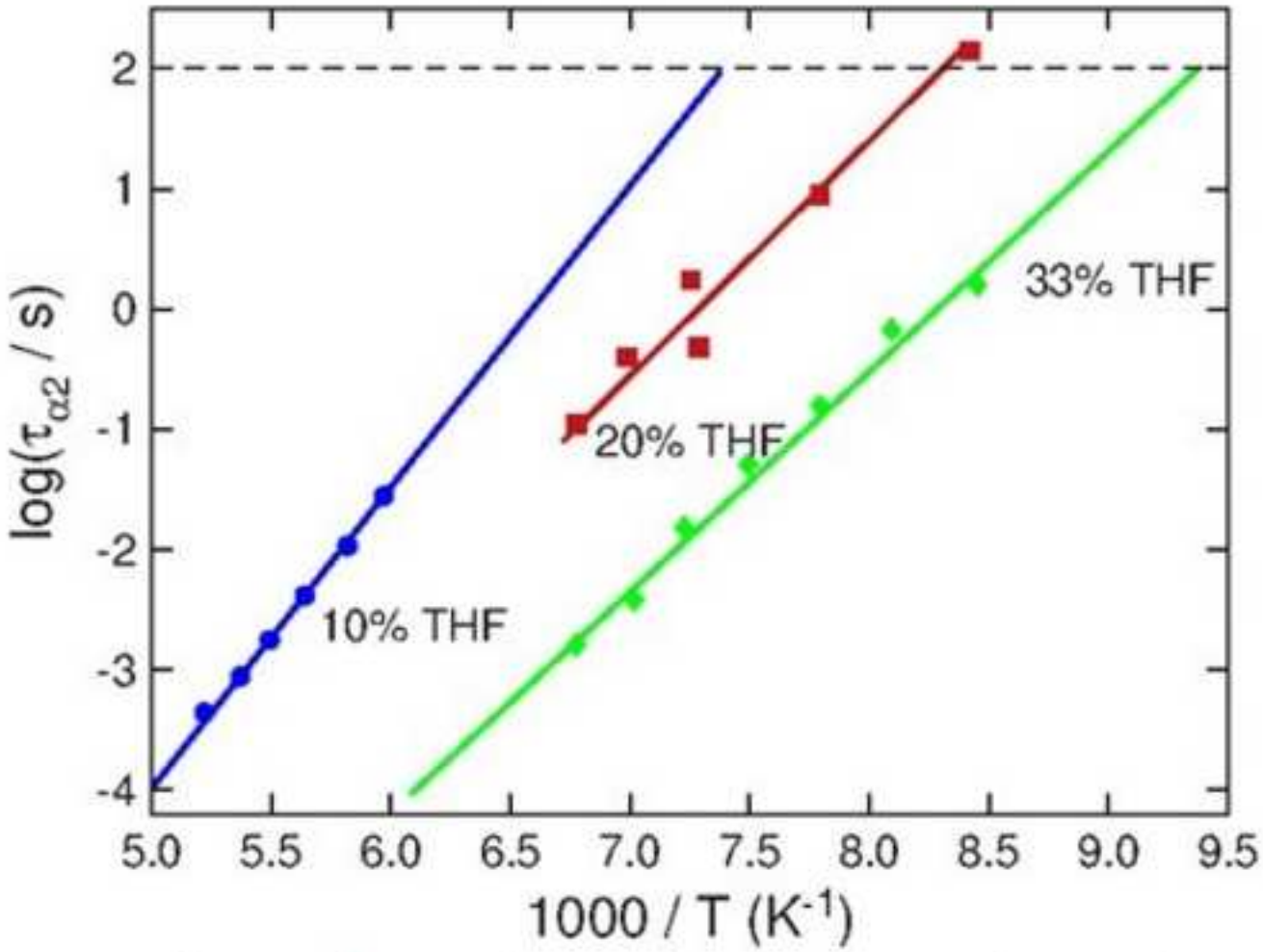

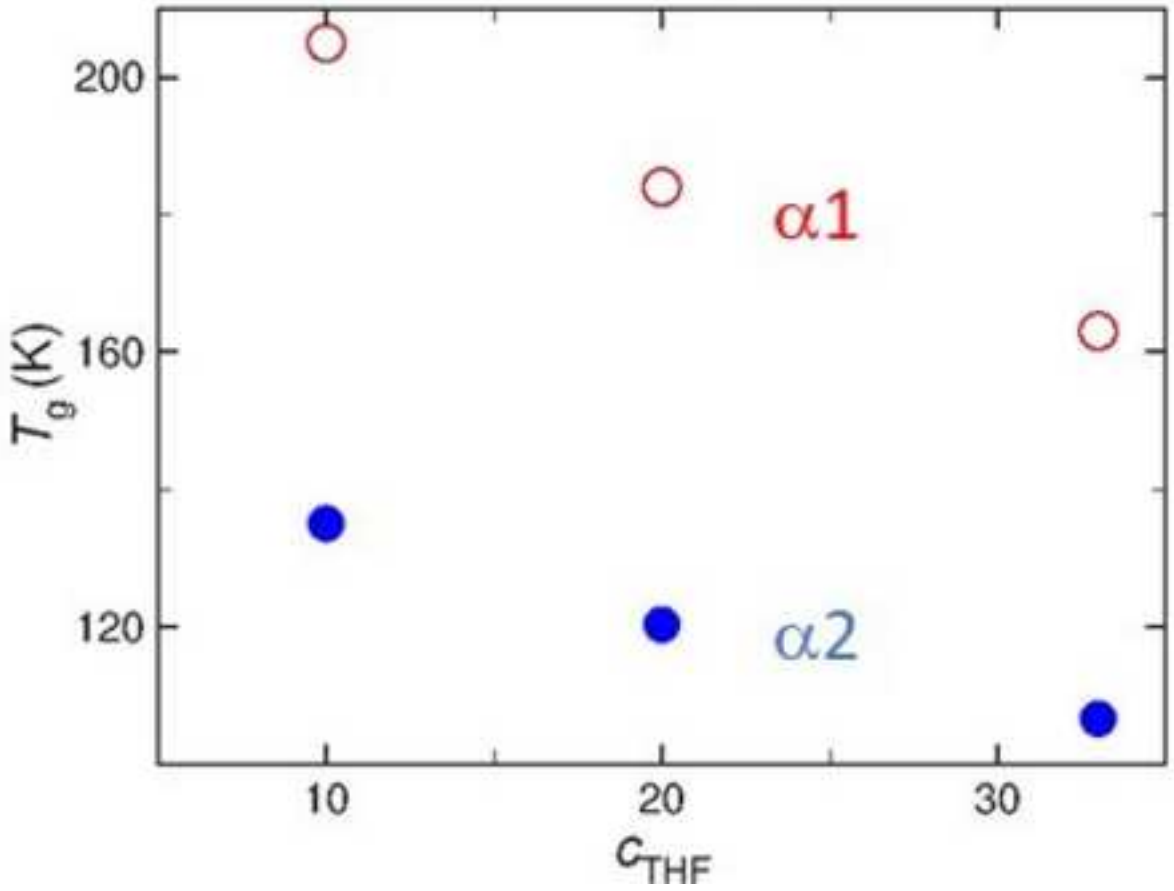

Figure 4

Click here to download high resolution image

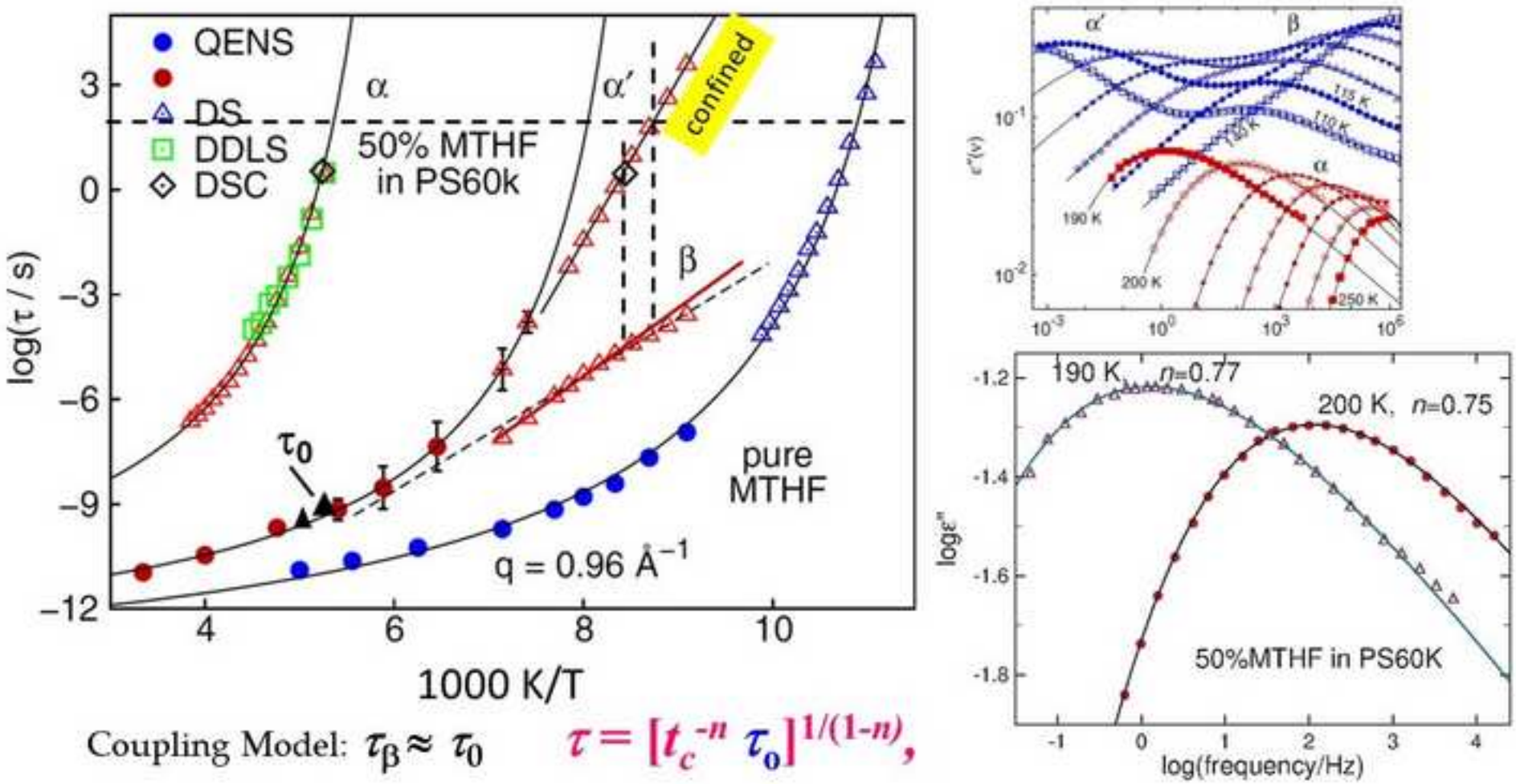

Figure 5

Click here to download high resolution image

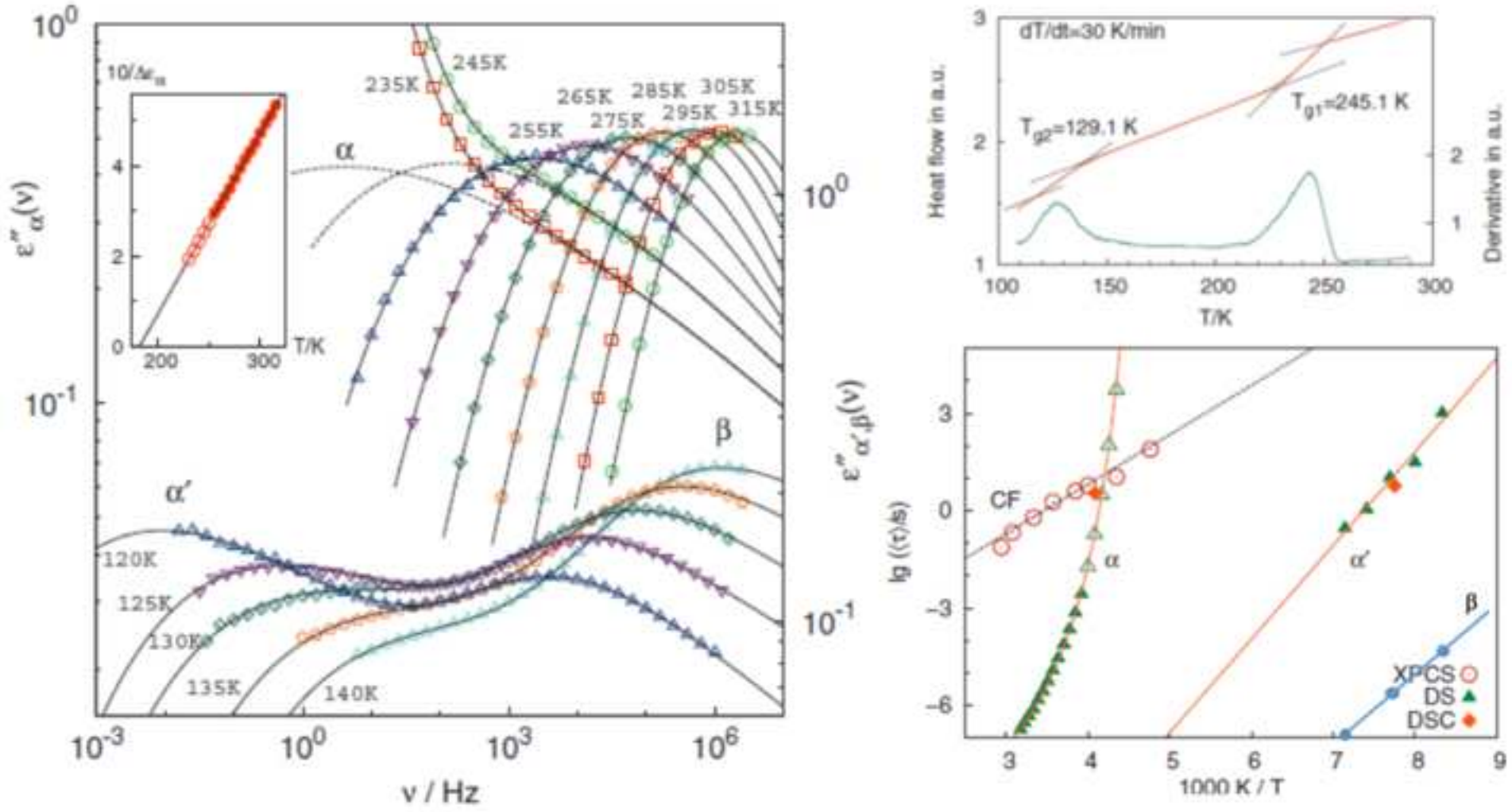

Figure 6

Click here to download high resolution image

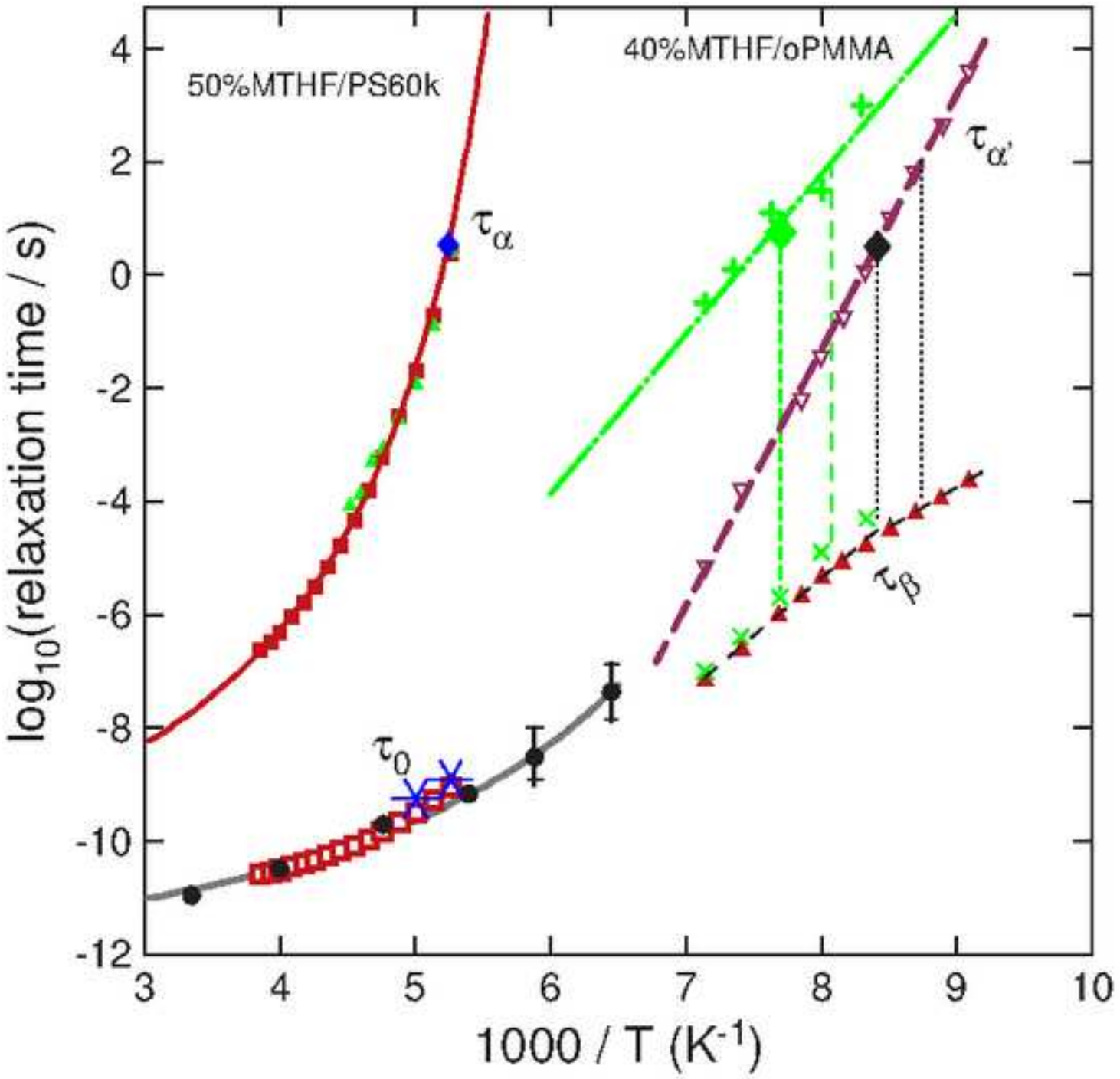

Figure 7

Click here to download high resolution image

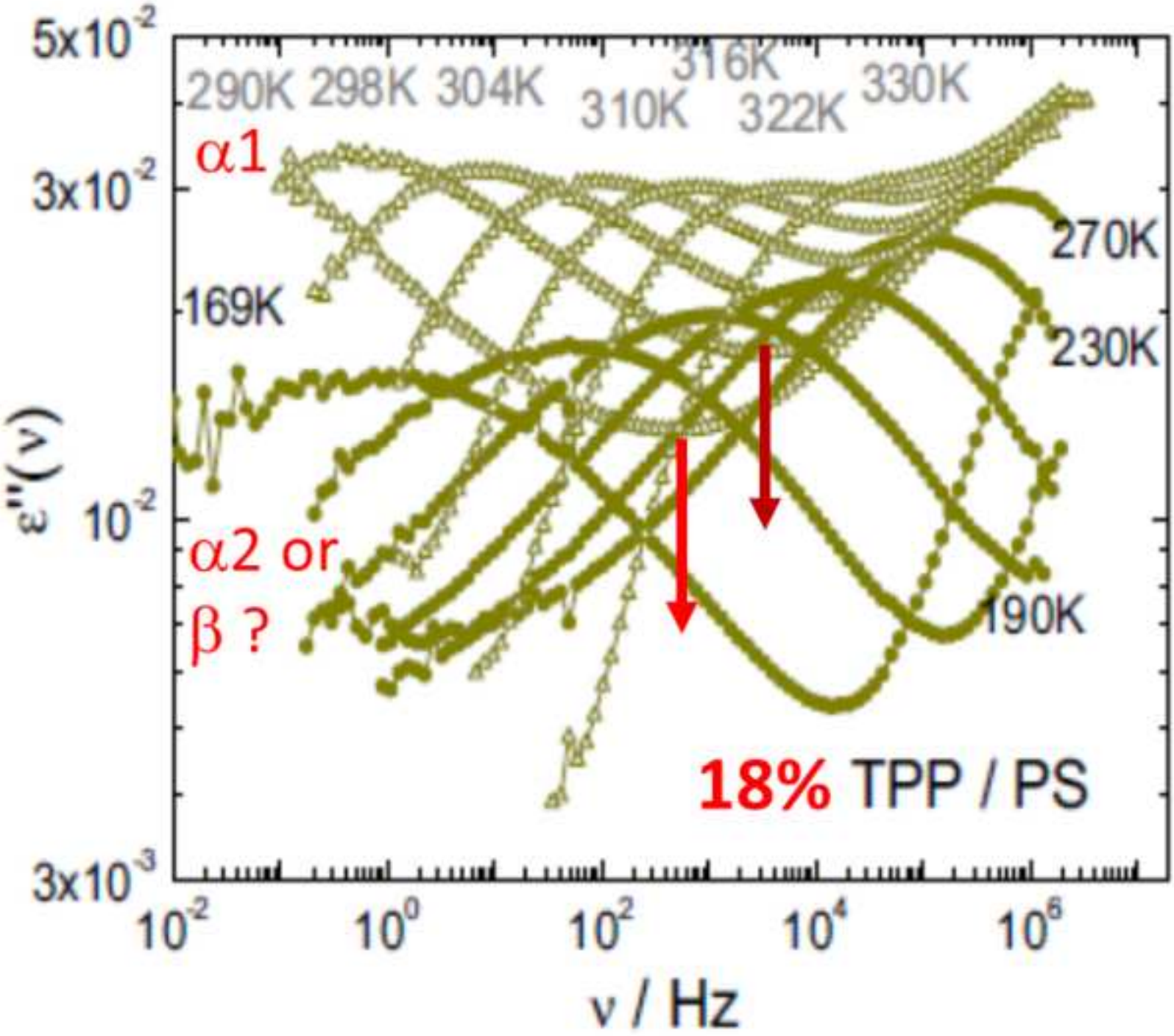

Figure 8

Click here to download high resolution image

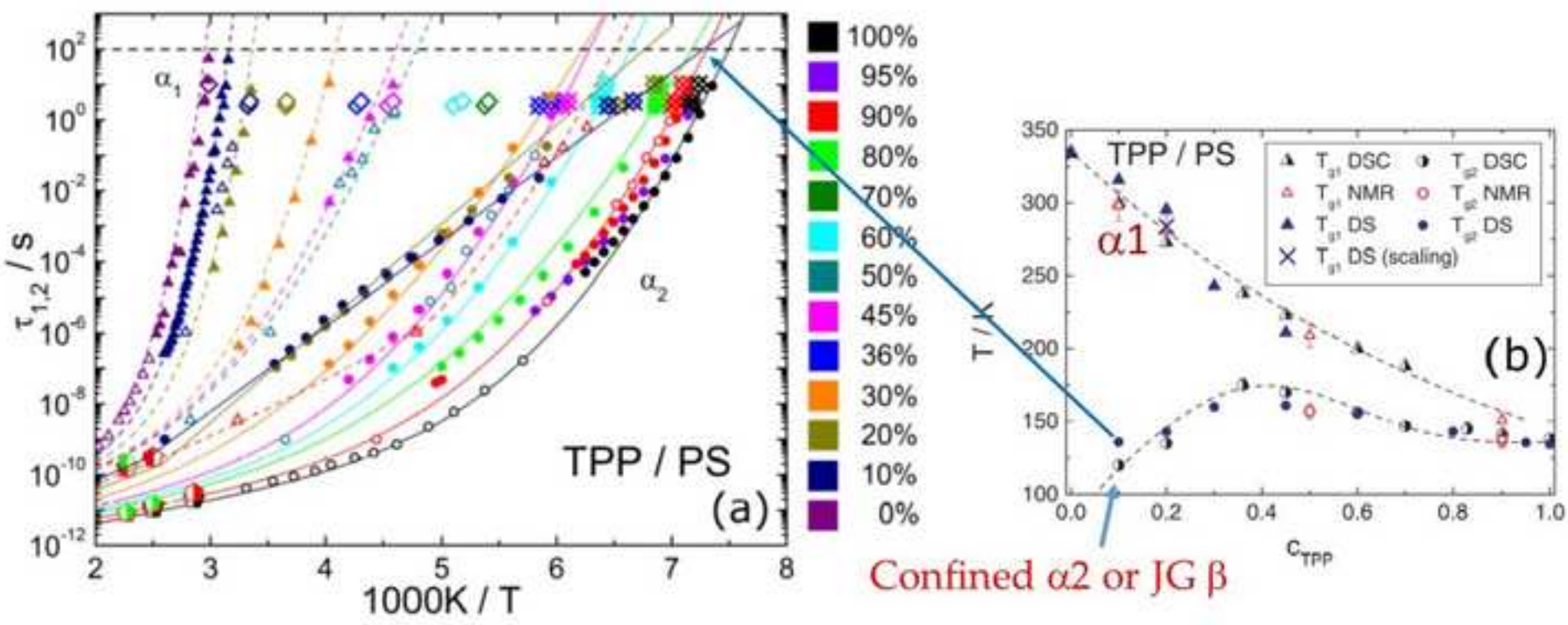

Figure 9

Click here to download high resolution image

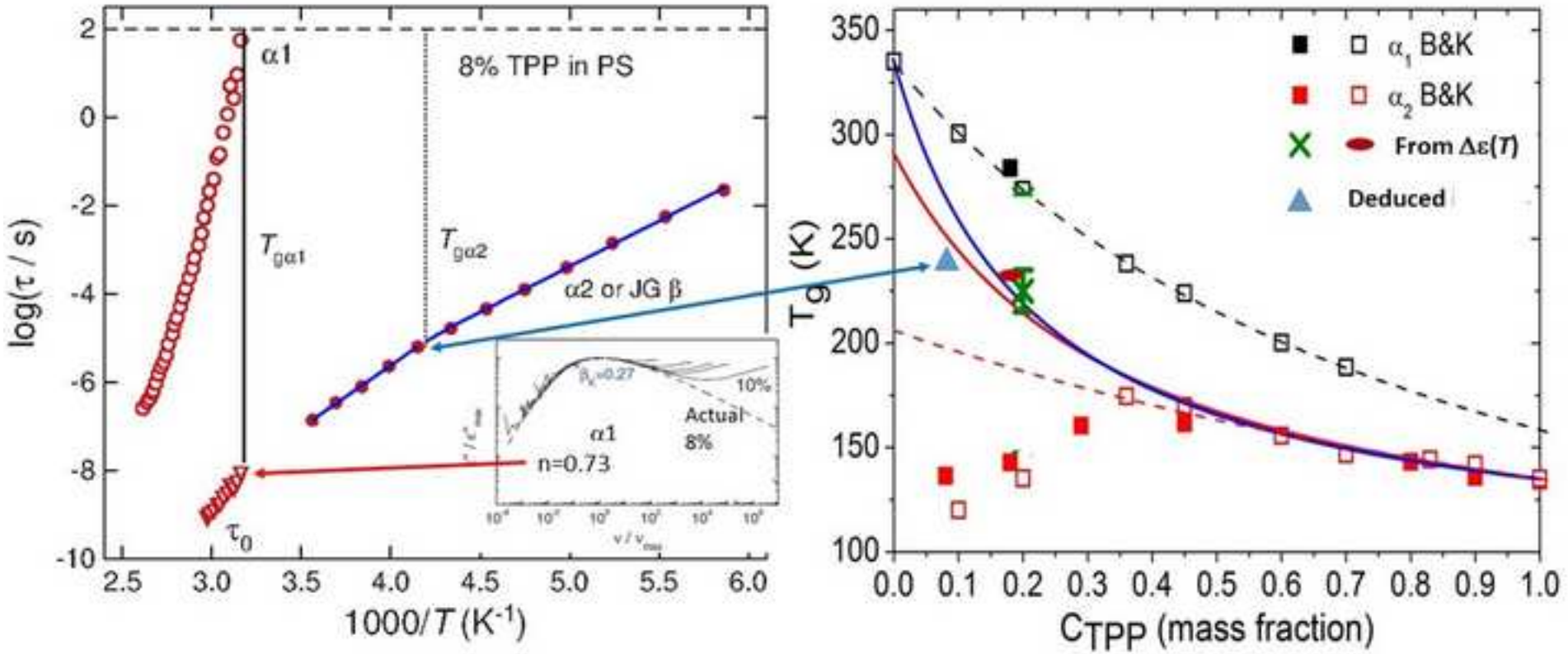

Figure 10

Click here to download high resolution image

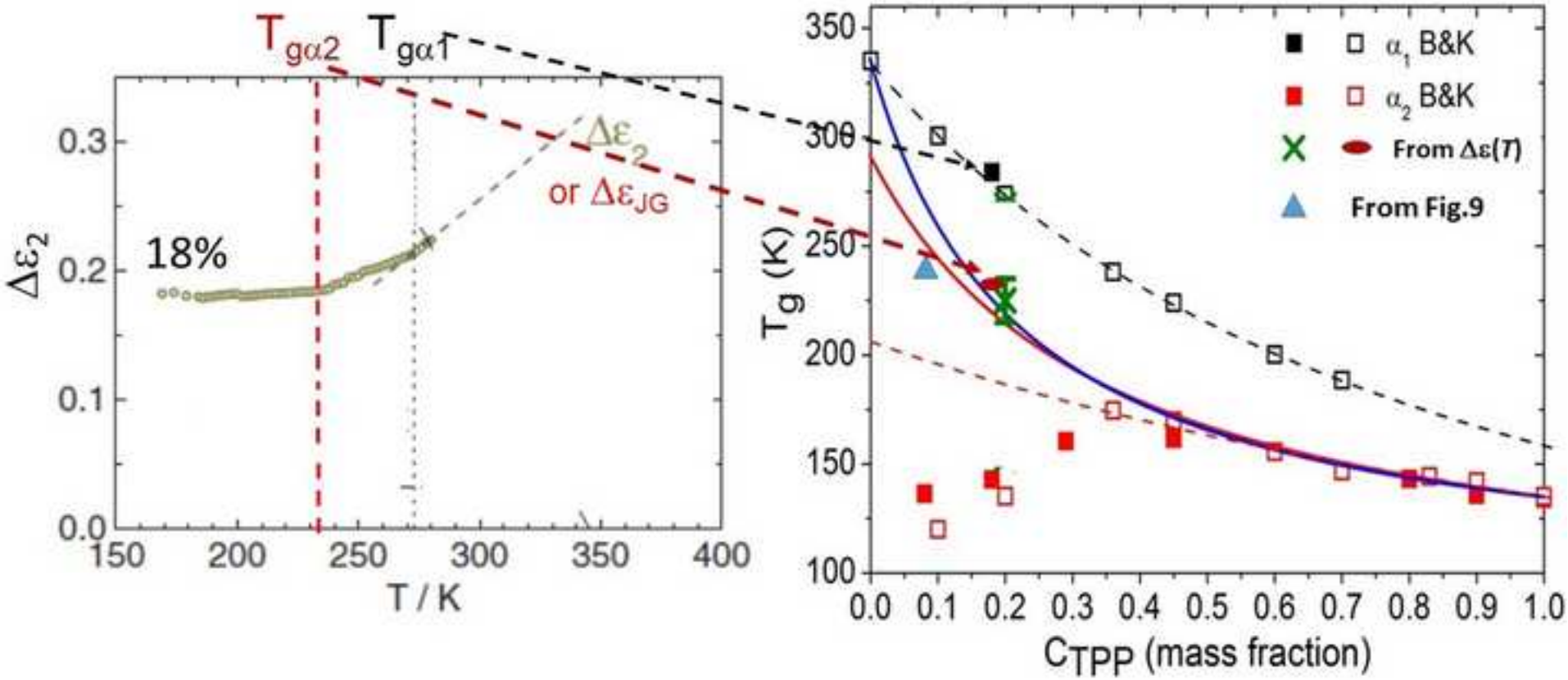

Figure 11

Click here to download high resolution image

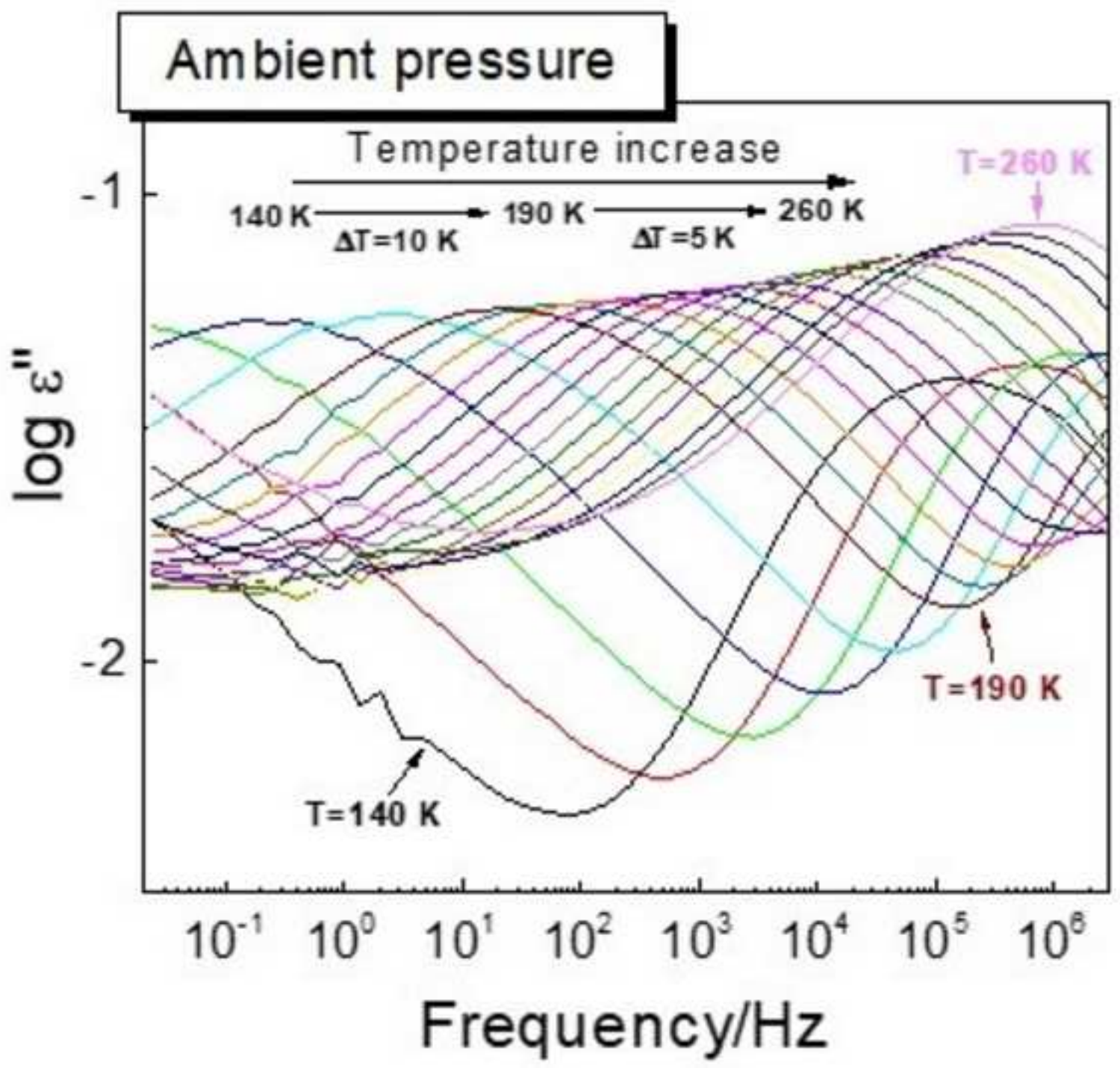

Figure 12

Click here to download high resolution image

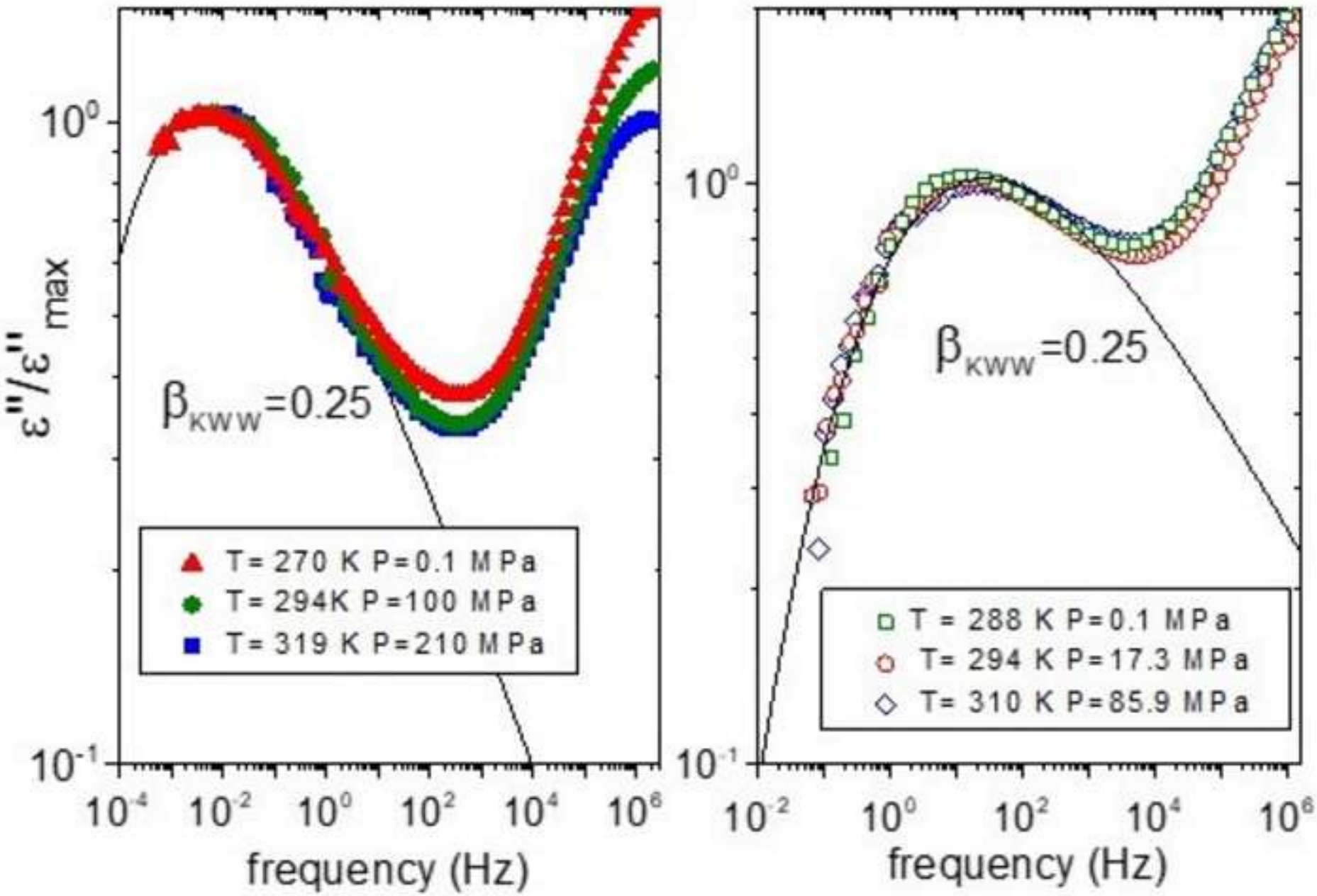

Figure 13

Click here to download high resolution image

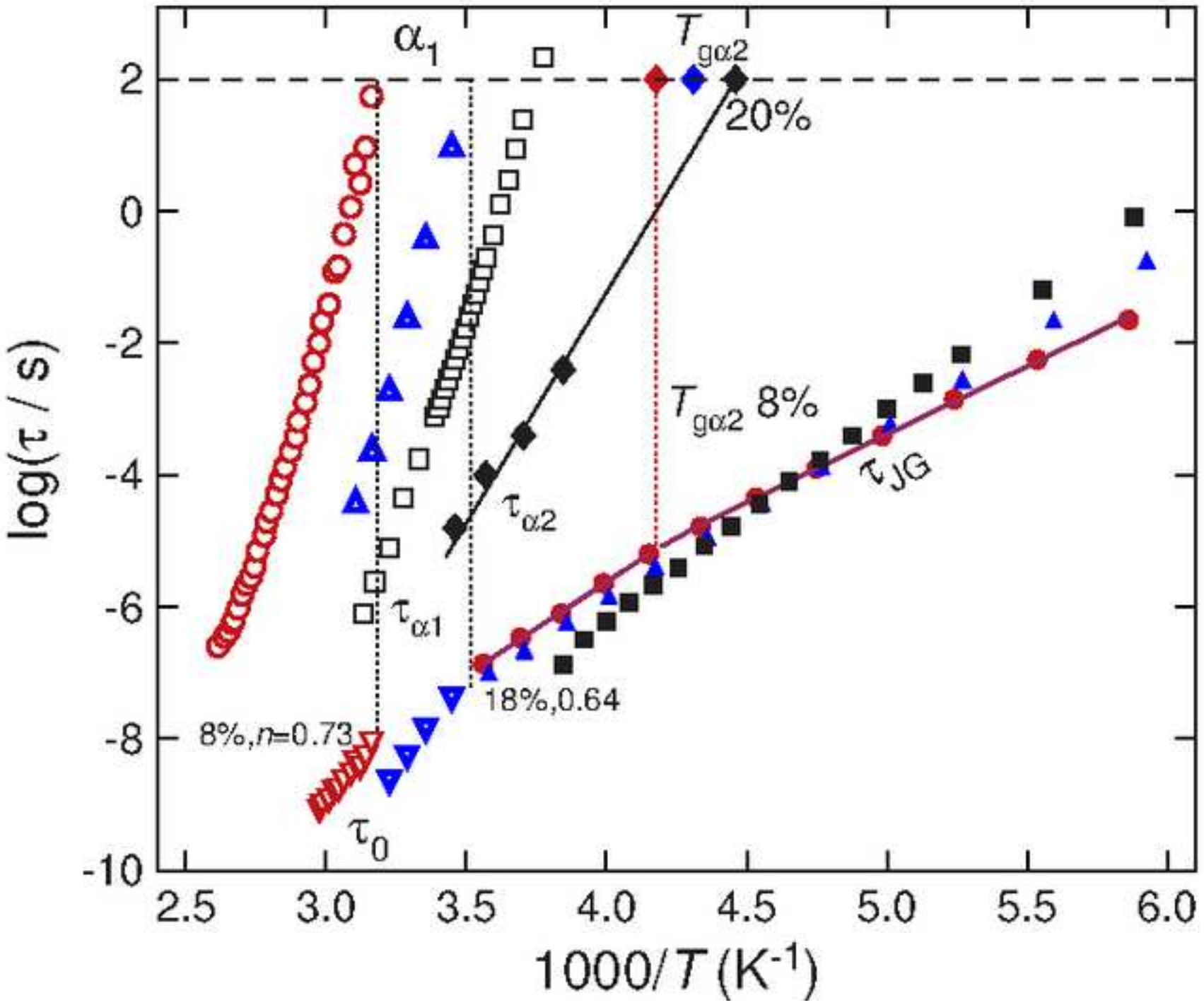

Figure 14

Click here to download high resolution image

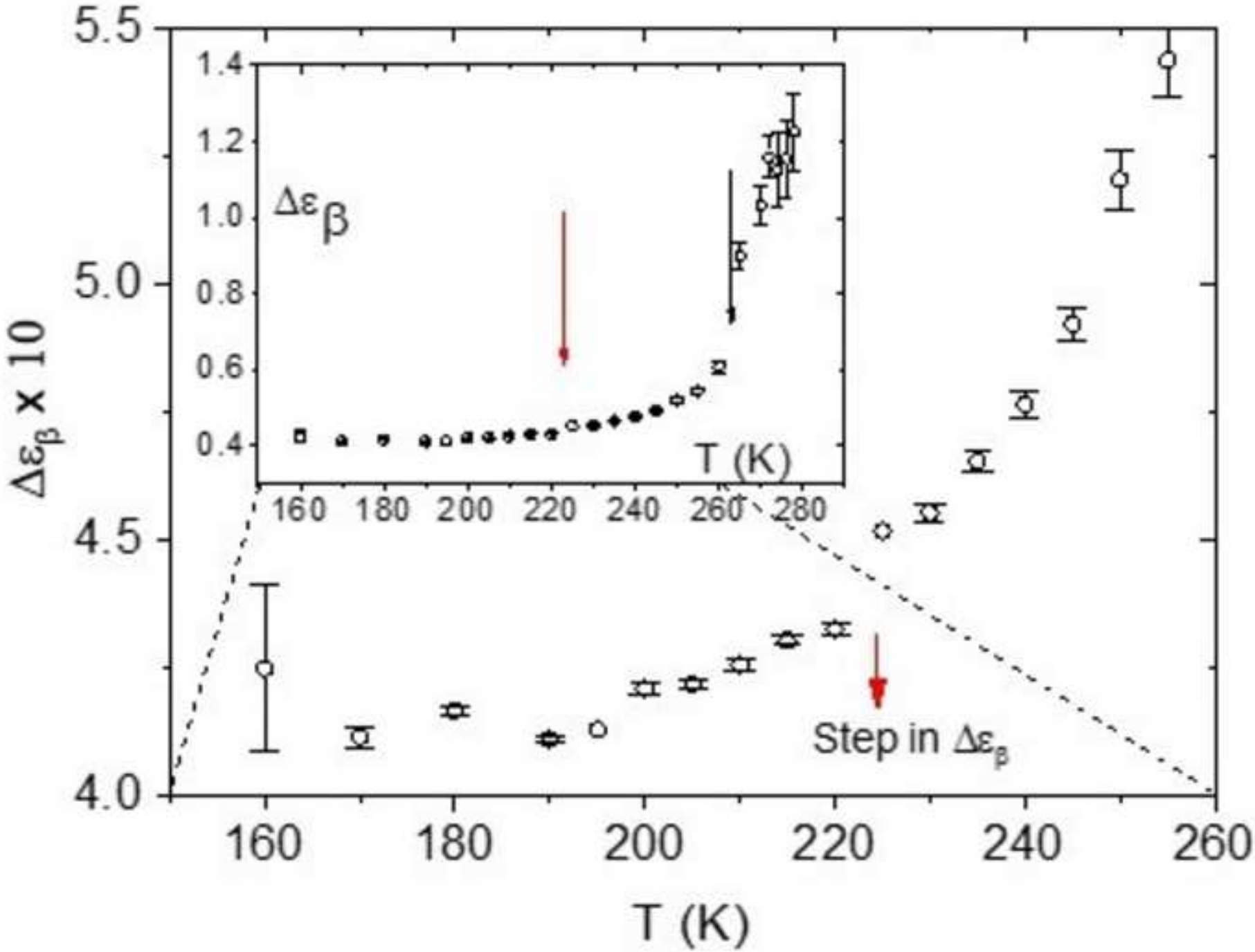

Figure 15

Click here to download high resolution image

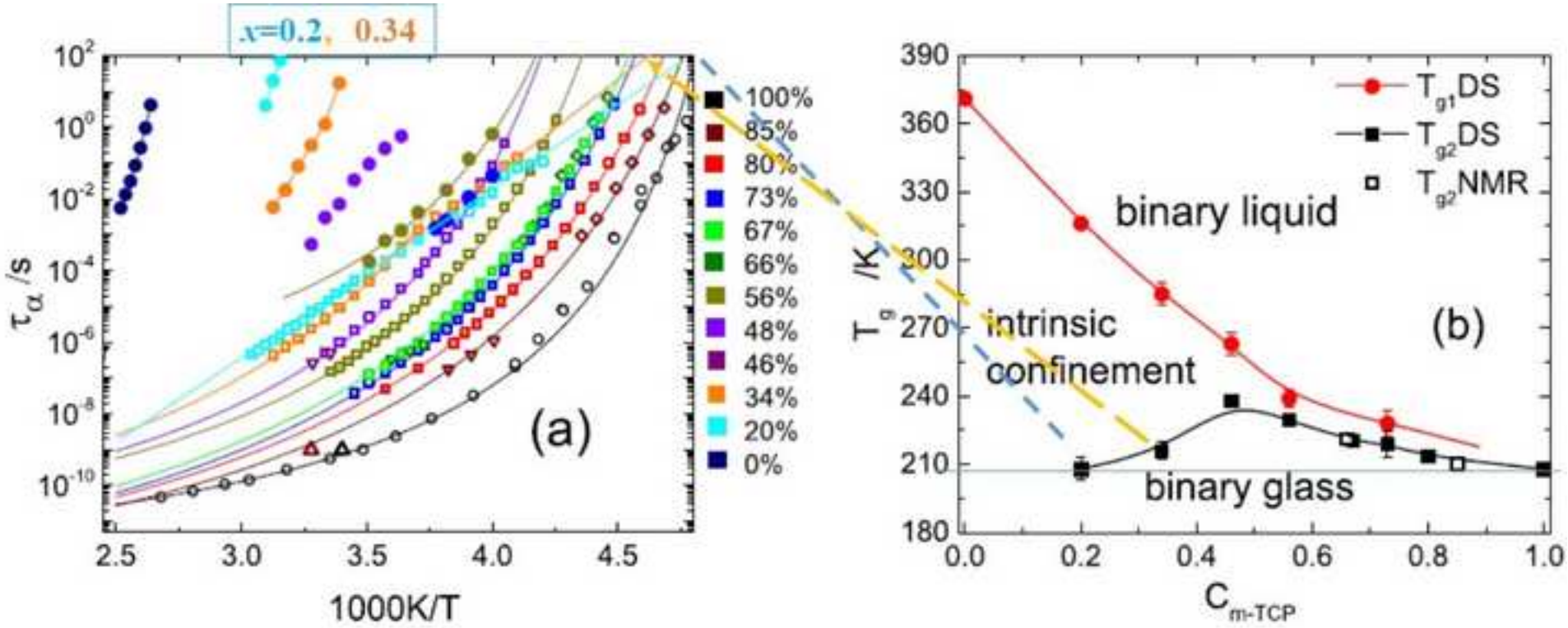

Figure 16

Click here to download high resolution image

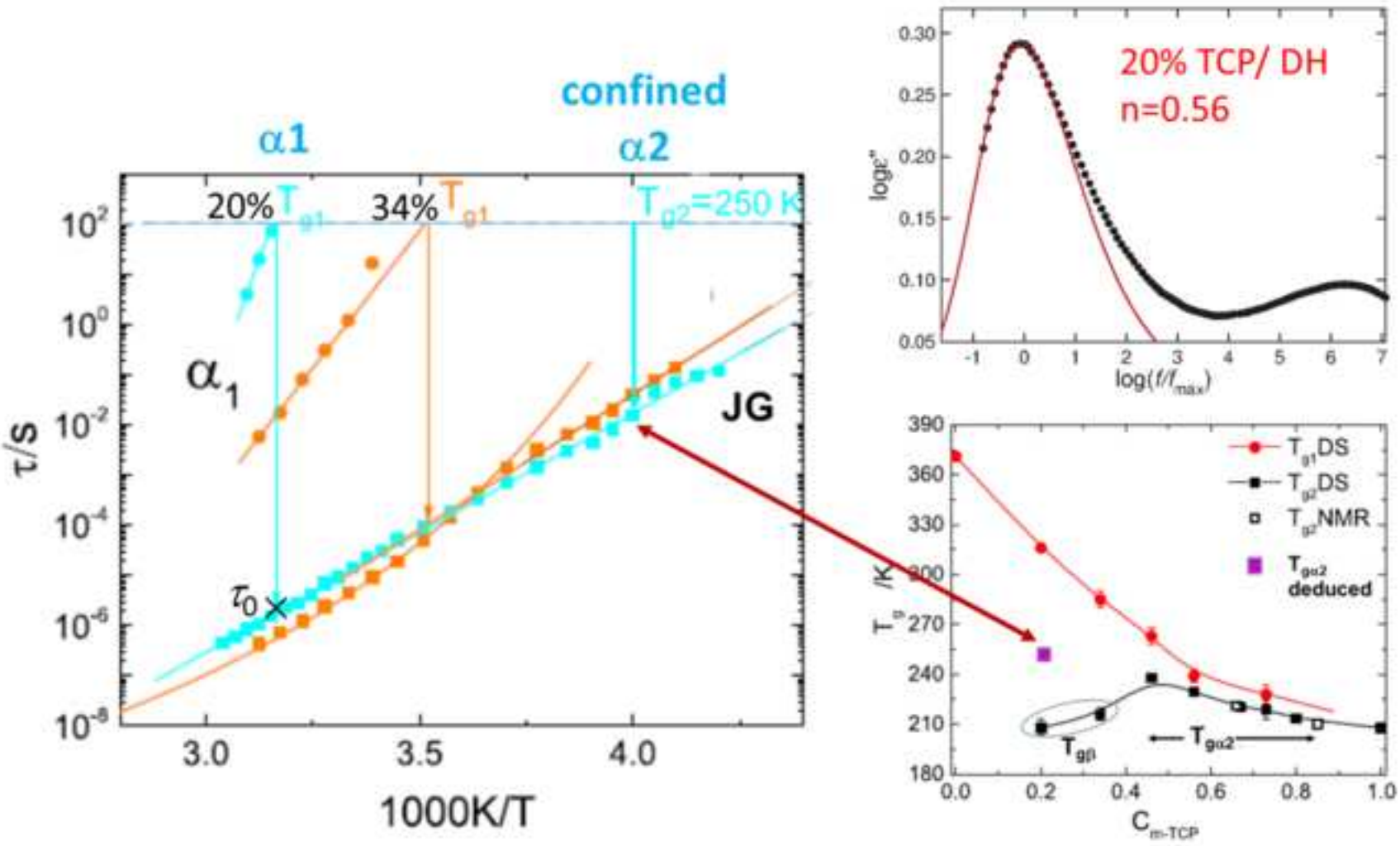

Figure 17
Click here to download high resolution image

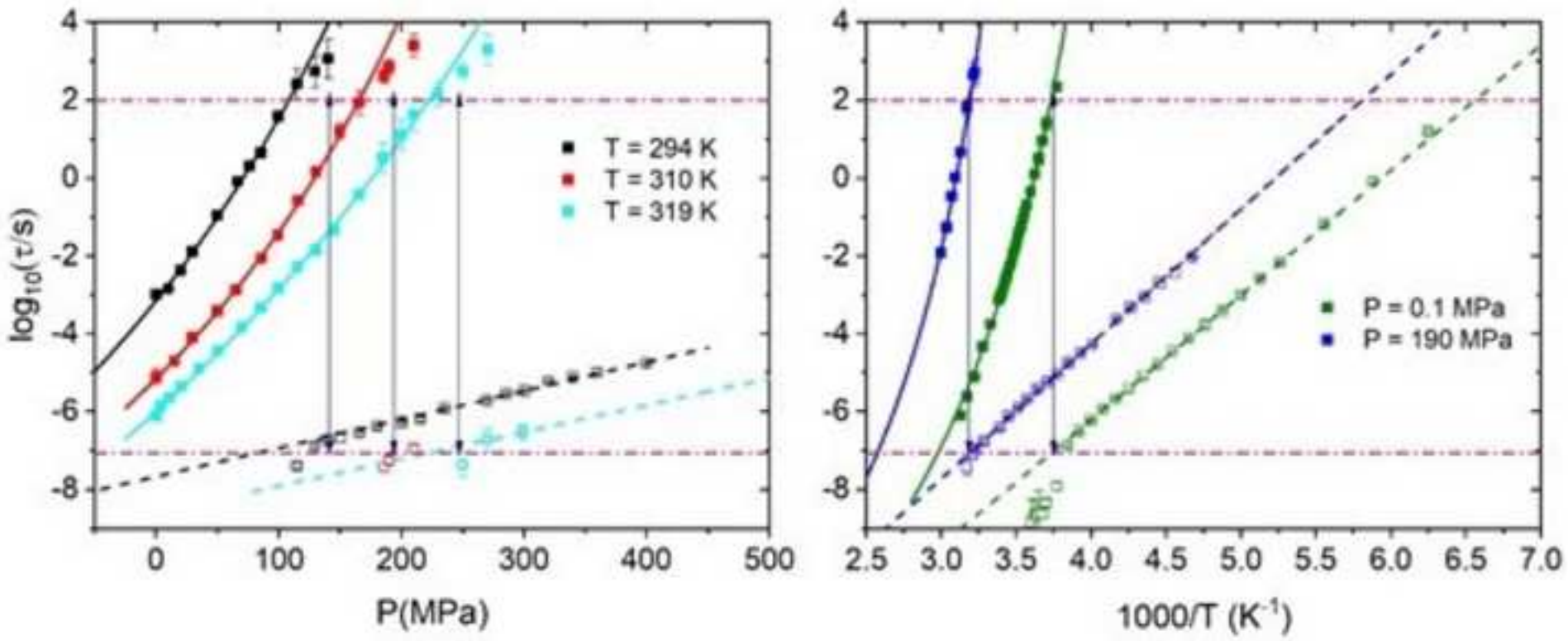

Figure 18

Click here to download high resolution image

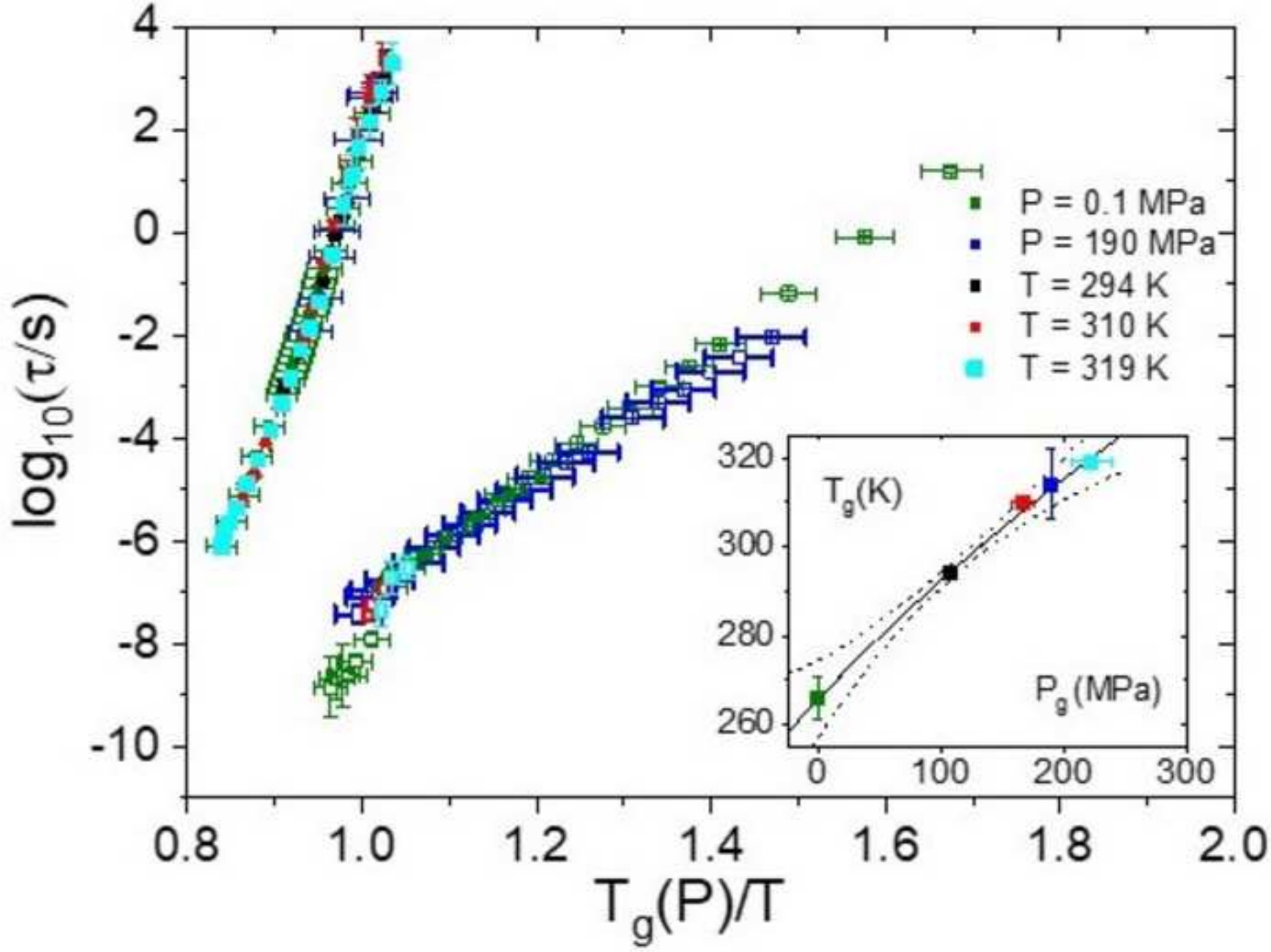

Figure 19

Click here to download high resolution image

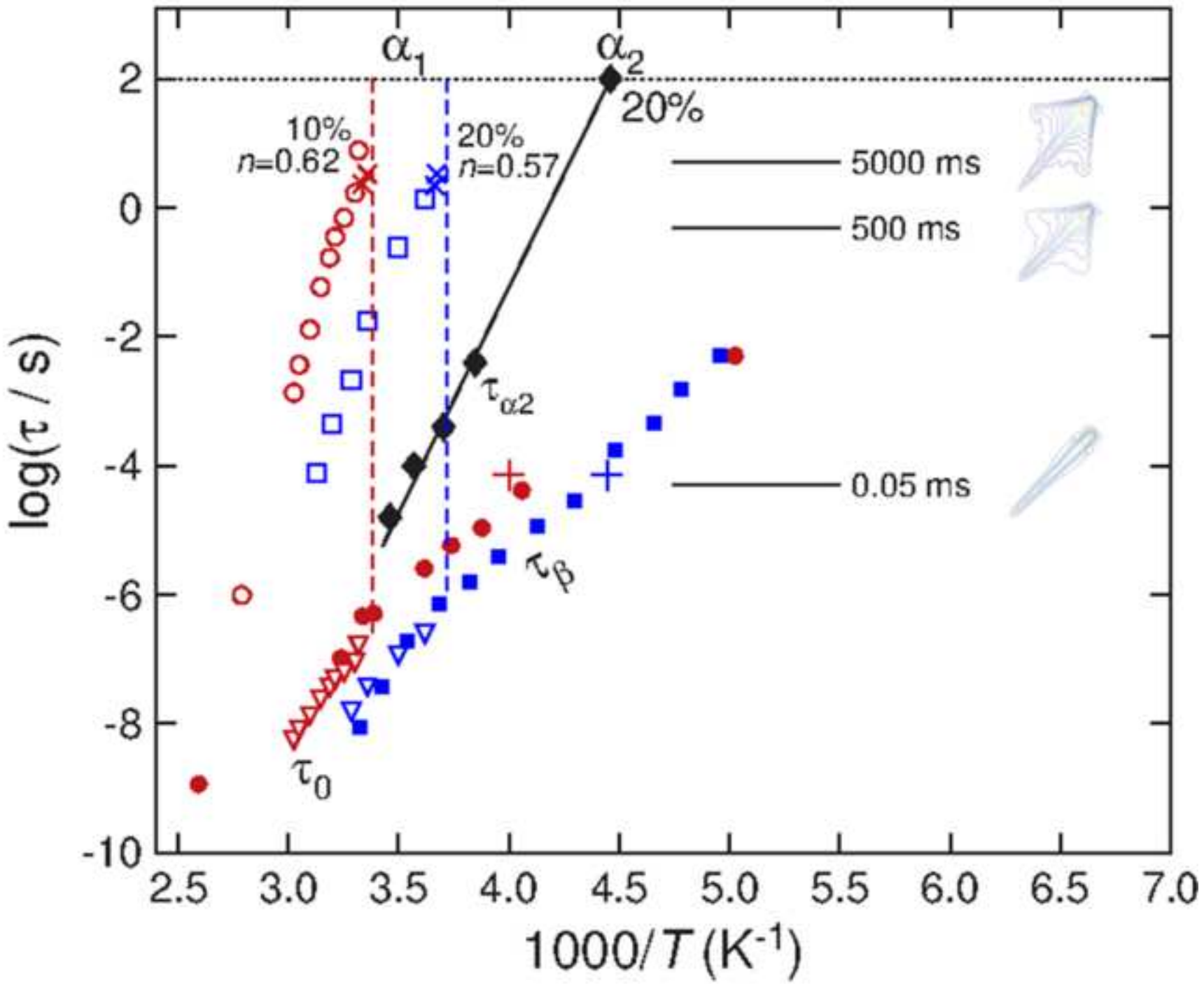

Figure 20
Click here to download high resolution image

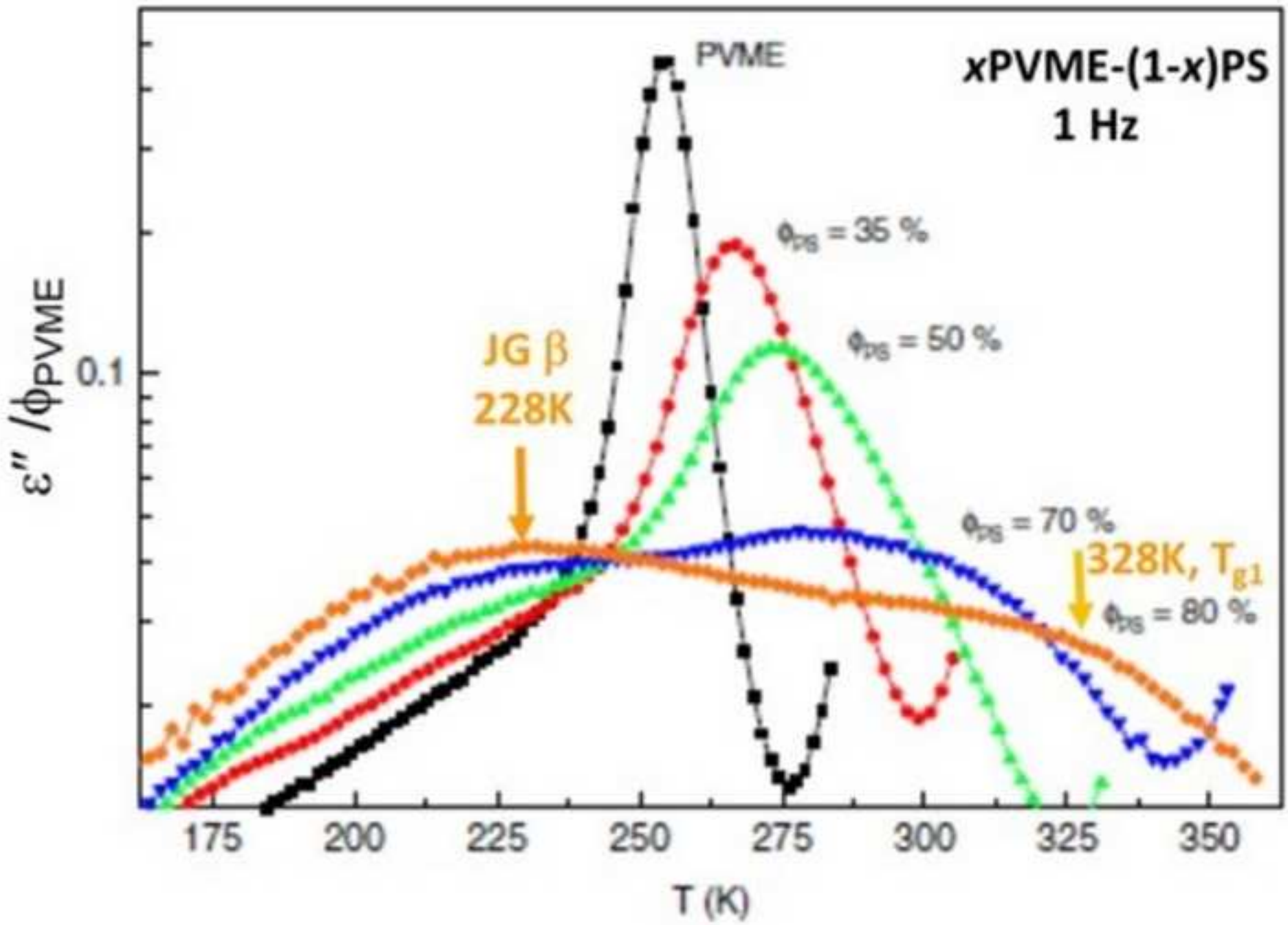

Figure 21

Click here to download high resolution image

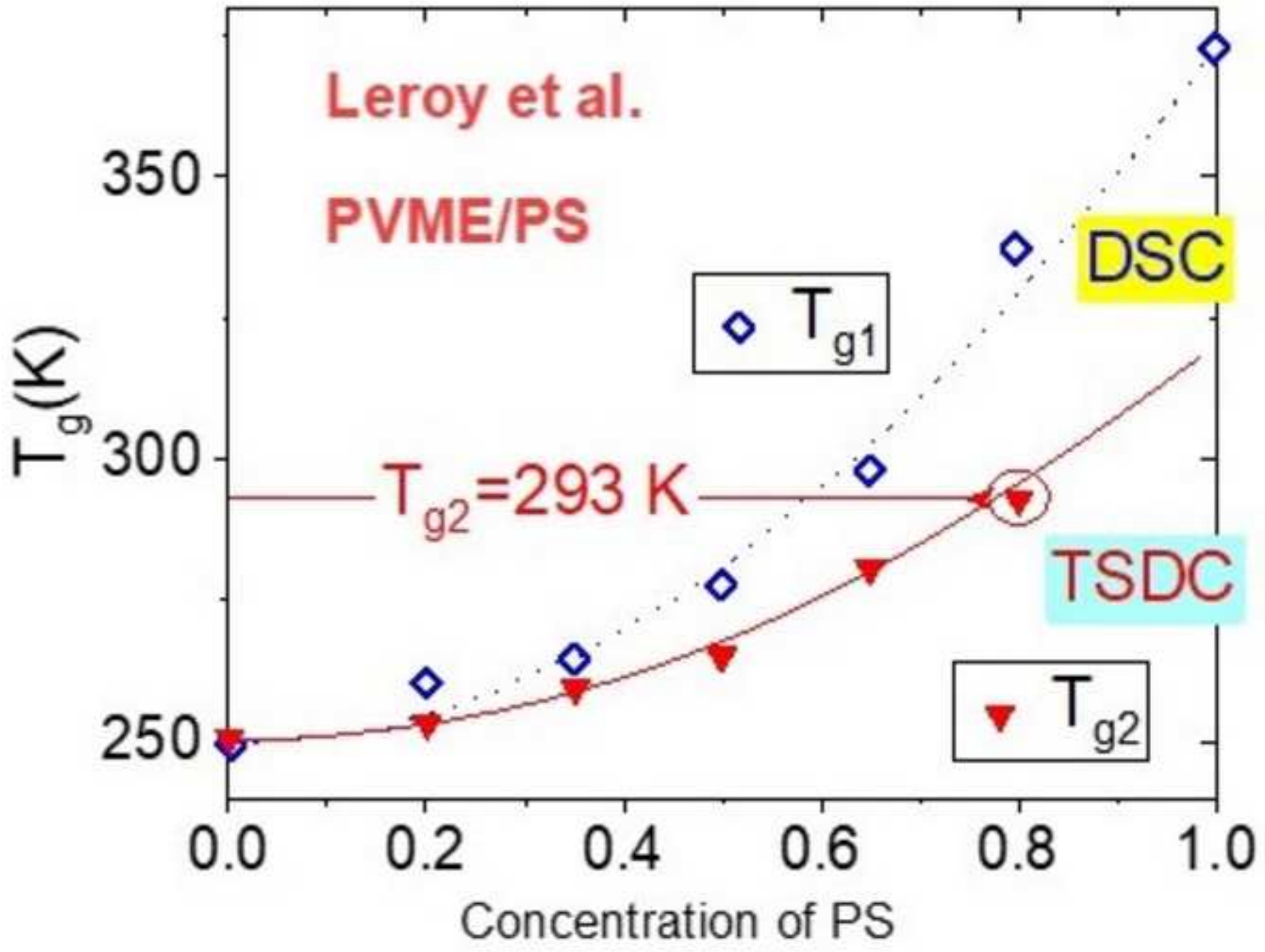

Figure 22

Click here to download high resolution image

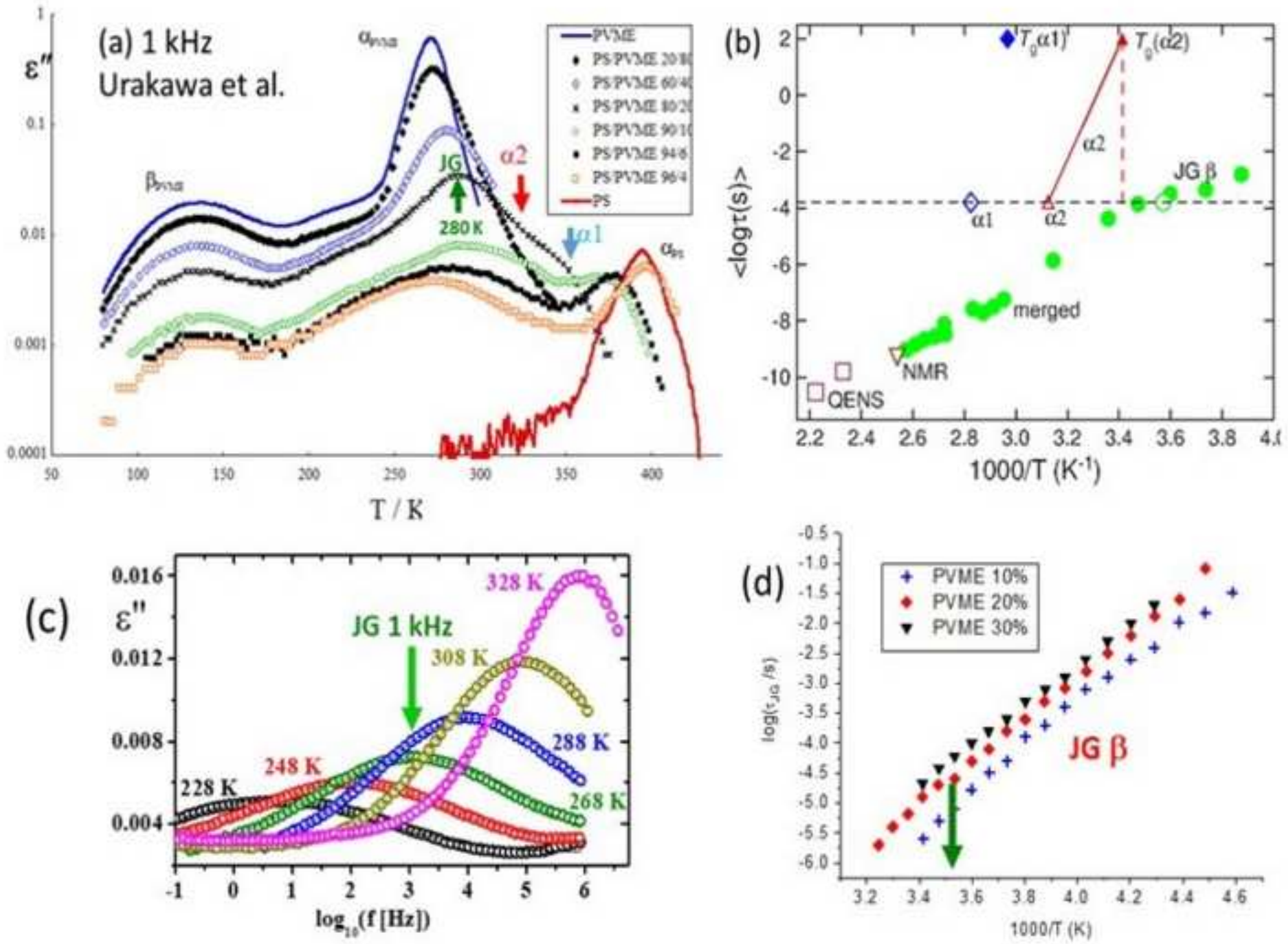

Figure 23

Click here to download high resolution image

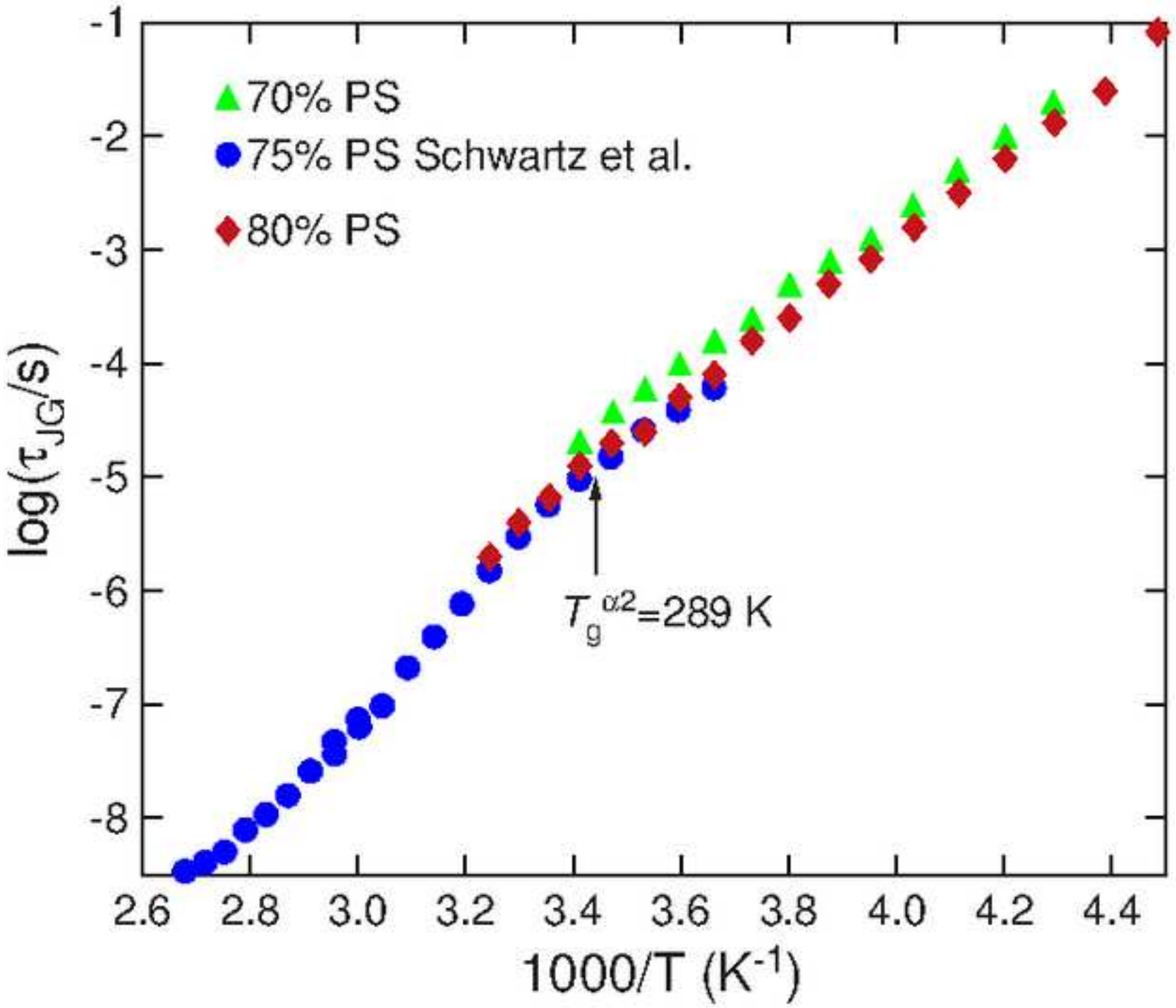

Figure 24

Click here to download high resolution image

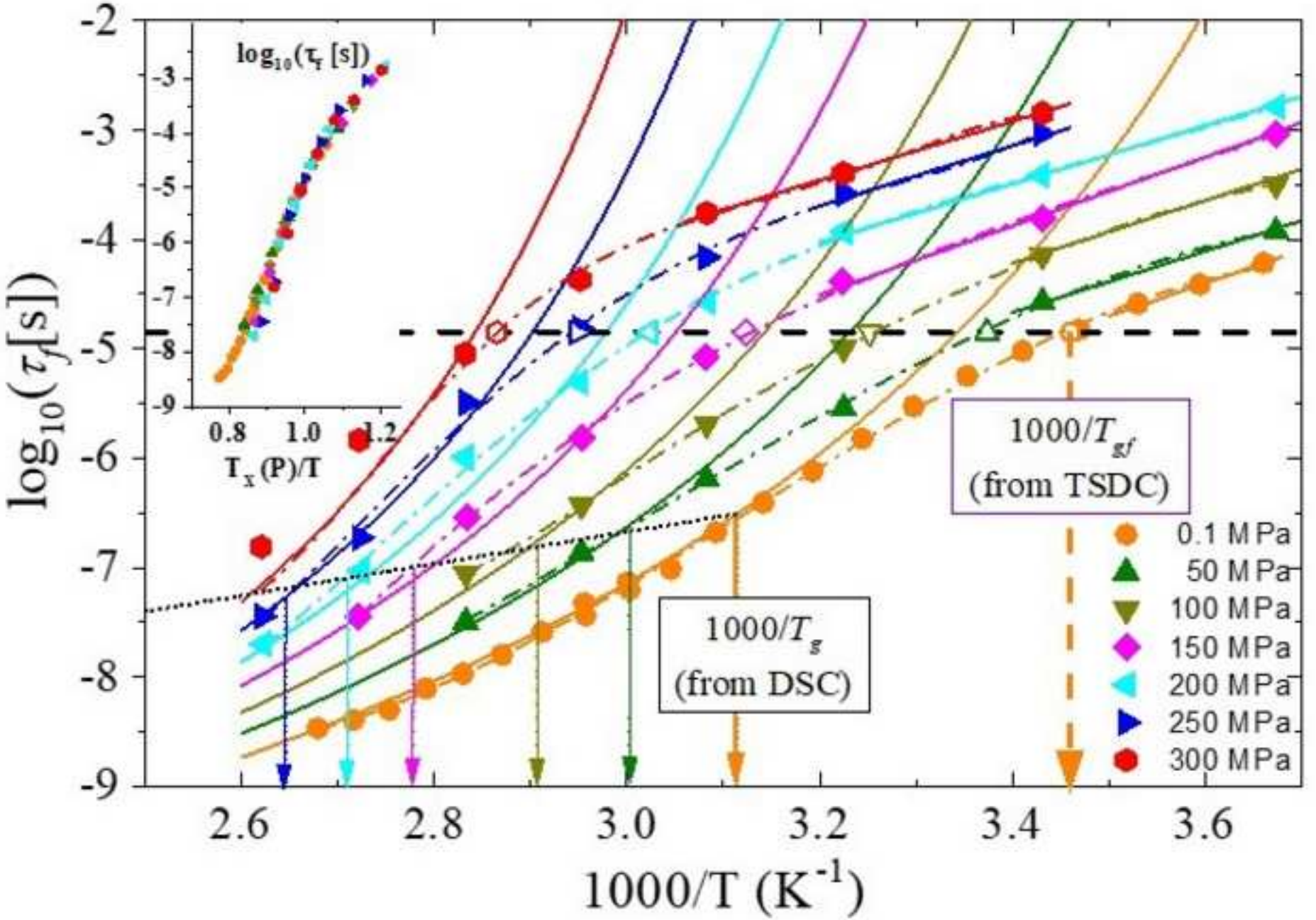

Figure 25

Click here to download high resolution image

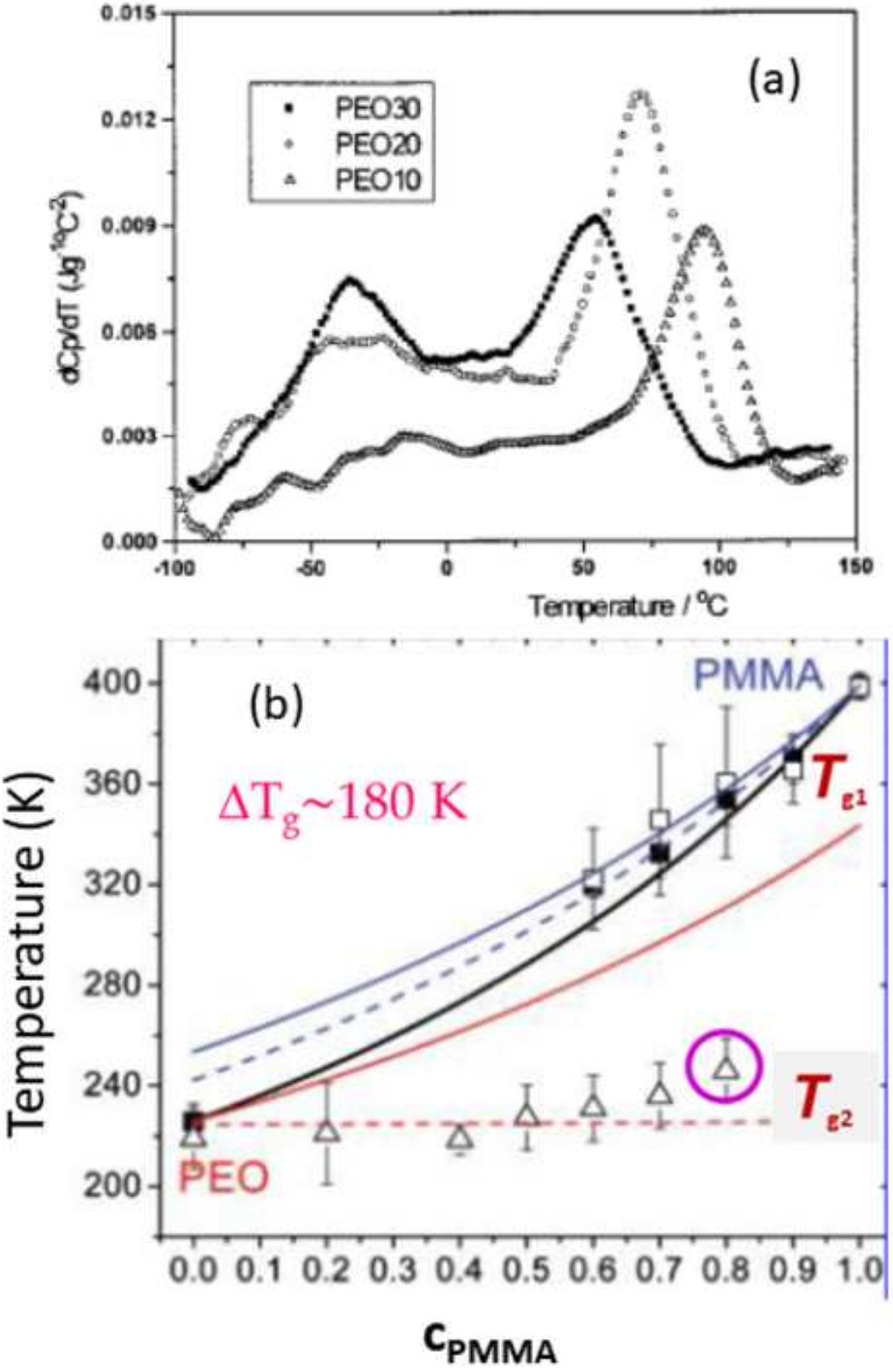

Figure 26

Click here to download high resolution image

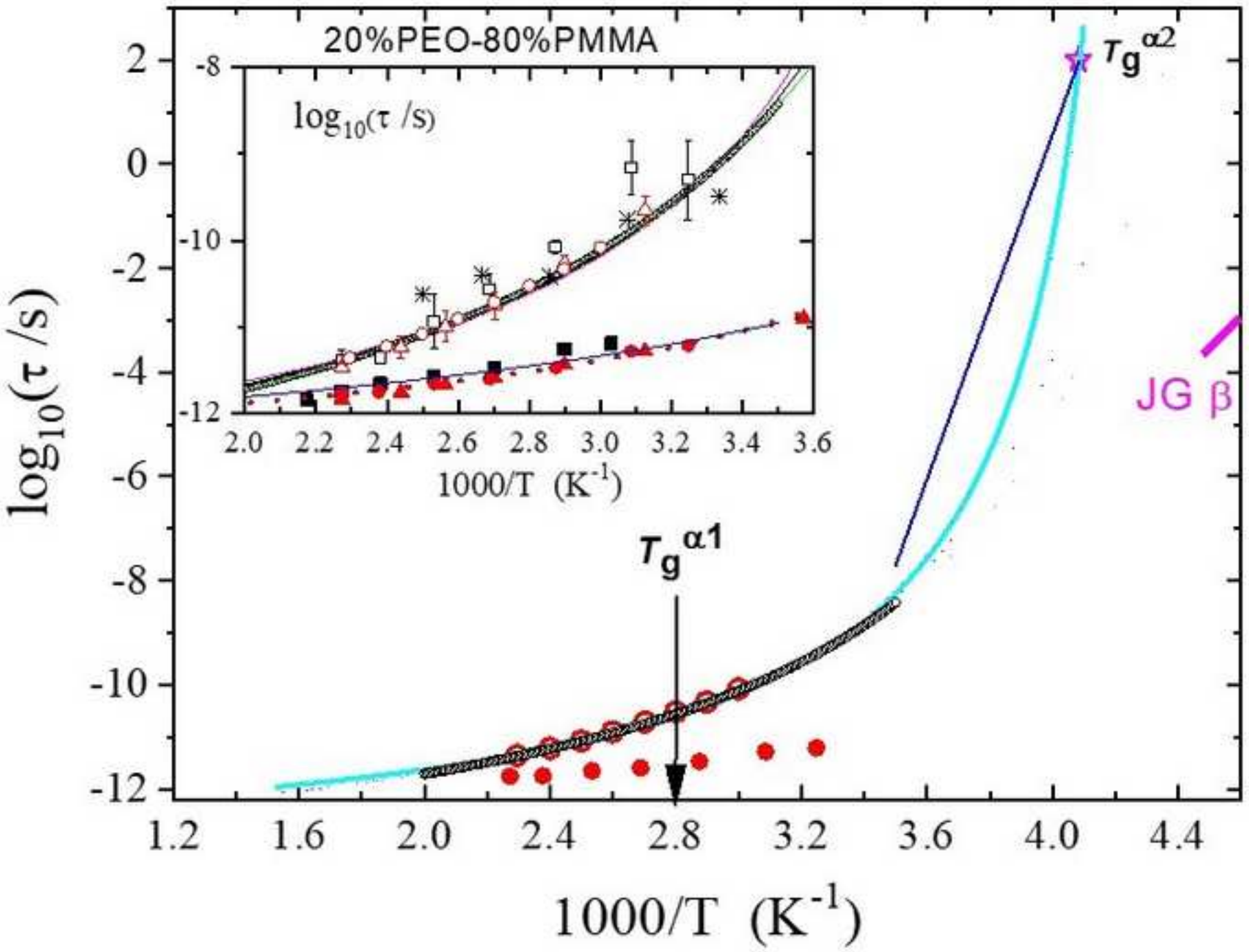

Figure 27

Click here to download high resolution image

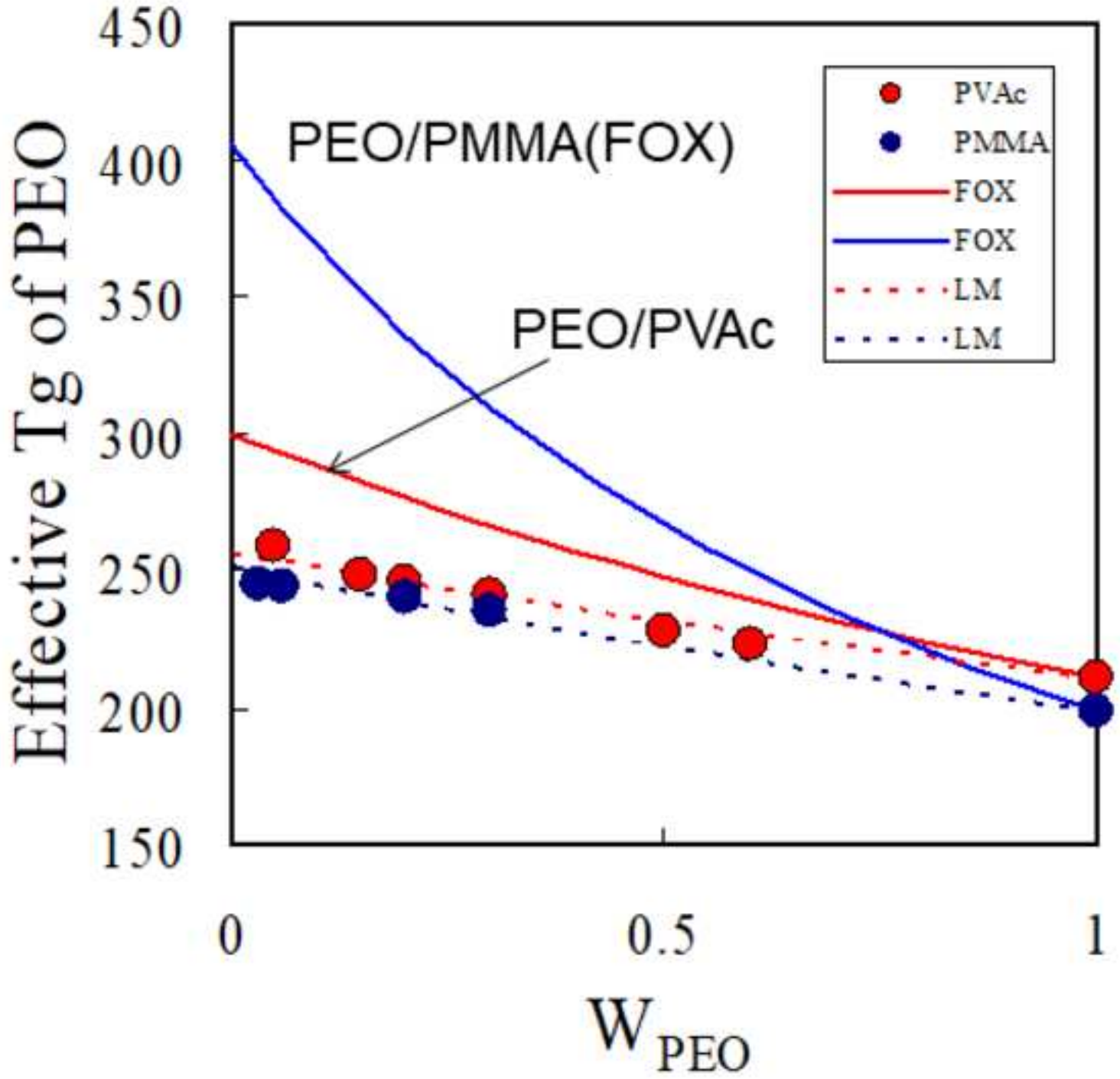

Figure 28

Click here to download high resolution image

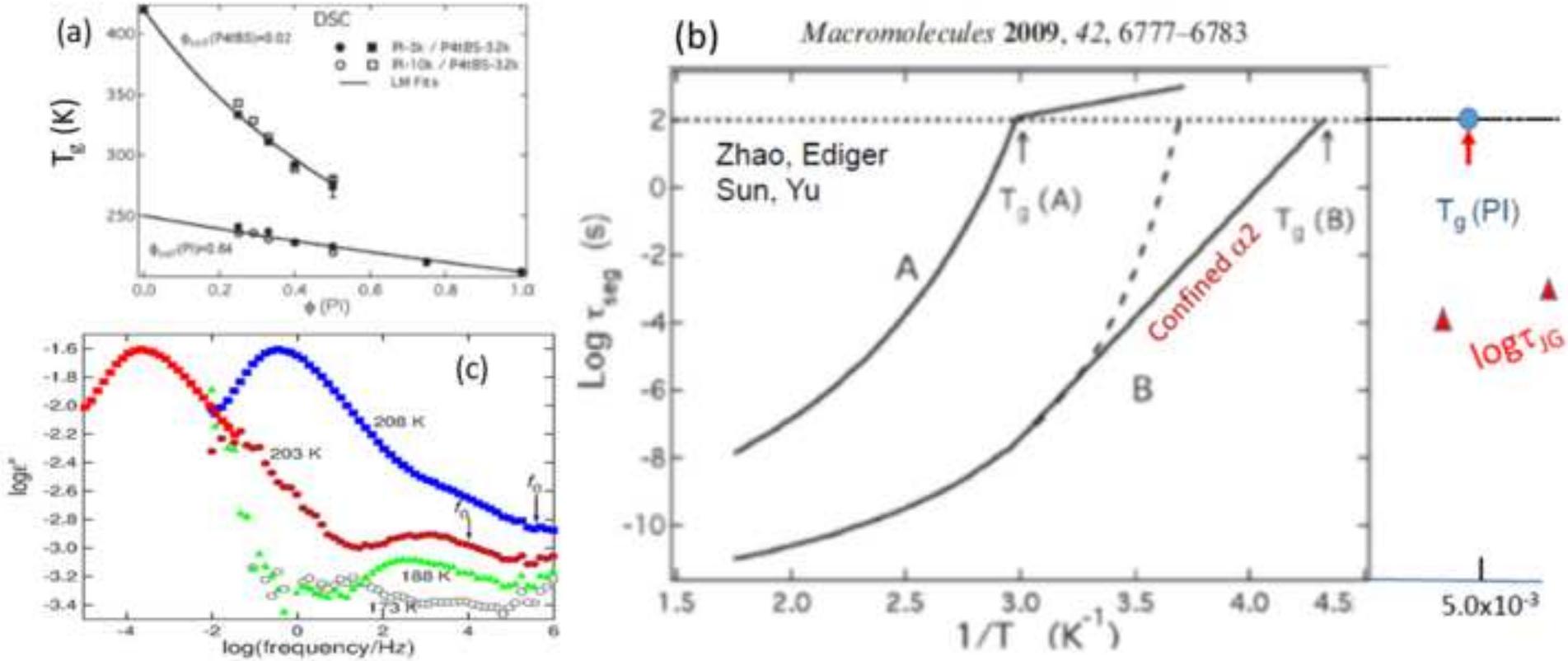

Figure 29

Click here to download high resolution image

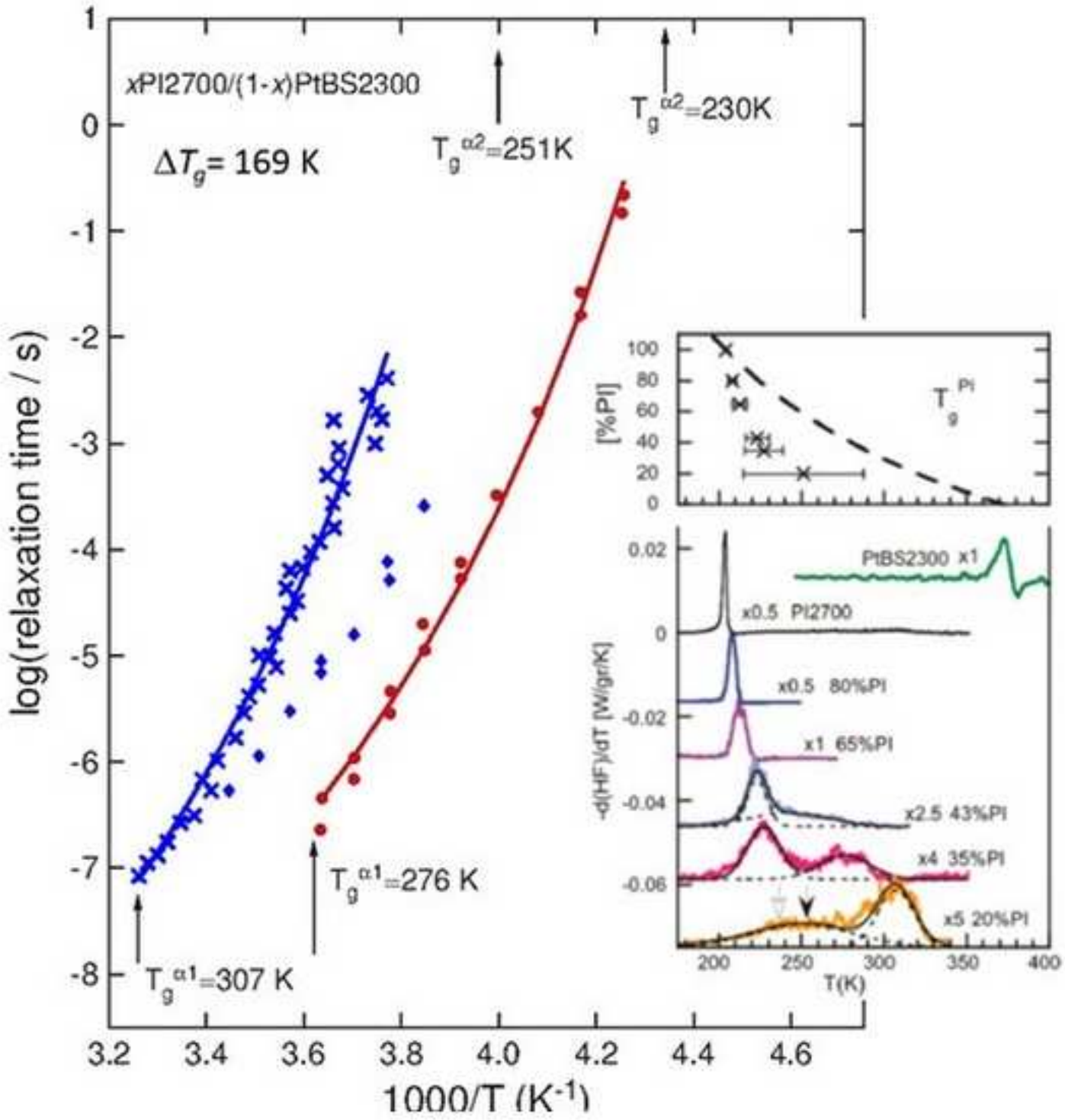

Figure 30

Click here to download high resolution image

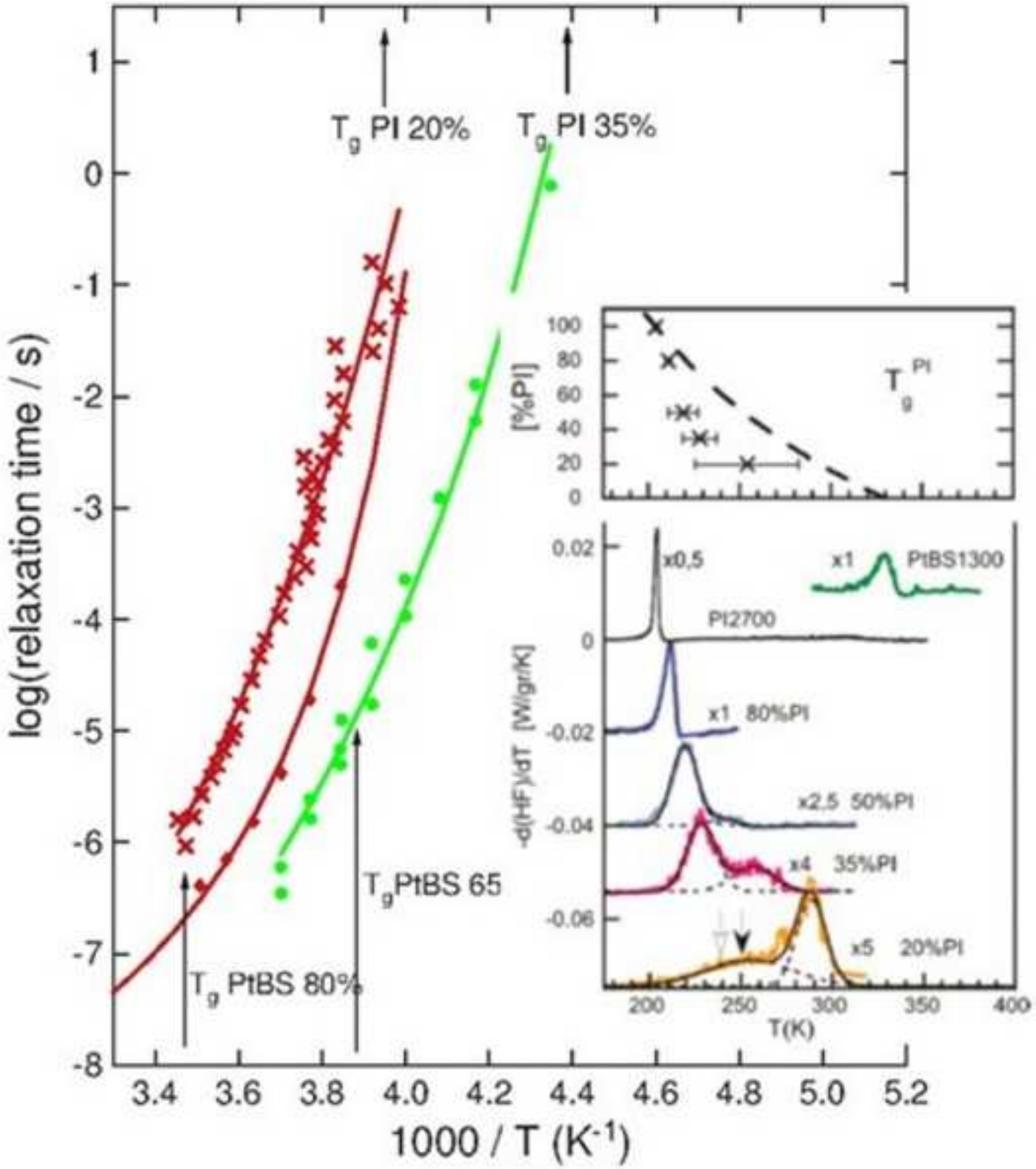

Supplemental material for on-line publication only

Click here to download Supplemental material for on-line publication only: Supplemental Material.docx

***Declaration of Interest Statement**

Declaration of interests

☒ The authors declare that they have no known competing financial interests or personal relationships that could have appeared to influence the work reported in this paper.

☐The authors declare the following financial interests/personal relationships which may be considered as potential competing interests: